

# **BIOAPPLICATIONS OF SOLID PHASE MICROEXTRACTION**

By

Haodan Yuan

A thesis

presented to the University of Waterloo

in fulfillment of the

thesis requirement for the degree of

Doctor of Philosophy

in

Chemistry

Waterloo, Ontario, Canada, 2000

© Haodan Yuan, 2000



**National Library  
of Canada**

**Acquisitions and  
Bibliographic Services**

**395 Wellington Street  
Ottawa ON K1A 0N4  
Canada**

**Bibliothèque nationale  
du Canada**

**Acquisitions et  
services bibliographiques**

**395, rue Wellington  
Ottawa ON K1A 0N4  
Canada**

*Your file Votre référence*

*Our file Notre référence*

**The author has granted a non-exclusive licence allowing the National Library of Canada to reproduce, loan, distribute or sell copies of this thesis in microform, paper or electronic formats.**

**The author retains ownership of the copyright in this thesis. Neither the thesis nor substantial extracts from it may be printed or otherwise reproduced without the author's permission.**

**L'auteur a accordé une licence non exclusive permettant à la Bibliothèque nationale du Canada de reproduire, prêter, distribuer ou vendre des copies de cette thèse sous la forme de microfiche/film, de reproduction sur papier ou sur format électronique.**

**L'auteur conserve la propriété du droit d'auteur qui protège cette thèse. Ni la thèse ni des extraits substantiels de celle-ci ne doivent être imprimés ou autrement reproduits sans son autorisation.**

**0-612-60577-9**

**Canada**

## **BORROWER'S PAGE**

The University of Waterloo requires the signatures of all persons using or photocopying this thesis. Please sign below, and give the address and date.

## ABSTRACT

Solid phase microextraction (SPME) has experienced rapid development in the recent decade. Especially for volatile organic compounds in environmental sample analysis, SPME features the special advantages of combining sampling, sample preparation, and sample transfer into a single step. However, due to the complexity of biomatrices and non-volatile and polar nature of the drug compounds, most drug analyses by SPME and in-tube SPME are still in their primary analytical optimization stage.

Based on the fact that SPME is an equilibrium extraction process, in this thesis, SPME has been successfully applied for drug-protein studies. The theory of protein binding study by headspace SPME was first illustrated with selected alkylbenzene compounds binding to bovine serum albumin (BSA) as the model system. Drug binding to human serum albumin (HSA) was subsequently studied by direct SPME due to the non-volatile and polar nature of the model drug, diazepam. This method can be easily adapted to other drugs. The theoretical as well as the experimental analysis demonstrated that, compared with the traditional methods, SPME is a simple and accurate method for protein binding studies. The small volume SPME method developed in this thesis is useful in the determination of drug binding to expensive proteins since only a very small volume (150  $\mu\text{L}$  for each extraction) of the protein solution is required.

The major difficulty in the analysis of the biological sample with the existing SPME coating materials is the lack of selectivity, which normally results in poor chromatographic separations or/and the poor sensitivity. To overcome the difficulties, immunoaffinity SPME has been developed based on two types of molecular recognition elements: antibodies (Abs) and molecular imprinted polymers (MIPs). Theophylline antibodies were covalently immobilized on the surface of fused silica fiber and on the inner surface of fused silica capillaries for immunoaffinity SPME/in-tube SPME analysis. This method has been successfully applied to human serum analysis.

The research performed in this thesis demonstrates that such materials could have great potential for selective extraction once they can be coated on fused silica surfaces more reliably and effectively.

## **ACKNOWLEDGEMENT**

I would like first and foremost to thank Dr. Janusz Pawliszyn for his guidance, encouragement and patience throughout my Ph.D. program. I also thank him for giving me this opportunity to work on this challenging and exciting research project.

Special appreciation is extended to Dr. Wayne Mullett and Heather Lord for the helpful scientific discussions and strong technical support, which greatly enhanced the way I carried out my research. They have also provided me assistance in preparing manuscripts and this thesis.

I would like to thank Dr. Taduesz Gorecki and Dr. Perry Martos for their encouragement and teaching when I first came to this group.

I would like to thank my committee members, Dr. Micheal Chong, Dr. David Josephy and Dr. Lew Brubacher, for their help and guidance when it was required.

I would like to thank Dr. Schulte in the Department of Biology for allowing me to use the Liquid Scintillation Counter and Dr. Mario Gauthier for the scientific discussions.

I would also thank all the group members, especially Alina Segal, Bryn Shurmer, Tiemin Huang, Li Sheng, Wei Xie, Jingcun Wu, Angelina So, Claudia Zini, Dr. Jacek Koziel, Dr. Zoltan Mester, for their assistance and friendship.

## **DEDICATION**

I dedicate this thesis to my husband Xiang He for his love, encouragement and tremendous help during the entire period of my Ph.D. program. I also dedicate this thesis to my lovely daughter Andrea. I have a special dedication for my parents for giving me so much to cherish and always encouraging me to going up.

# TABLE OF CONTENTS

|   | PAGE      |
|---|-----------|
| Declaration .....   | ii        |
| Borrower's Page .....   | iii       |
| Abstract .....  | iv        |
| Acknowledgement.....  | v         |
| Dedication .....  | vi        |
| List of Tables.....   | x         |
| List of Figures .....   | xii       |
| <br>  |           |
| <b>CHAPTER 1 INTRODUCTION .....</b>   | <b>1</b>  |
| <b>1.1 Solid Phase Microextraction (SPME).....</b>  | <b>1</b>  |
| 1.1.1 General Introduction .....  | 1         |
| 1.1.2 Practical Aspects of SPME .....   | 3         |
| 1.1.3 Theoretical Aspects of SPME .....   | 4         |
| 1.1.4 SPME/HPLC Interface .....   | 6         |
| 1.1.5 Detection Methods Coupled with SPME .....   | 10        |
| <b>1.2 Considerations in Biological Sample Analysis.....</b>                                | <b>12</b> |
| <b>1.3 Difficulties in Biological Sample Analysis by SPME.....</b>                          | <b>13</b> |
| <b>1.4 Molecular Recognition Materials .....</b>  | <b>14</b> |
| <b>1.5 Objectives of the Thesis .....</b>   | <b>15</b> |
| <b>1.6 References .....</b>   | <b>17</b> |
| <br>  |           |
| <b>CHAPTER 2 APPLICATION OF SPME TO THE STUDY OF PROTEIN-<br/>LIGAND INTERACTIONS .....</b> | <b>21</b> |
| <b>2.1 Introduction .....</b>   | <b>21</b> |
| 2.1.1 Definition and Significance of Protein Binding Study.....                             | 21        |
| 2.1.2 Techniques Used for the Measurement of Binding.....                                   | 23        |
| 2.1.3 Evaluation of the Binding Data .....  | 26        |
| <b>2.2 Study of Alkylbenzenes Binding to Bovine Serum Albumin by SPME .....</b>             | <b>30</b> |
| 2.2.1 Background .....  | 30        |
| 2.2.1.1 General Introduction .....  | 30        |
| 2.2.1.2 Headspace GC Method.....  | 31        |

|            |  |           |
|------------|--|-----------|
| 2.2.1.3    | Present SPME for Free Concentration Measurement .....                | 34        |
| 2.2.2      | Theory .....   | 34        |
| 2.2.3      | Experimental .....   | 38        |
| 2.2.4      | Methods .....  | 40        |
| 2.2.5      | Results and Discussion.....  | 41        |
| 2.2.6      | Determination of Equilibrium Constant without Calibration.....       | 57        |
| 2.2.7      | Conclusion.....  | 61        |
| <b>2.3</b> | <b>Study of Diazepam Binding to Human Serum Albumin by SPME.....</b> | <b>62</b> |
| 2.3.1      | Background .....   | 62        |
| 2.3.2      | Theory .....   | 64        |
| 2.3.3      | Experimental .....   | 68        |
| 2.3.4      | Results and Discussion.....  | 70        |
| 2.3.5      | Measurement of Equilibrium Constant without Calibration .....        | 75        |
| 2.3.6      | Conclusion.....  | 78        |
| <b>2.4</b> | <b>Diazepam Binding to HSA — Small Volume Analysis by SPME.....</b>  | <b>79</b> |
| 2.4.1      | Theory and Description of the Method .....                           | 79        |
| 2.4.2      | Experimental .....   | 81        |
| 2.4.3      | Results and Discussion.....  | 82        |
| 2.4.4      | Direct Measurement for Small Volume Binding Study .....              | 84        |
| 2.4.5      | Conclusion.....  | 85        |
| <b>2.5</b> | <b>Conclusions of Protein Binding Study by SPME .....</b>            | <b>87</b> |
| <b>2.6</b> | <b>References .....</b>  | <b>88</b> |

|                  |   |            |
|------------------|---|------------|
| <b>CHAPTER 3</b> | <b>DETERMINATION OF THEOPHYLLINE IN SERUM BY</b>      |            |
|                  | <b>IMMUNOAFFINITY SPME AND IN-TUBE SPME.....</b>      | <b>90</b>  |
| <b>3.1</b>       | <b>Introduction .....</b>                             | <b>90</b>  |
| 3.1.1            | Background .....                                      | 90         |
| 3.1.2            | Antibody and Antigen .....                            | 91         |
| 3.1.3            | Antibody Immobilization .....                         | 94         |
| 3.1.4            | Immunoassay.....                                      | 97         |
| 3.1.5            | Scintillation Detection.....                          | 100        |
| <b>3.2</b>       | <b>Experimental.....</b>                              | <b>102</b> |
| 3.2.1            | Method .....  | 104        |
| 3.2.1.1          | Preparation of the Antibody Immobilized Surface ..... | 104        |
| 3.2.1.2          | Test of the Antibody Immobilized Surface .....        | 110        |
| 3.2.2            | Results and Discussion.....                           | 111        |
| 3.2.2.1          | Reaction of Antibody Immobilization .....             | 111        |
| 3.2.2.2          | Binding Studies of Immobilized Antibodies.....        | 114        |
| 3.2.2.2.1        | Antibody Immobilized Fiber Surface Analysis.....      | 114        |
| 3.2.2.2.2        | Binding Study of In-tube Immunoaffinity SPME.....     | 121        |
| <b>3.3</b>       | <b>Conclusion.....</b>                                | <b>126</b> |
| <b>3.4</b>       | <b>References .....</b>                               | <b>127</b> |



|  |            |
|--|------------|
| <b>CHAPTER 4 APPLICATION OF MOLECULAR IMPRINTED POLYMER IN SPME: A PRELIMINARY STUDY .....</b> | <b>130</b> |
| <b>4.1 Introduction .....</b>  | <b>130</b> |
| 4.1.1 Molecularly Imprinted Polymer (MIP) .....  | 130        |
| 4.1.2 Preparation of MIPs .....  | 131        |
| 4.1.3 Advantages and Applications of MIPs.....   | 131        |
| 4.1.4 Objectives of This Study .....   | 132        |
| <b>4.2 Theory .....</b>  | <b>132</b> |
| 4.2.1 Preparation of MIP for Diazepam .....  | 132        |
| <b>4.3 Experimental.....</b>   | <b>136</b> |
| 4.3.1 Chemicals and Materials .....  | 136        |
| 4.3.2 Method .....   | 136        |
| 4.3.3 Results and Discussion.....  | 138        |
| <b>4.4 Conclusion.....</b>   | <b>143</b> |
| <b>4.5 References .....</b>  | <b>143</b> |
| <br>   |            |
| <b>CHAPTER 5 IN-TUBE SPME FOR BENZODIAZEPINE ANALYSIS.....</b>                                 | <b>145</b> |
| <b>5.1 Introduction .....</b>  | <b>145</b> |
| 5.1.1 Benzodiazepine .....   | 145        |
| 5.1.2 Electrospray Ionization Mass Spectrometry .....  | 146        |
| <b>5.2 Theory .....</b>  | <b>148</b> |
| <b>5.3 Experimental.....</b>   | <b>151</b> |
| 5.3.1 Methods .....  | 152        |
| 5.3.2 Results and Discussion.....  | 154        |
| 5.3.2.1 Optimization of Analytical Conditions .....  | 154        |
| 5.3.2.2 Quantitative Analysis .....  | 159        |
| 5.3.2.3 Mass Spectra of Benzodiazepines .....  | 162        |
| 5.3.2.4 Analysis of Urine and Serum Samples.....   | 170        |
| <b>5.4 Conclusion.....</b>   | <b>173</b> |
| <b>5.5 References .....</b>  | <b>174</b> |
| <br>   |            |
| <b>CHAPTER 6 CONCLUSIONS.....</b>  | <b>176</b> |
| <b>6.1 Scope of SPME in Biological Applications .....</b>                                      | <b>176</b> |
| <b>6.2 Protein Binding Study with SPME.....</b>  | <b>178</b> |
| <b>6.3 Immunoaffinity SPME.....</b>  | <b>179</b> |
| <b>6.4 The Potential of SPME in Biological Applications.....</b>                               | <b>180</b> |
| <b>6.5 References .....</b>  | <b>182</b> |
| <br>   |            |
| <b>GLOSSARY .....</b>  | <b>183</b> |

## LIST OF TABLES

### *Chapter 2*

|   |    |
|---|----|
| <b>Table 2.1:</b> Summary of physical-chemical properties of the target compounds .....   | 30 |
| <b>Table 2.2:</b> GC response factors of target alkylbenzenes determined by syringe injection<br>(/500 ng) .....  | 42 |
| <b>Table 2.3:</b> Regression coefficients of the calibration curves shown in Figure 2.4.....  | 44 |
| <b>Table 2.4:</b> Summary of $K_{fh}$ and $K_{fs}$ SPME/PDMS data for selective alkylbenzene<br>compounds .....   | 45 |
| <b>Table 2.5:</b> Summary of the data obtained from calibration of alkylbenzenes.....   | 46 |
| <b>Table 2.6:</b> Summary of the experimental results of alkylbenzenes binding to BSA.....  | 49 |
| <b>Table 2.7:</b> Comparison of $\log K$ values obtained from the SPME method and from<br>headspace GC analysis .....   | 50 |
| <b>Table 2.8:</b> The geometric dimensions of selected fibers .....   | 51 |
| <b>Table 2.9:</b> Summary of the experimental data of total amount of the analyte spiked into<br>the system, on the fiber and in the headspace. Henry's law constant (12) is also listed...   | 52 |
| <b>Table 2.10:</b> Summary of the data of the direct equilibrium constant measurement.....  | 59 |
| <b>Table 2.11:</b> Summary of the data for diazepam analysis in buffer solution.....  | 71 |
| <b>Table 2.12:</b> Summary of the experimental data of diazepam binding to HSA.....   | 74 |
| <b>Table 2.13:</b> Experimental data of diazepam binding to HSA for direct equilibrium<br>constant measurement. Note that for reference system, $C_s^{(0)}$ was 1000 ppb without<br>protein. Its corresponding area count $A^{(0)}$ was 135,109 ..... | 77 |

**Table 2.14:** Summary of the experimental data of diazepam binding to HSA in small volume analysis. The protein concentration was 0.05 mg/mL..... 83

**Table 2.15:** Experimental data for diazepam binding to HSA (small volume) for direct equilibrium constant measurement..... 85

**Chapter 3**

**Table 3.1:** Analysis of theophylline in human serum sample with antibody immobilized silica fiber..... 121

**Table 3.2:** Analysis of theophylline in human serum sample with antibody immobilized capillary..... 125

**Chapter 5**

**Table 5.1:** Comparison of direct injection and in-tube SPME on the extraction of benzodiazepines ..... 158

**Table 5.2:** The regression coefficients of the calibration curves for benzodiazepines analysis by in-tube SPME ..... 161

**Table 5.3:** The limits of detection of benzodiazepine compounds by in-tube SPME ..... 162

**Table 5.4:** The identified characteristic ions of the selected benzodiazepines ..... 166

**Table 5.5:** Recoveries of seven benzodiazepines spiked into urine and serum samples 173

## LIST OF FIGURES

### *Chapter 1*

|   |    |
|---|----|
| <b>Figure 1.1:</b> The SPME device .....  | 2  |
| <b>Figure 1.2:</b> Schematic of fiber SPME interface for SPME/LC and SPME/LC/MS using Hewlett-Packard HP1100 LC/MS .....                      | 7  |
| <b>Figure 1.3:</b> Configuration of the in-tube SPME using Hewlett-Packard HP1100 LC/MS. (A) Extraction process; (B) Desorption process ..... | 9  |
| <b>Figure 1.4:</b> Septum-equipped temperature programmable injector (SPI) interface.....   | 11 |

### *Chapter 2*

|   |    |
|---|----|
| <b>Figure 2.1:</b> A schematic diagram representing the pharmacokinetic consequences of drug binding in blood .....   | 22 |
| <b>Figure 2.2:</b> A schematic diagram of equilibrium in a four-phase system .....  | 35 |
| <b>Figure 2.3:</b> Gas chromatogram of alkylbenzenes .....  | 43 |
| <b>Figure 2.4:</b> The calibration curves of the area count of fiber injection vs. the spiked concentration of the analyte in the buffer solution.....  | 44 |
| <b>Figure 2.5:</b> Calibration curves of the area count obtained from fiber injection vs. the free analyte concentrations in solution, for each of the five compounds .....   | 47 |
| <b>Figure 2.6:</b> The free toluene concentration calibration curves of a) two-phase system (buffer-dissolved protein), b) three-phase system (buffer-dissolved protein-headspace) and c) four-phase system (buffer-dissolved protein-headspace-fiber)..... | 55 |
| <b>Figure 2.7:</b> Curves to directly calculate the equilibrium constant.....   | 60 |

**Figure 2.8:** Loop structure of HSA indicating disulphide bonds forming loops, subdomains and domains. (Adapted from (3)). —: disulfide bond) ..... 62

**Figure 2.9:** Structure and some physical properties of diazepam..... 63

**Figure 2.10:** Schematic of equilibrium in three-phase system (sample solution-dissolved protein-fiber coating)..... 66

**Figure 2.11:** Extraction profile of diazepam by a PDMS 100 μm fiber in 0.067 M pH= 7.4 phosphate buffer. Agitation speed was 800 rpm ..... 70

**Figure 2.12:** Calibration curve of diazepam. The x-axis is the total concentration of diazepam..... 72

**Figure 2.13:** Scatchard plot for diazepam binding to HSA ..... 75

**Figure 2.14:** Direct measurement of diazepam-HSA binding equilibrium constant..... 77

**Figure 2.15:** Experiment configurations for diazepam binding to HSA in small volume analysis..... 81

**Figure 2.16:** Scatchard plot for small volume diazepam-HSA binding analysis ..... 83

**Figure 2.17:** Direct measurement of diazepam HSA binding equilibrium constant (small volume)..... 86

**Chapter 3**

**Figure 3.1:** Schematic of the structure of IgG antibody molecule. The four polypeptide chains, two heavy and two light chains, are linked via disulfide groups. The number of these disulfide groups can vary depending on the source of the antibody ..... 93

**Figure 3.2:** Non-competitive (a) and competitive solid-phase radioactiveimmunoassay.

◀: Antigen (analyte); ◀: Radiolabelled antigen; —: Antibody molecule;

▨—: Immobilized antibody ..... 99

|   |     |
|---|-----|
| <b>Figure 3.3:</b> The scintillation process .....  | 100 |
| <b>Figure 3.4:</b> Chemical structures of theophylline and caffeine.....  | 103 |
| <b>Figure 3.5:</b> The schematic diagram represents the configuration of the capillary interfaced with the syringe pump for the inside-tube reactions .....   | 105 |
| <b>Figure 3.6:</b> Reactions involved in the antibody immobilization process. a. Silanization of silica surface with APTES; b. Surface modification with glutaraldehyde; c. Immobilization of antibody .....  | 109 |
| <b>Figure 3.7:</b> Scanning electronic micrographs (SEM) of (a) cleaned fused silica surface; (b) glutaraldehyde activated surface; (c) antibody-immobilized surface.....   | 114 |
| <b>Figure 3.8:</b> Binding of <sup>3</sup> H-theophylline on the anti-theophylline immobilized surface in the presence of various amounts of unlabeled diazepam .....   | 115 |
| <b>Figure 3.9:</b> Binding isotherm of anti-theophylline immobilized surface .....  | 116 |
| <b>Figure 3.10:</b> Calibration curve of mass of <sup>3</sup> H-theophylline on the fiber vs. the scintillation response .....  | 117 |
| <b>Figure 3.11:</b> Competitive binding of cold theophylline with the <sup>3</sup> H-theophylline to the anti-theophylline immobilized on a fused silica surface. The <sup>3</sup> H-theophylline was kept at saturation value (4 ng/mL), while the cold theophylline concentration was varied. Duplicates were measured for each point ..... | 119 |
| <b>Figure 3.12:</b> Competitive binding of caffeine to <sup>3</sup> H-theophylline on anti-theophylline coated fused silica fibers .....  | 120 |
| <b>Figure 3.13:</b> The comparison of the immunoaffinity capillary with the bare fused silica capillary in the binding to <sup>3</sup> H-theophylline. The concentration of <sup>3</sup> H-theophylline was 12.4 ng/mL .....  | 122 |

**Figure 3.14:** The competition of non-radiolabeled theophylline to <sup>3</sup>H-theophylline in the binding with the anti-theophylline immobilized capillary. The concentration of <sup>3</sup>H-theophylline was kept at 12.4 ng/mL ..... 123

**Figure 3.15:** Cross reactivity study of caffeine to <sup>3</sup>H-theophylline in the binding to anti-theophylline immobilized capillary..... 124

#### **Chapter 4**

**Figure 4.1:** Typical hydrogen bond interactions between diazepam (target) and MIP binding site are depicted by broken lines (adapted from (20)) ..... 134

**Figure 4.2:** Preparation of a diazepam MIP and binding vs. desorption ..... 135

**Figure 4.3:** The schematic diagram representing the polymerization of MIP and the SEM pictures showing the MIP powder after it is glued on the fiber surface..... 139

**Figure 4.4:** The comparison of anti-diazepam MIP and controlled polymer in binding the 1 ng/mL <sup>3</sup>H-diazepam in CH<sub>2</sub>Cl<sub>2</sub> solution. The blank value is the blank test (extraction of blank solvent) of anti-diazepam fiber..... 140

**Figure 4.5:** The competitive binding of cold diazepam with <sup>3</sup>H-diazepam in the binding to anti-diazepam MIP fiber. The concentration of <sup>3</sup>H-diazepam was 1 ng/mL ..... 141

**Figure 4.6:** The competitive binding to nordazepam with <sup>3</sup>H-diazepam in the binding to the anti-diazepam MIP fiber. The concentration of <sup>3</sup>H-diazepam was 1 ng/mL ..... 142

#### **Chapter 5**

**Figure 5.1:** An LC/ESI/MS interface ..... 147

**Figure 5.2:** ESI ion generation process ..... 148

**Figure 5.3:** Structures of the target benzodiazepine compounds..... 150

|   |     |
|---|-----|
| <b>Figure 5.4:</b> Comparison of various types of capillaries for the in-tube SPME to the extraction of benzodiazepine compounds .....  | 155 |
| <b>Figure 5.5:</b> The effect of pH on in-tube SPME efficiency of benzodiazepine compounds using Supelco-Q PLOT capillary as the extraction media .....   | 156 |
| <b>Figure 5.6:</b> Extraction profile of benzodiazepine compounds illustrating the effect of draw/eject cycles on the in-tube SPME efficiency.....  | 157 |
| <b>Figure 5.7:</b> Calibration curves for benzodiazepines analysis by in-tube SPME .....  | 160 |
| <b>Figure 5.8:</b> Influence of the capillary voltage to the fragmentation of the benzodiazepine compounds .....  | 165 |
| <b>Figure 5.9:</b> Influence of the fragmentor voltage to the fragmentation of benzodiazepine compounds .....   | 167 |
| <b>Figure 5.10:</b> Mass spectra of benzodiazepam compounds obtained from HP 1100 LC/ESI/MS.....  | 170 |
| <b>Figure 5.11:</b> Total ion and SIM chromatograms obtained from urine samples (0.5µg/mL) by in-tube SPME/LC/MS. A: Total ion chromatograms obtained from spiked urine sample. 1. 7-aminoflunitrazepam, 2. N-desmethylflunitrazepam, 3. clonazepam, 4. oxazepam, 5. temazepam, 6. nordazepam, 7.diazepam. B: SIM chromatograms obtained from spiked urine samples..... | 171 |
| <b>Figure 5.12:</b> Total ion and SIM chromatograms obtained from serum samples (0.2µg/mL) by in-tube SPME/LC/MS. A: Total ion chromatograms obtained from spiked urine sample. 1. 7-aminoflunitrazepam, 2. N-desmethylflunitrazepam, 3. clonazepam, 4. oxazepam, 5. temazepam, 6. nordazepam, 7.diazepam. B: SIM chromatograms obtained from spiked urine samples..... | 172 |



**Chapter 6**

**Figure 6.1: SPME for biological applications – scope of the research performed in this thesis..... 177**

# CHAPTER 1

## INTRODUCTION

### 1.1 Solid Phase Microextraction (SPME)

#### 1.1.1 General Introduction

Solid Phase Microextraction (SPME) is a solvent-free sample preparation technique first introduced by Dr. Janusz Pawliszyn and his coworkers in 1990 (1). In its early development stage, SPME was considered primarily suitable for the extraction of volatile organic compounds from environmental samples (1-3). It has been demonstrated that SPME provides many significant advantages over the traditional sample preparation methods by integrating sampling, sample pre-concentration and sample introduction into a single step.

A schematic of the SPME device is shown in Figure 1.1. There are two basic components of this device: the holder and the needle assembly. The needle assembly includes a septum piercing needle, a tubing for fiber attachment and a piece of coated fused silica rod with diameter around 100  $\mu\text{m}$  and length about 1 cm. The holder is carefully designed for the protection of the needle assembly and for the convenience of the sample extraction and injection. The whole SPME device looks like a syringe. Prior to the extraction or injection process, the fiber is withdrawn into the septum piercing needle by retracting the plunger of the holder. In the beginning of the process, the needle first pierces through the septum of the vial or of the hot GC injector. The plunger is then depressed, exposing the fiber to the sample matrix to be analyzed or GC carrier gas. During this period, the plunger is locked by its retaining screw to keep the fiber at a fixed

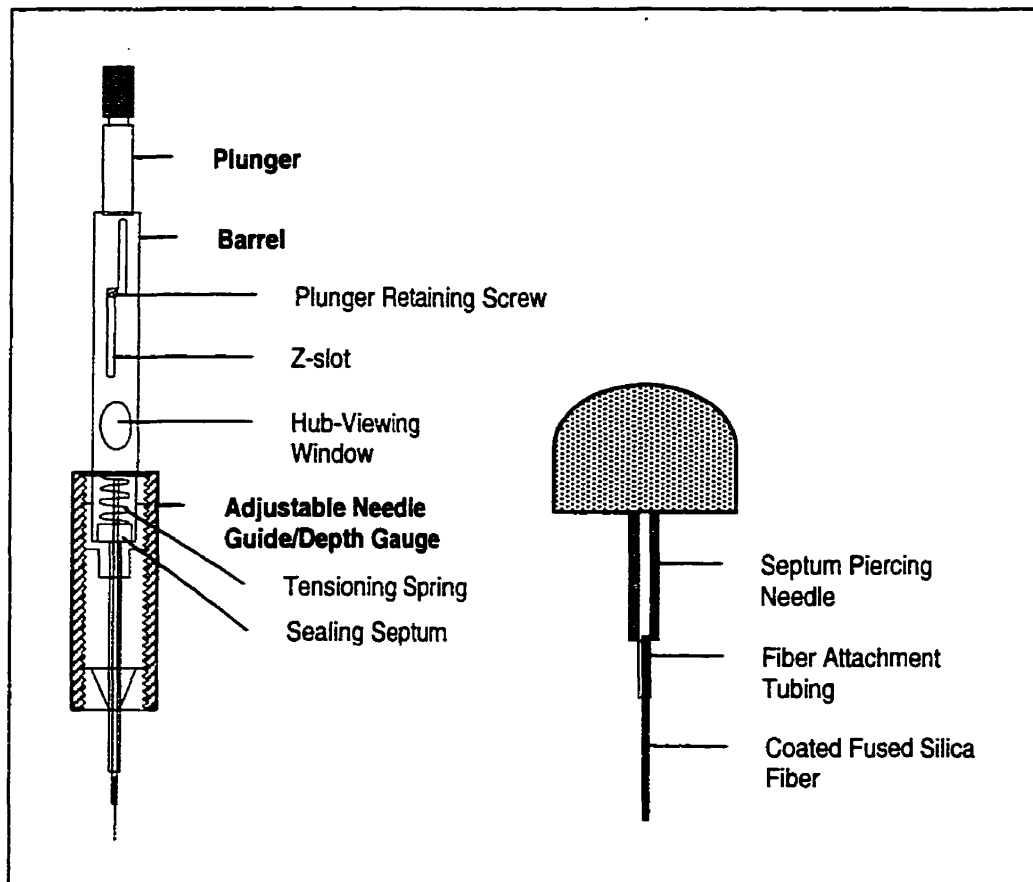


**Figure 1.1:** The SPME device.

position until the extraction or injection process is completed. The plunger is then retracted before the SPME device is removed from the septum to avoid possible damage to the fiber.

The major component of the sampling device is the fused silica rod coated with a layer of polymer. The polymer coating is responsible for extracting analytes from the sample for further analysis. The properties of the coating, obviously, play a very important role in the sample analysis. Many factors are used to evaluate the performance

of the fiber coating, such as the selectivity, the linearity of the response, the stability, the carryover, etc. Much effort has been made to find possible effective coatings.

### **1.1.2 Practical Aspects of SPME**

SPME became commercially available with the introduction of the 100  $\mu\text{m}$  Poly(dimethylsiloxane) (PDMS) coated fiber by Supelco in 1993. Since then, many different fiber coatings have been introduced, dramatically enhancing the scope of the SPME applications. Now, SPME can be used to sample many matrices, including air, water and soil. For aqueous samples, sampling can be carried out directly from the sample solution or from the sample headspace, depending on the volatility of the analytes. SPME has found numerous applications in many applications (4). Some examples include the determination of substituted benzene compounds in water (5,6), volatile organic compounds (7-9), polycyclic aromatic hydrocarbons and polychlorinated biphenyls (10), chlorinated hydrocarbons (11), pesticides (12-18), phenols (19-21), and fatty acids (22), as well as lead and tetraethyllead (23, 24).

While initially SPME studies were concentrated on environmental sample analysis, recently, interest has shifted towards biological sample analysis. Fibers coated with different types of polymers have been employed for the analysis of many drugs and drug classes, including tricyclic antidepressants (25-28), phenothiazines (29), benzodiazepines (30), local anaesthetics (31, 32), meperidine (33), cocaine (35), phencyclidine (36), amphetamines (34), 1-phenylethylamine (37), and diphenylmethane antihistaminics and their analogues (38).

### 1.1.3 Theoretical Aspects of SPME

The theoretical aspects of SPME analysis have been studied in detail (39). Louch *et al* (40) developed a theory for the two-phase system (sample solution-fiber coating), and Zhang and Pawliszyn (41) for the three-phase systems (sample solution-headspace-fiber coating). The effect of sample volume on the amount of the sample extraction by SPME in two-phase (sample solution-fiber coating) and three-phase (sample solution-headspace-fiber coating) systems has been further discussed by Górecki and Pawliszyn (42, 43). Some of the basic conclusions are described in the following paragraphs, while the theory for four-phase systems (sample solution-pseudo phase-headspace-fiber coating) will be discussed in detail in Chapter 2 of this thesis.

SPME extraction is based on an equilibrium process, where analytes distribute between the polymeric coating of the fiber and the sample. Two different types of processes are involved in SPME, depending on characteristics of the fiber utilized for the extraction. The most widely used poly(dimethylsiloxane) (PDMS) is a liquid coating. Although it looks like a solid, it is in fact a high viscosity rubbery liquid. Poly(acrylate) (PA) is a solid glassy coating that can turn into liquid at certain desorption temperatures. Both PDMS and PA extract analytes via absorption. The remaining coatings, including PDMS/DVB (divinylbenzene), Carbowax/DVB (CW/DVB), Carbowax/Template Resin (CW/TR) and Carboxen, are mixed coatings, in which the primary extracting phase is a porous solid. Those coatings extract analyte via adsorption rather than absorption. The only common feature is that both processes begin with analyte molecules getting attached to the surface of the coating. However, in absorption, analytes stick on the coating

surface and then diffuse into the bulk of it during the extraction process, while in adsorption they stay on the surface of the solid (42).

Absorption (PDMS and PA fibers) is a non-competitive process. Therefore, the composition of the matrix generally does not affect the extraction. Exhaustive extraction can be accomplished only when the volume of a sample is small and the analyte has a very high affinity towards the fiber coating (39). At equilibrium, the amount of analyte extracted ( $n_f$ ) by an absorption-type SPME in a two-phase system of limited sample volume only depends on the fiber/sample partition coefficient ( $K_{fs}$ ), the volumes of the fiber coating and the sample ( $V_f$  and  $V_s$ , respectively), and the initial concentration of the analyte in the sample ( $C_0$ ), as illustrated in Equation 1.1.

$$n_f = \frac{K_{fs} V_f C_0 V_s}{K_{fs} V_f + V_s} \quad \text{Equation 1.1}$$

When a large volume is sampled, or  $K_{fs}$  is very small (i.e.  $V_s \gg K_{fs} V_f$ ), which means that the analyte has low affinity towards the fiber, the system can be described by Equation 1.2, where the amount of the analyte ( $n_f$ ) absorbed by the SPME fiber is proportional to the partition coefficient ( $K_{fs}$ ), fiber volume ( $V_f$ ) and initial concentration of the analyte in the sample ( $C_0$ ):

$$n_f = K_{fs} V_f C_0 \quad \text{Equation 1.2}$$

For a three-phase system (sample-headspace-coating), the mass of the analyte extracted by the polymeric coating is related to the overall equilibrium of the analyte. The mass of the analyte absorbed by the coating,  $n_f = C_f^{\infty} V_f$ , can be expressed as:

$$n_f = \frac{K_{fh} K_{hs} V_f C_0 V_s}{K_{fh} K_{hs} V_f + K_{hs} V_h + V_s} \quad \text{Equation 1.3}$$

where  $C_f^\infty$  is the equilibrium concentration of the analyte in the coating;  $V_h$  is the headspace volume. The coating/gas distribution constant was defined as

$K_{fh} = C_f^\infty / C_h^\infty$  and the gas/sample matrix distribution constant as  $K_{hs} = C_h^\infty / C_s^\infty$ , where  $C_h^\infty$  and  $C_s^\infty$  are the equilibrium concentrations of the analyte in the headspace and the sample solution, respectively;

The equilibrium theory developed for the liquid PDMS coating does not apply to the adsorption-type coatings. The theoretical description of the extraction process for this type of fiber was described by Górecki *et al.* (43). The model was based on the Langmuir adsorption isotherm. In general, there is a non-linear correspondence between the amount of an analyte extracted by the fiber and its concentration in the sample. Their dependence can only be approximated by a straight line at sufficiently low concentrations.

Adsorption is a competitive process. Therefore, the matrix composition can significantly affect the amount extracted. Interference compounds co-extracted with the analyte of interest may reduce the amount of analyte extraction and its quasi-linear range of the response. Therefore, great care should be exercised when performing quantitative analysis with porous polymer SPME fibers.

#### **1.1.4 SPME/HPLC Interface**

While the majority of the work to date on drug analysis by SPME has focused on GC (gas chromatograph) or GC/MS (mass spectrometry) analysis, the use of SPME coupled to HPLC and LC/MS is gaining more attention. There are two modes by which SPME can be coupled to HPLC: conventional fiber coupling and the more recent in-tube SPME. With the conventional fiber coating, analysts are currently limited to performing

manual extractions and desorptions. However, for automated extraction and analysis, in-tube SPME is much simpler to implement.

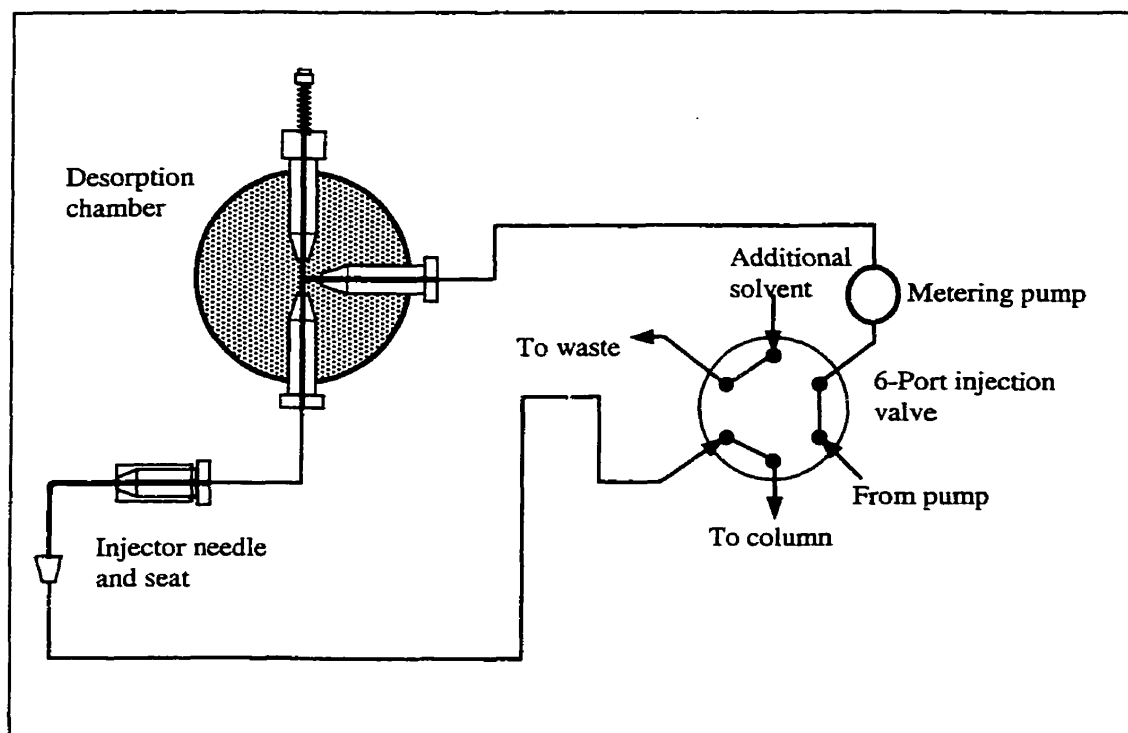


**Figure 1.2:** Schematic of fiber SPME interface for SPME/LC and SPME/LC/MS using Hewlett-Packard HP1100 LC/MS.

A schematic of the conventional fiber couplings is shown in Figure 1.2. In this interface, a three-way tee is used, with two of the ports connected in the position of the sample loop. The third position, a finger-tight fitting which compresses a standard 0.4 mm i.d. GC ferrule around the inner stainless steel tube of the fiber assembly, gives a convenient port to introduce the fiber to fluid flow for analyte desorption. Depending on the type of the analytes, sample desorption may be accomplished using only the flow of HPLC mobile phase, if the desorption process is fast enough to provide a sharp peak. Otherwise, another desorption solvent may be introduced to the interface to aid the



desorption. The desorbed analyte solution will be transferred to the column via the HPLC mobile phase. In order to achieve acceptable performance, it is important to select a tee with sufficiently small internal diameter to allow a high linear flow rate of mobile phase to pass the fiber, and to allow the analyte be desorbed into as small a volume of liquid as possible.

For in-tube SPME, a section of fused silica GC column, which has been internally coated with an appropriate material, is placed between the injection loop and the injector needle of the HPLC autosampler. In this technique, organic compounds in aqueous samples are extracted directly from the sample into the internal capillary coating. All the capillary connections were facilitated with PEEK sleeve tubings of appropriate i.d. over the ends of the capillary, and then adding standard stainless steel fittings and ferrules. A schematic of this arrangement, as incorporated into Hewlett-Packard 1100 LC system, is shown in Figure 1.3.

In the early research, sections of standard commercial GC capillaries, primarily PDMS and poly(ethylene glycol) based phases have been employed. Recently the conducting polymer polypyrrole (PPY) was coated on the inside wall of the capillary and used for the drug analysis (44). In this thesis, the characteristics of an antibody coating (both in SPME fiber and in-tube SPME) have been investigated.

During extraction (as shown in Figure 1.3(a)), sample solution is aspirated from the sample vial to the capillary, and then dispensed back into the sample. This process is repeated until either an equilibrium been accomplished, or sufficient amount of analyte has been extracted to achieve the desired sensitivity.

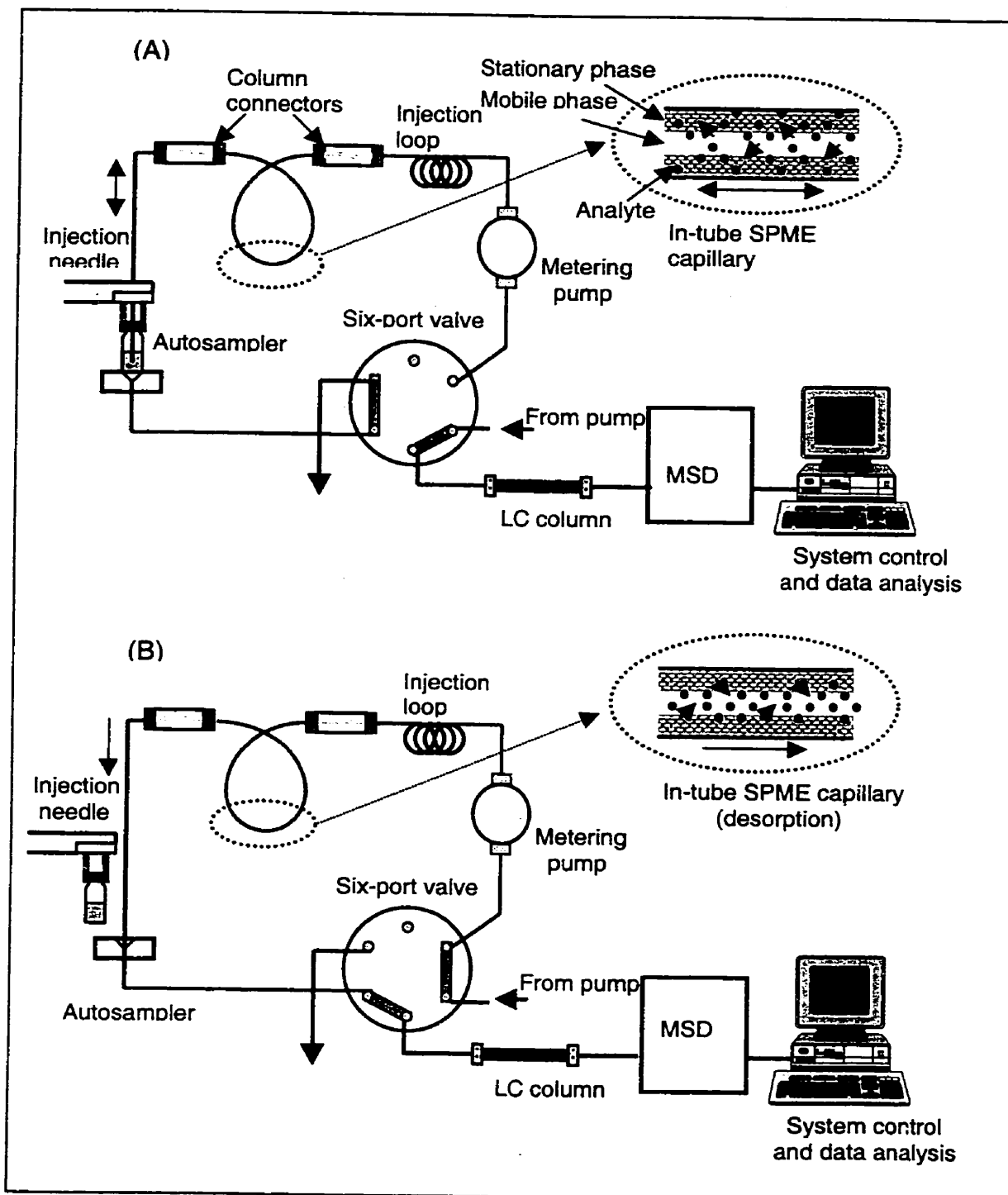


**Figure 1.3:** Configuration of the in-tube SPME using Hewlett-Packard HP1100 LC/MS.

(A) Extraction process; (B) Desorption process.

Compared with the conventional fiber coupling, in-tube SPME is an easy and automatic sample extraction technique. Due to its larger inner surface area to contact with the sample solution, in-tube SPME normally has a higher sensitivity than the conventional fiber coupling. GC capillary was selected so that it would withstand the aggressive HPLC conditions. The possible selections of coating materials have been greatly enhanced, especially for highly polar compounds. In-tube SPME has been applied to many cases of drugs and pesticides analysis. Kataoka and Pawliszyn *et al.* utilized automated in-tube SPME coupled with Liquid Chromatography/Electrospray Ionization Mass Spectrometry (LC/ESI/MS) to determine  $\beta$ -blockers and metabolites in urine and serum samples (45). Other compounds, such as heterocyclic amines (46), ranitidine (47), amphetamine, methamphetamine and their methylenedioxy derivatives (48) and carbamate pesticide (49-51), have also been analyzed by this method.

### **1.1.5 Detection Methods Coupled with SPME**

SPME was initially developed for the volatile organic compound analysis. Its syringe-like configuration is very convenient for the GC injection. In SPME, the high temperature carrier gas flow in the injector port of a GC system is the driving force for the analyte desorption, as Figure 1.4 illustrated. The volatile organic compounds could be readily analyzed by GC or GC/MS.

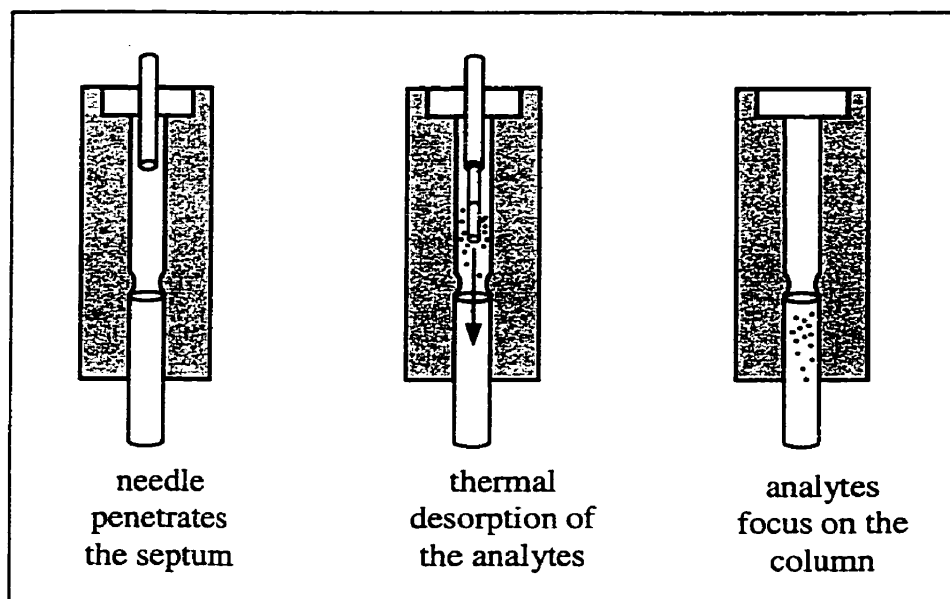


**Figure 1.4:** Septum-equipped temperature programmable injector (SPI) interface.

An SPME/HPLC interface was then developed for semi- or non-volatile, polar organic compounds, such as various drugs and pesticides, analysis. Recently, with the progress of the development of LC/MS, SPME coupled with LC/MS has been used in many applications (44-51). By sampling ions directly from solution in mass spectrometric analysis, the electrospray technique provides a simultaneous logical coupling of solution introduction of compound and the facility for ionization of highly polar and nonvolatile compounds. Therefore, compared to the conventional mass spectrometer, LC/ESI/MS features much higher sensitivity and lower detection limits. Recently, the direct coupling of SPME and ESI/MS has also been investigated by Mester *et al.* (52).

## 1.2 Considerations in Biological Sample Analysis

Biological samples are frequently encountered in pharmaceutical, clinical, and forensic analyses. Therefore, analysis of drugs in biological liquids is a very important subject. A biological fluid is not a simple mixture, but a very complex one containing many different components, which may subtly interact and hence contribute to some interference during the analysis. For example, interferences may elevate or mask the analyte response or alter the actual values by degradation.

Two important biological matrices encountered are plasma and urine. The chief feature of plasma and serum to the analysts is the presence of a large amount of protein. Obviously, the proteins themselves are chemically and physically different from the small drug molecule normally being measured. However, there is often a strong affinity between such proteins and drugs. Straightforward removal of protein by means of ultrafiltration or dialysis could also remove a large fraction of the drug. Therefore, any direct measurement of drug could miss the "total" drug present in the sample and only measure the "free" drug component. This problem can be solved by destroying the binding of drug to protein, followed by extracting the total drugs for analysis. Many methods have been investigated for this purpose (53). On the other hand, the measurement of "free" drug and the affinity of drug to protein is a fundamental problem in pharmacokinetics as well as in metabolism analysis. In such applications, considerations should be given to prevent the drug-protein binding equilibrium from being interfered with, in any procedures.

Unlike plasma or serum, urine is generally free of protein and lipids and therefore can usually be extracted directly with an organic solvent. However, urine does have a

wide variation in its gross composition, which depends very largely on the diet, and this can account for a quite startling range of colors. The normal types of compound found in urine are water-soluble small organic compounds, which have similar properties to the drug compounds. The greatest difficulty arises because these water-soluble compounds could be extracted together with the drug and interfere with the analysis.

Drug analysis can be subsequently classified as two aspects: drug confirmation and concentration analysis, and drug-protein binding analysis. Many methods have been used for drug confirmation and concentration analysis in biological samples, such as GC, HPLC, radioimmunoassay and other analytical methods. A suitable method should be chosen according to the properties of the analyte, and the requirements of the analysis.

Many techniques have been applied in drug-protein binding study, including equilibrium dialysis, ultrafiltration, gel filtration, and many other methods (54).

In this thesis, SPME is investigated as an alternative method for drug analysis in both of these two aspects. Compared with the previously mentioned methods, SPME is simpler, more efficient and effective.

### **1.3 Difficulties in Biological Sample Analysis by SPME**

To date, most of the methods published in biological sample analysis by SPME are still at their preliminary method optimization stage. The main difficulty arises from the complexity of the biological fluid matrices and the fact that most of the biologically active species are polar and non-volatile organic compounds. For the absorption-type SPME coatings, compounds other than the analyte of interest can be coextracted and interfere with the analysis. For adsorption type coating, the coextraction will not only

interfere with the chromatography, but also reduce the sensitivity due to the competition for the adsorption sites.

One way to overcome this difficulty is to develop a type of coating that has high selectivity to the analyte of interest. The extraction of other compounds presented in the system is highly inhibited since they do not have the specific binding to the coating material. The feasible candidates for such kind of the coating include antibodies (Ab) and molecularly imprinted polymers (MIPs), which have been studied in this thesis.

#### **1.4 Molecular Recognition Materials**

The ability to selectively recognize a target analyte, known as molecular recognition, is very useful in the development of rapid and sensitive analytical methods (55). Molecular recognition depends on non-covalent forces. Due to the immense numbers of the binding interactions and the variety of non-covalent interactions, unlimited capacity for recognition at the molecular level is possible. The challenge for the modern analytical chemist is the enhancement of analyte selectivity. Complex matrices, such as biological samples, often require time-consuming and error-prone cleanup steps to remove interferents prior to analysis. Although commercially available solid phase adsorbents provide sample pretreatment solutions, they impart little analyte selectivity. Research in natural and alternative molecular recognition techniques is becoming more and more important to the progress of health care and environmental studies.

In classical bioanalytical techniques, the selective recognition elements are antibodies. They are the most common recognition structures in practical use today. The versatility was demonstrated by their use in therapeutics, diagnostic assays and

purification systems. Immunoassay employs antibodies for the determination of sample components. The selective binding nature of the antibodies with antigens allows the compounds to be employed in the development of immunoassay methods that are highly specific and that can often be used directly with even complex biological matrices such as blood, plasma, or urine (56).

Alternatives to natural recognition elements for chemical analysis are desired. To date, the most successful approach for producing synthetic recognition sites has been the technique of molecular imprinting. The imprinted polymer material is composed of a three-dimensional network that has memory of the shape and functional group positions of the template molecule. It has offered new possibilities for sensor technology as well for use in solid phase extraction (SPE) materials (57-59).

### **1.5 Objectives of the Thesis**

The major objective of this thesis is to establish SPME as a viable tool for biological sample analysis. The research presented in this thesis consists of two aspects. The first aspect is the drug-protein binding study by SPME, based on the fact that SPME extraction is an equilibrium process and the amount of the analyte partitioned onto the SPME fiber reaches equilibrium only with the free form of the analyte in the solution. The introduction of dissolved protein as a “pseudo phase” to the solution certainly makes the system more complicated. It is demonstrated that SPME is an alternative method, which is accurate and simple, to investigate the protein binding phenomenon based on the understanding of the thermodynamic and kinetic properties of SPME.



The second aspect of the research is to identify and validate selective coatings for SPME in complex matrix analysis. Two materials have been investigated: antibody, a molecular recognition material that exists in nature, and molecularly imprinted polymer (MIP), which is a synthesized material having molecular recognition ability. This part of the work is mainly presented in Chapter 3 and Chapter 4. In Chapter 3, the antibody was investigated for the fiber SPME as well as in-tube SPME extraction. In Chapter 4, MIP is employed for SPME analysis.

As an integrated part of this thesis, benzodiazepines are analyzed with in-tube SPME by commercial extraction capillary with LC/ESI/MS. This work is presented in Chapter 5.

Finally, an overall summary of the scientific advancement from the compiled work presented herein and possible future work are provided in Chapter 6.

## 1.6 References

---

1. Arthur, C. L.; Pawliszyn, J. *Anal. Chem.*, **1990**, 62, 2145-2148.
2. Potter, D. W.; Pawliszyn, J. *J. Chromatogr.*, **1992**, 625, 247-255.
3. Louch, D.; Motlagh, S.; Pawliszyn, J. *Anal. Chem.*, **1992**, 64, 1187-1199.
4. Pawliszyn, J. *Application of Solid Phase Microextraction*. RSC, Cornwall, UK, **1999**.
5. Arthur, C. L.; Killam, L. M.; Motlagh, S.; Lim, M.; Potter, D. W.; Pawliszyn, J. *Environ. Sci. Technol.* **1992**, 26, 979-983.
6. Wittkamp, B.L.; Tilotta, D.C. *Anal. Chem.* **1995**, 67, 600-605.
7. Arthur, C. L.; Pratt, K.; Motlagh, S.; Pawliszyn, J.; Belardi, R. P. *J. High Resolut. Chromatogr.* **1992**, 15, 741-748.
8. Langenfeld, J. J.; Hawthorne, S. S.; Miller, D. J. *Anal. Chem.* **1996**, 68, 144-155.
9. Nilsson, T.; Ferrari, F.; Facchetti, S.; *Proc. 18<sup>th</sup> Int. Symp. on Capillary Chromatogr.* Riva Del Garda (Italy), May 20-24, **1996**, 618.
10. Potter, D.; Pawliszyn, J. *Environ. Sci. Technol.* **1994**, 28, 298.
11. Chai, M.; Arthur, D.; Pawliszyn, J.; Belardi, R. P.; Pratt, K. F. *Analyst*, **1993**, 118, 1501-1505.
12. Boyd-Boland, A. A.; Pawliszyn, J. *J. Chromatogr.* **1995**, 704, 163-172.
13. Eisert, R.; Levsen, K.; Wuensch, G. *J. Chromatogr.* **1994**, 683, 175-183.
14. Popp, P.; Kalbitz, K.; Oppermann, G. *J. Chromatogr.* **1994**, 687, 133-140.
15. Eisert, R.; Levsen, K. *Fresenius J. Anal. Chem.* **1995**, 351, 555-562.
16. Graham, K. N.; Sarna, L. P.; Webster, G. R. B.; Gaynor, J. D.; Ng, H. Y. F. *J. Chromatogr.* **1996**, 725, 129-136.

17. Magdic, S.; Pawliszyn, J. *J. Chromatogr.* **1996**, 723, 111-122.
18. Górecki, T.; Mindrup, R.; Pawliszyn, J. *Analyst*, **1996**, 121, 1381-1386.
19. Buchholz, K.; Pawliszyn, J. *Environ. Sci. Technol.* **1993**, 27, 2844.
20. Buchholz, K.; Pawliszyn, J. *Anal. Chem.* **1994**, 66, 160-167.
21. Schaefer, B.; Engewald, W. *Fresenius J. Anal. Chem.* **1995**, 352, 535-536.
22. Pan, L.; Adam, M.; Pawliszyn, J. *Anal. Chem.* **1995**, 67, 4396-4403.
23. Górecki, T.; Pawliszyn, J. *Anal. Chem.* **1996**, 68, 3008-3014.
24. Yu, X.; Yuan, H.; Górecki, T.; Pawliszyn, J. *Anal. Chem.* **1999**, 71, 2998-3002.
25. Kumazawa, T.; Lee, X.-P.; Tsai, M.-C.; Seno, H.; Ishii, A.; Sato, K. *Jpn. J. Forensic Toxicol.*, **1995**, 13, 25-30.
26. Lee, X.-P.; Kumazawa, T.; Sato, K.; Suzuki, O. *Chromatogr. Sci.*, **1997**, 35, 302-308.
27. Moffat, A. C.; Jackson, J. V.; Moss, M. S.; Widdop, B. *Clark's Isolation and Identification of Drugs*, Pharmaceutical Press, London, England, **1986**.
28. Ulrich, S.; Martens, J. *Chromatogr. B.*, **1997**, 696, 217-234.
29. Seno, H.; Kumazawa, T.; Ishii, A.; Nishikawa, M.; Watanabe, K.; Hattori, H.; Suzuki, O. *Jpn. J. Forens. Toxicol.*, **1996**, 14, 30-33.
30. Seno, H.; Kumazawa, T.; Seno, H.; Watanabe, K.; Hattori, H.; Suzuki, O. *Jpn. J. Forens. Toxicol.*, **1997**, 15, 16-19.
31. Kumazawa, T.; Lee, X.-P.; Sato, K.; Seno, H.; Ishii, A.; Suzuki, O. *Jpn. J. Forensic Toxicol.*, **1995**, 13, 182-188.
32. Kumazawa, T.; Sato, K.; Seno, H.; Ishii, A.; Suzuki, O. *Chromatographia*, **1996**, 43, 59-62.

33. Seno, H.; Kumazawa, T.; Ishii, A.; Nishikawa M.; Hattori, H.; Suzuki, O. *Jpn. J. Forensic Toxicol.*, **1995**, 13, 211.
34. Lord, H.; Pawliszyn, J. *Anal. Chem.*, **1997**, 69, 3899-3906.
35. Kumazawa, T.; Watanabe, K.; Sato, K.; Seno, H.; Ishii, A.; Suzuki, O. *Jpn. J. Forensic Toxicol.*, **1995**, 13, 207-210.
36. Ishii, A.; Seno, H.; Kumazawa, T.; Watanabe, K.; Hattori, H.; Suzuki, O. *Chromatographia*, **1996**, 43, 331-314.
37. Ishii, A.; Seno, H.; Guan, F.; Watanabe, K.; Kumazawa, T.; Hattori, H.; Suzuki, O. *Jpn. J. Forensic Toxicol.*, **1997**, 15, 189-132.
38. Nishikawa M.; Seno, H.; Ishii, A.; Suzuki, O.; Kumazawa, T.; Watanabe, K.; Hattori, H. *Chromatogr. Sci.*, **1997**, 35, 275-279.
39. Pawliszyn, J. *Solid Phase Microextraction: Theory and Practice*. Wiley-VCH, Inc.: New York, **1997**.
40. Louch, Y.; Pawliszyn, J. *J. Micro. Sepa.*, **1994**, 6, 443-448.
41. Zhang, Z.; Pawliszyn, J. *Anal. Chem.*, **1993**, 65, 1843-1852.
42. Górecki, T.; Pawliszyn, J. *Applications of Solid Phase Microextraction*. RSC, Cornwall, UK, **1999**, Chapter 7.
43. Górecki, T.; Yu, X.; Pawliszyn, J. *Analyst*, **1999**, 124, 643-649.
44. Wu, J. C.; Lord, H.; Pawliszyn, J.; Kataoka, H. *J. Micro. Sepa.*, **2000**, 12, 255-266.
45. Kataoka, H.; Narimatsu, S.; Lord, H.; Pawliszyn, J. *Anal. Chem.* **1999**, 71, 4237-4244.
46. Kataoka, H.; Pawliszyn, J. *Chromatographia*, **1999**, 50, 532-538.
47. Kataoka, H.; Lord, H.; Pawliszyn, J. *J. Chromatog. B*, **1999**, 731, 353-359.

48. Kataoka, H.; Lord, H.; Pawliszyn, J. *J. Anal. Toxicol.*, **2000**, 24, 257-265.
49. Gou, Y.; Pawliszyn, J. *Anal. Chem.*, **2000**, 72, 2774-2779.
50. Gou, Y.; Eisert, R.; Pawliszyn, J. *J. Chromatogr. A*. **2000**, 873, 137-147.
51. Gou, Y.; Tragas, C.; Lord, H.; Pawliszyn, J. *J. Micro. Sepa.*, **2000**, 12, 125-134.
52. Mester, Z.; Lord, H.; Pawliszyn, J. *J. Chromatogr. A*, **2000**, 880, 35-62
53. Chamberlain, J. *The Analysis of Drugs in Biological Fluid*, CRC Press, Inc., **1995**
54. La Du, B. N.; Mandel, H. G.; Way, E. L. *Fundamentals of Drug Metabolism and Drug Disposition*, The William & Wilkins Company, **1971**, 67.
55. Mullett, W. M. *Ph.D. Thesis*, Carleton University, **2000**, 2-6.
56. Hage, D.S. *Anal. Chem.*, **1999**, 71, 294R-304R.
57. Kriz, D.; Ramstrom, O.; Mosbach, K. *Anal. Chem.*, **1997**, 69, 345A-349A.
58. Owens, P. K.; Karlsson, L.; Lutz, E.S.M.; Andersson, L.I. *Trends Analy. Chem.*, **1999**, 18, 138-145.
59. Vlatakis, G.; Andersson, L. I.; Muller, R.; Mosbach, K. *Nature*, **1993**, 361, 645-647.

## **CHAPTER 2**

# **APPLICATION OF SPME TO THE STUDY OF PROTEIN-LIGAND INTERACTIONS**

### **2.1 Introduction**

#### **2.1.1 Definition and Significance**

Drug binding is a reversible interaction between a drug molecule and a protein or other macromolecules. It is analogous to the enzyme-substrate interaction, except that the complex does not decompose to yield new products; it is also analogous to most drug-receptor complexes, unless they involve covalent bonding (1).

The process of drug transformation and drug storage usually involves the binding of a drug to the relative protein. The fate of a drug in the body is controlled by protein interactions.

As shown in Figure 2.1, the importance of the drug-protein binding study lies in three aspects. The first is the investigation of possible multiple binding interactions of a drug in the blood. Although serum albumin is the main protein binding to drugs in the blood, many other components and proteins, as well as cells, can also bind drugs. Therefore, to study drug binding is important for us to know the distribution and biotransformation pathways of the drug.

The second aspect is the pharmacokinetic consequence of drug binding in blood. Drug binding can modify the apparent distribution volume, facilitate or prevent cell penetration or govern the elimination clearance. Therefore, drug-protein binding study

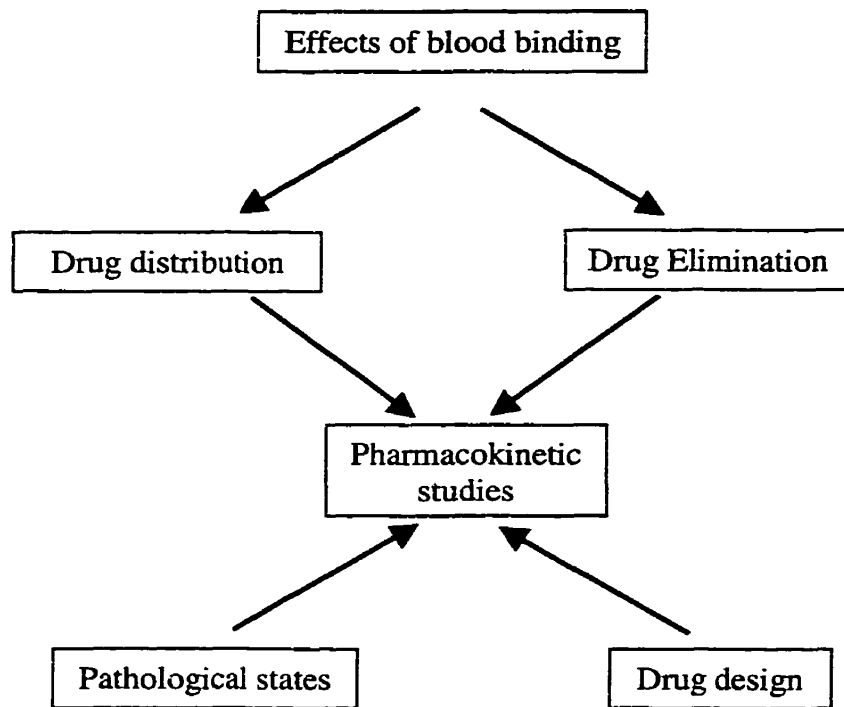


**Figure 2.1:** A schematic diagram representing the pharmacokinetic consequences of drug binding in blood.

has implications for pathology since binding may be modified in disease state, due to changes in nature or amount of protein, dehydration, or alteration of pH.

The third aspect is that the bound drug complex is of high molecular weight and is unavailable for tissue membrane transport. Only the unbound drug is capable of diffusing across tissue membranes to reach the target site (2). Therefore, only the free drug is considered to be pharmacologically active. If the bound drug is rapidly dissociable, the rate of transport will not be greatly affected since the free drug passing a membrane could be immediately replaced by newly dissociated drug. However, not all dissociations are so rapid. Therefore, the stability of the bound form must be analyzed (3). This will affect the process of drug design.

Among the plasma proteins, serum albumin is undoubtedly the most important carrier for drugs and other small molecules. Therefore, the attention of many scientists has been drawn to the phenomenon of the interactions between drugs and serum albumin. Because of the relative ease of the experiments, most standard binding assays use serum albumin.

### **2.1.2 Techniques Used for the Measurement of Drug-Protein Binding**

*Equilibrium Dialysis.* Equilibrium dialysis is a very commonly used procedure for the protein binding studies. The method involves equilibration of a given volume of protein solution within a dialysis bag with a known volume of drug solution. Once equilibrium has been attained, measurement of the free drug concentration outside the bag will permit the calculation of the amount of drug, which has been taken up by the protein. The equilibrium dialysis technique is very simple and convenient for multiple samples. Drawbacks include time-scale: the period of 12 hours or more is required to obtain equilibrium, permitting possible decomposition of unstable compounds. While these problems may be minimized by carrying out the experiments at lower temperatures, binding will thereby be altered. Often compounds will bind not only to the glass containers, but also, to a greater degree, to the dialysis bag. This can be a serious problem particularly for highly lipophilic drugs. Appropriate controls without protein should be run to detect such problems. Additionally, significant overestimation of the free fraction can result from even a slight leakage of protein into the dialysate. Thus, the postdialysis stability of protein and its absence from the dialysate should be confirmed by protein assay in a validation study.



*Ultrafiltration.* Ultrafiltration has been introduced widely for routine free drug monitoring in clinical laboratories (1). If a solution of drug and protein is exposed under pressure to a dialysis membrane, the protein-free filtrate containing free drug only will be collected beyond the membrane. Knowing the initial concentration of the drug present, and of that in the ultrafiltrate, will permit the calculation of the appropriate protein binding parameters. Compared with equilibrium dialysis, this method offers significant advantages such as its short analysis time, simplicity, commercially available kits and the lack of dilution effects.

Ultrafiltration is faster than equilibrium dialysis since the drug is initially in direct contact with the protein. However, it is perhaps not so readily adapted for large numbers of samples, and uses somewhat more expensive and complicated apparatus. An important reservation is that a portion of the aqueous phase is forced away from the protein and the latter solution becomes more concentrated, thereby tending to increase binding. If the amount of solution removed by filtration is a relatively small portion of the whole, such concentration change is quite small.

*Gel Filtration.* Gel filtration is a very popular technique for measuring protein binding (1). In this technique, a solution of drug and protein passes through a column containing dextran molecular exclusion gel. The protein-bound drug is separated from the free drug by emerging before the free drug peak.

If the equilibrium between bound and free drug is rapidly reversible, this simple approach would not be appropriate. One would expect that the molecules of bound drug should dissociate as the protein-drug complex begins to separate from the free drug and that the drug should emerge from the column as a smear rather than a discrete peak.

Nevertheless in certain cases, such as salicylate binding (4), the binding survives. This suggests that the equilibrium constant is so great that the amount of drug, which dissociates is not readily detectable.

*Chromatographic Methods.* Despite the fact that chromatographic methods have been used for a long time for the determination of drug-protein binding parameters, they have earned only limited attention. In recent years, progress in chromatographic technology has led to the development of highly automated systems yielding high resolution on small columns, allowing shorter analytical times, consuming less chemicals and avoiding the use of radio labeled-ligands. In general, binding data obtained by chromatographic methods offers much higher precision and reproducibility than those measured by the previously described methods.

The most widely used chromatographic method is affinity chromatography. This method provides the possibility to detect very small differences in the binding affinity of ligands. Originally designed for the isolation and purification of biologically active compounds, the introduction of HPLC stationary phase materials with immobilized biopolymers (enzymers, receptors, ion channels, or antibodies) provided a powerful tool for studying the interactions of small ligands and biomacromolecules. The advantages of these approaches are represented particularly by the stability and constant binding behavior of immobilized biopolymers, the precision and reproducibility of the chromatographic system, and the effectiveness of using a small amount of ligands. However, because column preparation is a very time consuming process and column life is normally short, these methods are inconvenient.

*Miscellaneous Methods.* Many other methods have been employed in measuring the binding parameters. Differential spectrophotometry takes advantage of the fact that the bound form of the drug will exhibit an absorption spectrum that is unlike that of the free drug (1). The magnitude of such an absorption peak can be used as a measure of drug binding.

The degree of binding could also be determined from changes in electro-magnetic field (EMF), conductivity, vapor pressure, boiling point, freezing point and osmotic pressure, which depend on the interactions of substances and proteins.

Since only the unbound form of a drug can exert antibacterial or other biological action, bioassays that measure the differences in the activity of a drug in the presence or absence of protein can also be used as methods for determination of the binding affinity.

### **2.1.3 Evaluation of the Binding Data**

One of the predominant values measured in a protein binding study is the free drug concentration. Knowing the total concentration of the drug and protein and the concentration of the free drug, the percentage of the drug bound can be calculated. Experimental observations show that a high percentage of the drug is bound at low concentrations. If an accurate concentration of a pure protein solution can be prepared, and measurements are made at several concentrations of drug, more meaningful treatments can be employed to determine: the number of classes of identical binding sites; the number of binding sites of each class; and the corresponding equilibrium constant for each class.

Binding is commonly considered as a simple reversible reaction.



where  $[P]$  is the free protein concentration;  $[D]$  is the free drug concentration;  $[PD]$  is drug-protein complex concentration. At equilibrium, it will have the equilibrium constant ( $K$ ):

$$K = \frac{[PD]}{[P][D]} \quad \text{Equation 2.2}$$

Therefore,

$$[PD] = K[P][D] \quad \text{Equation 2.3}$$

and the quantity  $r$  may be defined as

$$\begin{aligned} r &= (\text{moles of drug bound}) / (\text{total moles of protein}) \\ &= \frac{[PD]}{[PD] + [P]} = \frac{K[P][D]}{K[P][D] + [P]} = \frac{K[D]}{1 + K[D]} \end{aligned} \quad \text{Equation 2.4}$$

If there are a number ( $N$ ) of identical independent sites, a series of independent equations can be written and summed:

$$r_1 + r_2 + \dots + r_N = r_{(total)} = \frac{NK[D]}{1 + K[D]} \quad \text{Equation 2.5}$$

There is often more than one type of site on a given protein, each with its own equilibrium constant, so that a more general form of the equation 2.5 is:

$$r_{(total)} = \frac{N_1 K_1 [D]}{1 + K_1 [D]} + \frac{N_2 K_2 [D]}{1 + K_2 [D]} + \dots + \frac{N_n K_n [D]}{1 + K_n [D]} \quad \text{Equation 2.6}$$

This is an equation for a hyperbola. The value of  $[D]$  may be measured and  $r_{(total)}$  calculated from the free and total drug concentration and protein concentration. The data may then be plotted in several ways so as to determine the values of  $N$  and  $K$ .

*Scatchard Method.* The most commonly used method to analyze the binding data and determine the values of  $N$  and  $K$  is Scatchard's method (5), which plots  $r/[D]$  vs.  $r$ . The advantage of this method is that both the low values and high values of  $1/r$  spread well.

By rewriting Equation 2.5

$$r + rK[D] = NK[D] \quad \text{Equation 2.7}$$

and by rearranging

$$r/[D] = NK - rK \quad \text{Equation 2.8}$$

where the y-intercept =  $NK$ , slope =  $K$  and x-intercept =  $N$ .

While certain substances yield straight line plots, curvilinear plots can also be obtained, in some cases. This indicates that there are at least two classes of binding sites. Such curves may be fitted as the summation of two or more straight lines, each due to a different class of binding site. In such cases, computer programs are normally used to analyze the data (6).

The above derivations assume that binding sites of a given class are independent of each other and that binding of the first molecule does not affect that of subsequent molecules. While this appears to be generally true, there are some recognized examples, such as the binding of oxygen to hemoglobin, where pronounced interactions do occur (7), i.e. cooperative binding.

It is obvious that the binding of a charged molecule alters the over-all electrostatic environment of the macromolecule, which increases the difficulty of adding another similar ion. If the experiments are carried out in buffer, this problem will be more obvious. On the other hand, the competition between drug and buffer ion for the same

site may produce much greater changes in the degree of association. An alteration in pH can also affect the overall charge on the drug, as well as the charge on individual amino acids on the protein, thereby affects the drug interaction. Binding experiments conducted in distilled water will avoid the competition problem, but bear little relationship to the physiological situation.

## 2.2 Study of Alkylbenzenes Binding to Bovine Serum Albumin by SPME

### 2.2.1 Background

#### 2.2.1 General Introduction

Small chain alkylbenzenes are a class of toxic, volatile organic compounds. The physical-chemical properties, such as boiling point (B.P.) and vapor pressure (V.P.), of the compounds used in this study are listed in Table 2.1. Since these analytes are volatile organic compounds, headspace SPME would be suitable for their analysis. The introduction of dissolved protein into the solution as a pseudo-phase certainly increases the complexity of the system. The system changes from a three-phase system (sample-headspace-coating) to a four-phase system (sample-dissolved protein-headspace-coating).

**Table 2.1:** Summary of physical-chemical properties of the target compounds.

| Analyte         | Formula /<br>MW                       | B. P. (°C) | V.P. (mm Hg) (20°C) |
|-----------------|---------------------------------------|------------|---------------------|
| Benzene         | C <sub>6</sub> H <sub>6</sub> / 78    | 80         | 75                  |
| Toluene         | C <sub>7</sub> H <sub>8</sub> / 92    | 111        | 21                  |
| Ethylbenzene    | C <sub>8</sub> H <sub>10</sub> / 106  | 136        | 7                   |
| n-Propylbenzene | C <sub>9</sub> H <sub>12</sub> / 120  | 159        | 2                   |
| n-Butylbenzene  | C <sub>10</sub> H <sub>14</sub> / 134 | 183        | 1                   |

### 2.2.1.2 Headspace GC Method

The conventional methods for the protein binding study, such as dialysis, ultrafiltration and gel filtration, are suitable for the analysis of non-volatile compounds binding to a protein. They are not suitable for studying the analysis of binding of volatile organic compounds to a protein. The headspace GC method could be employed for this purpose (8). This method requires no standard solution of the analyte and no calibration of the GC detector. It only requires that the analyte is volatile enough to be measurable in the headspace and that the detector response is linear.

In reference (8), the partition coefficient of water-hexadecane was determined as an example by headspace GC method. The basic idea behind this method was to measure the analyte concentration change in the vapor phase, which was in equilibrium with a dilute solution of the analyte in water, upon the addition of a known volume of hexadecane. The change is directly related to the partition coefficient of the analyte between water and hexadecane. Obviously, this method can be easily adapted for the study of binding of a volatile organic compound to protein.

For this system, an initial aqueous solution is made and the analyte peak area is measured. Then a given amount of hexadecane is added and the peak area is again measured. From the measured change (ratio) of analyte peak areas, the partition coefficient of the analyte between water and hexadecane can be calculated.

Based on the fact that the mutual solubility of water and hexadecane is very low (the solubility of water in hexadecane is  $2 \times 10^{-3}$  mol/L and that of hexadecane in water



is  $4 \times 10^{-4}$  mol/L), the water-hexadecane system can be regarded as a system containing two pure solvents (if the hexadecane portion is large enough).

The analyte partition coefficient between the headspace and water  $K_{hw}$  is defined as  $K_{hw} = C_h / C_w$ , where  $C_h$  and  $C_w$  are the analyte concentration in headspace and water, respectively. Also one can define the partition coefficient between the headspace and hexadecane ( $K_{h16}$ ) as  $K_{h16} = C_h / C_{16}$ , where  $C_{16}$  is the analyte concentration in hexadecane. Then the partition coefficient between water and hexadecane  $P_{w,16}$  can be determined by  $P_{w,16} = K_{hw} / K_{h16}$ . Suppose the total amount of analyte in the system is  $n_{total}$ , we have:

$$\begin{aligned} n_{total} &= C_h V_h + C_w V_w + C_{16} V_{16} \\ &= C_h (V_h + V_w / K_{hw} + V_{16} / K_{h16}) \end{aligned} \quad \text{Equation 2.9}$$

Therefore, the peak area ratio, which is the same as the ratio of the headspace analyte concentration before and after the hexadecane is added, can be written as

$$\begin{aligned} A^0 / A^f &= C_h^0 / C_h^f \\ &= \frac{V_h + V_w / K_{hw} + V_{16} / K_{h16}}{V_h + V_w / K_{hw}} \\ &\approx 1 + P_{w,16} V_{16} / V_w \end{aligned} \quad \text{Equation 2.10}$$

The superscript  $^0$  and  $^f$  stand for 'initial' and 'final', respectively. The approximation in the above equation is correct only if the amount of analyte in the headspace is only a very small portion, which means  $V_h \ll V_w / K_{hw}$ . From Equation 2.10, we can see that ratio of the analyte peak is linearly proportional to the volume of hexadecane added. Partition coefficient  $P_{w,16}$  can be determined from the plot of the ratio of  $A^0 / A^f$  vs.  $V_{16}$  (8).

The described method can be modified to determine the protein binding parameters. In such a study, the protein is dissolved in the water solution. The protein binding equilibrium constant  $K$  is defined as  $K = \frac{C_b}{C_s \cdot C_p}$ , where  $C_s$ ,  $C_b$  and  $C_p$  are the concentrations of the free drug ( $C_s = n_s/V_s$ ), bound ( $C_b = n_b/V_s$ ) and free protein ( $C_p = n_p/V_s$ ), respectively.

The total amount of analyte in the system  $n_{total}$  can be written as:

$$\begin{aligned} n_{total} &= C_h V_h + C_s V_s + C_b V_s \\ &= C_h (V_h + V_s / K_{hs} + C_p V_s K / K_{hs}) \end{aligned} \quad \text{Equation 2.11}$$

where  $V_h$  and  $V_s$  are the volumes of the head space and solution and  $K_{hs}$  is the partition coefficient of the analyte between the headspace and the water. Therefore, if the amount of analyte in the headspace is negligible ( $V_h \ll V_s / K_{hs}$ ), the peak area ratio can be expressed as:

$$\begin{aligned} A^0 / A^f &= n_h^0 / n_h^f \\ &= \frac{V_h + V_s / K_{hs} + C_p V_s K / K_{hs}}{V_h + V_s / K_{hs}} \approx 1 + C_p K \end{aligned} \quad \text{Equation 2.12}$$

Since the total protein concentration  $C_{p,total}$  is known, the concentration of free protein  $C_p$  can be determined as the following:

$$C_p = C_{p,total} - C_b = C_{p,total} - (C_s^0 - C_s^f)$$

The concentration of free analyte  $C_s^f$  is available from the following relationship:

$$\frac{C_s^f}{C_s^0} = \frac{C_h^f}{C_h^0} = \frac{A^f}{A^0}$$

Therefore,  $C_p$  can be written as

$$C_p = C_{p,total} - (1 - A^f / A^0) \cdot C_s^0 \quad \text{Equation 2.13}$$

From the plot of  $A^0 / A^f$  vs.  $C_p$ , the equilibrium constant  $K$  between the protein and analyte can be determined. The case where the amount of analyte partitioned into the headspace cannot be neglected will be presented in section 2.2.3.6.5.

### 2.2.1.3 Present SPME for Free Concentration Measurement

A few applications have been published using SPME for free concentration measurements in either a phospholipid/water system or a protein/water system (9). The theoretical background of these measurements is that the depletion of analyte from the sample with SPME extraction is so small that it is negligible. In other words, the amount of analyte extracted is insignificant and would not influence the equilibrium among the phases. The assumption that there is a linear correlation between the amount of the analyte on the fiber vs. the total concentration of the analyte added into the system was used. While in most of the cases, this assumption is true, in some cases where analytes have large affinity for the SPME fiber, the validity of this assumption and the method of plotting the calibration curve needs to be verified. This is one of the objectives of the research work described in this chapter.

## 2.2.2 Theory

SPME is based on the overall equilibrium of an analyte among all the phases. The absorption-type fiber is considered in this analysis. The schematic for the SPME headspace sampling from a four-phase system (dissolved protein-sample-headspace-coating) is illustrated in Figure 2.2. In this four-phase system, with the presence of

dissolved protein, the analyte in the solution is actually partitioned into two phases: the analyte freely dissolved in the solution and the analyte bound to the dissolved protein. However, in SPME, the equilibrium is attained for the species in each phase. Therefore, the amount of analyte on the fiber will only reach equilibrium individually

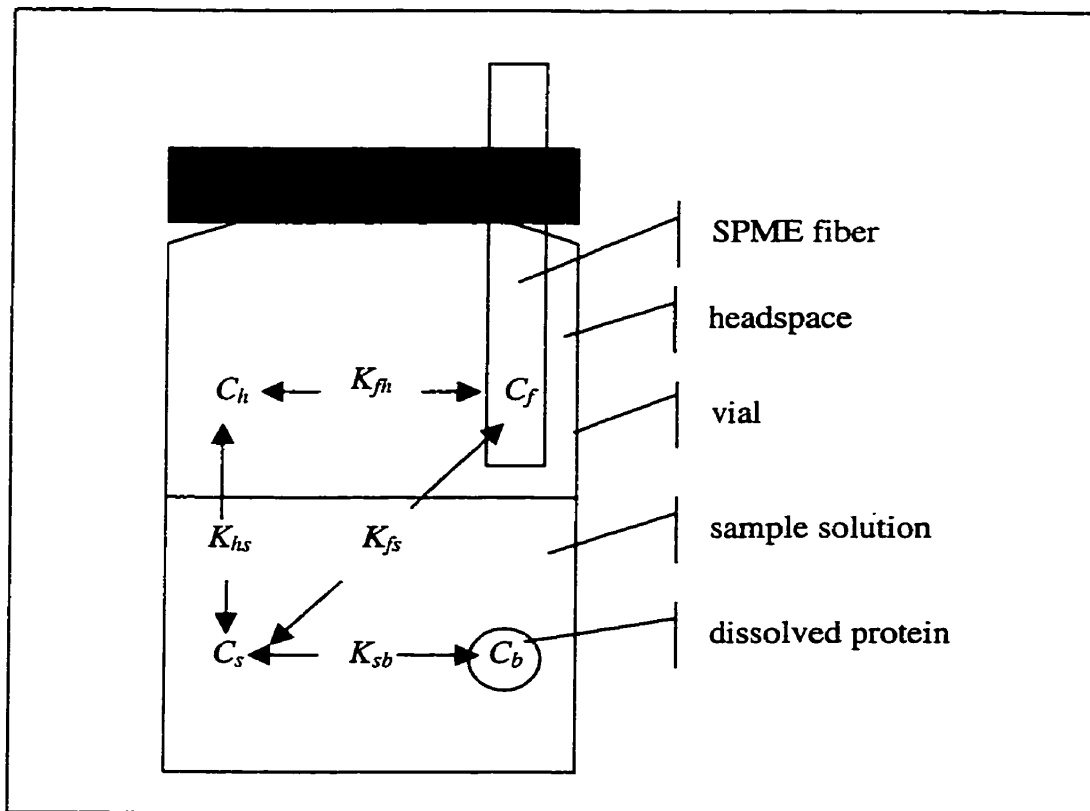


**Figure 2.2:** A schematic diagram of equilibrium in a four-phase system.

with the concentration in headspace, free concentration in solution, and the bound concentration in the solution, which was illustrated in Figure 2.2. It does not reach equilibrium with the sum of free and bound analyte in sample solution.

Since the total mass of the analyte remains the same before and after the extraction, we have:

$$C_0V_s = C_f^\infty V_f + C_h^\infty V_h + C_s^\infty V_s + C_b^\infty V_s \quad \text{Equation 2.14}$$

where  $C_0$  is the initial concentration of the analyte;  $C_f^\infty$ ,  $C_h^\infty$ ,  $C_s^\infty$  and  $C_b^\infty$  are the equilibrium concentrations of analyte in the fiber coating, in the headspace, freely dissolved in solution and bound to dissolved protein respectively. The symbol ' $\infty$ ' and footnote ' $b$ ' stand for 'at equilibrium' and 'bound concentration', respectively. The value of  $C_b^\infty$  is defined as the concentration of the bound drug in the sample solution at equilibrium ( $C_b^\infty = n_b/V_s$ ). The coating/headspace distribution constant is defined as  $K_{fh} = C_f^\infty / C_h^\infty$  and the headspace/ sample matrix distribution constant as  $K_{hs} = C_h^\infty / C_s^\infty$ . Since only the equilibrium states are discussed in this chapter, the symbol ' $\infty$ ' will be omitted in the following discussions unless specified.

To determine the free concentration of the analyte, a calibration curve showing the relationship of the amount of the analyte on the fiber and free analyte concentration in the solution at equilibrium, should be obtained without the protein present. The 'free concentration' here means the actual concentration in the solution since 'free' is relative to the 'bound'. Because there is no protein involved in the calibration step, the word 'free' is used here only for the convenience of further discussion.

The calibration curve should correctly represent the situation where the unknown sample, which is the sample with the dissolved protein, is measured. Since the analyte on the fiber reaches equilibrium with the analyte in each phase individually, theoretically the calibration curve obtained only represents the relationship between the amount of the

analyte on the fiber and free analyte concentration in the solution after the system reaches equilibrium. Therefore, from the calibration curve, we can only measure the free analyte concentration in the solution with protein added at the moment when the equilibrium has been established among the fiber, headspace and solution. We cannot directly measure the initial free analyte concentration, which involves no headspace and SPME fiber. However, that parameter can be indirectly measured if the experimental configurations such as volumes of headspace, sample solution, headspace-fiber partition coefficient, and the protein binding equilibrium constant are known.

In the experiment, the amount of the total analyte in the system was a known value. However, there is always confusion with respect to the meaning of the free concentration used in the calibration curve. The initial analyte concentration spiked into the system is often considered to be the free concentration that reaches equilibrium with the analyte on the fiber. But, this is incorrect, especially in the situation where the analyte is highly volatile and headspace contribution cannot be neglected. The correct interpretation is that only the free analyte, which is the portion of analyte after the amount of the analyte in the headspace and on the fiber have been subtracted from the total concentration, is the portion that reaches equilibrium with the amount of the analyte on the fiber. It is important to realize that this portion of the analyte should be used to construct the calibration curve.

In the calibration step, which is a three-phase system (sample-headspace-fiber), at equilibrium, the mass balance is:

$$n_{total} = n_f + n_h + n_s, \quad \text{Equation 2.15}$$

where  $n_f$ ,  $n_h$  and  $n_s$  are the amount of the analyte on the fiber, in headspace and in the solution, respectively. The amount of the analyte on the fiber  $n_f$  can be obtained from the GC analysis by the fiber injection with the pre-determined GC response factor, which can be obtained from syringe injection. There are two approaches to estimate the amount of the analyte partitioned in the headspace ( $n_h$ ). One method is to calculate it from the  $K_{fh}$  value, which can be obtained from the literature (9). The other method is to calculate it from the Henry's law constant. With the knowledge of  $n_{total}$ , the free analyte in the solution ( $n_s$ ), is easily obtained.

With this calibration curve, the free concentration in the protein binding study can be obtained from the fiber injection of the analyte with the GC system. Once the free concentration is available, the bound concentration of the analyte can be determined by the knowledge of the total concentration, the amount of the analyte on the fiber (obtained from response factor) and in the headspace (calculated by two previously mentioned methods). The equilibrium constant of the analyte protein binding can be calculated from equation 2.2, ensuring that the molar concentration is used.

### 2.2.3 Experimental

*Chemicals and Materials.* Benzene, toluene, ethylbenzene, n-propylbenzene, n-butylbenzene and bovine serum albumin (BSA) (98% purity) were all purchased from Sigma-Aldrich (Mississauga, ON, Canada). After a GC purity check, all chemicals were used as purchased.

The SPME holder and fibers (coated with 30  $\mu\text{m}$  PDMS) were purchased from Supelco (Bellefonte, PA). Fibers were conditioned according to the manufacturer's

instructions under a flowing helium stream in the GC injector before each usage. The 15 mL glass vials and syringes were also purchased from Supelco. A VWR Dylastir hot plate/stirrer (VWR Scientific Canada) was used to agitate the aqueous samples. The 15 mm stir bars were from Fisher Scientific (Nepean, ON, Canada).

Ultra high purity nitrogen and hydrogen gases for flame ionization detection (FID) and helium for the carrier gas were purchased from Praxair (Waterloo, ON, Canada). Air for the flame ionization detector was generated from a Balston (Scotch Plains, NJ) air generator.

*Instrumentation.* All analyses were performed on a Varian (Sunnyvale, CA) GC 3400CX gas chromatograph equipped with 30 m  $\times$  0.25 mm id  $\times$  0.25  $\mu$ m SPB-5 column (Supelco, Bellefonte, PA), a septum-equipped programmable injector (SPI) with SPME insert and FID. The carrier gas was helium (25 psi head pressure).

The column temperature program used in the experiments was 60 °C held for 1 min, increased at 20 °C min<sup>-1</sup> to 120 °C and held for 2 min. In all SPME analysis, the injector temperature was kept at 250 °C. Detector response factors were determined by syringe injection of a standard solution of the alkylbenzenes in methanol, using the following column temperature program: 40 °C held for 1 min, increased at 10 °C min<sup>-1</sup> to 120 °C and held for 1 min. In this experiment, the SPI injector was temperature programmed as follows: 43 °C held for 1 min, increased at 250 °C min<sup>-1</sup> to 250 °C and held for the rest of the run. Liquid CO<sub>2</sub> was used to cool the injector before sample injection.



*Preparation of Buffer and Analytical Mixture.* The pH 7.4 buffer solution was prepared by combining 100 mM disodium hydrogen orthophosphate ( $\text{Na}_2\text{HPO}_4$ ) and 100mM sodium dihydrogen orthophosphate ( $\text{NaH}_2\text{PO}_4$ ) solution with a certain ratio under the monitoring of pH meter. The calibration was performed in this buffer solution. In the protein binding measurement, the protein solution was prepared with this buffer solution and employed for the experiment.

A 1 mg/mL standard mixture of benzene, toluene, ethylbenzene, propylbenzene and butylbenzene each was prepared by adding 10 mg analyte each into a 15 mL vial, which was prefilled with 10 mL methanol. Standard solutions were prepared by dilution of the stock standard with methanol.

#### **2.2.4 Methods**

*Calibration.* All experiments were carried out at 23°C using the set up shown in Figure 2.2. The nominal volume of the vial was 15 mL. The actual volume of the vial was determined by measuring the volume of the water required to completely fill the vial with the stirring bar in it. The volumes of the buffer solution and headspace used were 8 mL and 7.8 mL, respectively. A certain amount of the analyte stock solution was spiked into the buffer solution to give the desired concentration. The vial was mounted on the stirrer plate for agitation. The fiber was inserted into the headspace of the vial to perform the extraction. After each extraction, the fiber was taken out the vial and introduced into the GC injector port for further analysis.

*Protein Binding Analysis.* The same procedure was used in the protein binding measurement, except that the protein buffer solution of the analytes was used instead of the pure buffer solution.

*GC Response Factors.* Syringe injections were used to calibrate the absolute mass of the analytes injected into the GC. By comparing the area count of the syringe injection and fiber injections, the absolute mass of the analyte that was injected into the GC injector by the fiber was determined. The so-called “sandwich” method was used for the syringe injection to make sure that the all the amount of the analyte was injected into the GC system. A 5.0  $\mu\text{L}$  gas tight syringe was used for this purpose. A segment of 0.5  $\mu\text{L}$  methanol was first withdrawn into the syringe and then a segment of air (1  $\mu\text{L}$ ) and then the sample (no more than 1  $\mu\text{L}$ ). Another segment of air was finally withdrawn before injection.

*Calculation.* The calculation was finally processed to obtain the free concentration, bound drug percentage and binding equilibrium constant.

### **2.2.5 Results and Discussion**

*GC Response Factor.* The GC response factors for each of the five compounds were measured by the injection of an aliquot of 0.5  $\mu\text{L}$  of a 1mg/mL standard mixture of the five compounds repeatedly for nine replicates. The mass of the compounds injected into the system was 500 ng. The area counts from each injection for each compound and their mean values, standard deviations (STD) and percent relative standard deviations (%STD) are listed in Table 2.2.

**Table 2.2:** GC response factors of the target alkylbenzenes determined by syringe injection (/500 ng).

|      | Benzene | Toluene | Ethylbenzene | Propylbenzene | Butylbenzene |
|------|---------|---------|--------------|---------------|--------------|
| 1    | 94521   | 93791   | 91369        | 84608         | 82238        |
| 2    | 94845   | 95657   | 95897        | 89903         | 89336        |
| 3    | 98637   | 99800   | 100035       | 94554         | 94090        |
| 4    | 92787   | 93564   | 93756        | 88573         | 88541        |
| 5    | 99341   | 101037  | 102131       | 96324         | 95969        |
| 6    | 88686   | 99902   | 109225       | 109228        | 113755       |
| 7    | 83404   | 87459   | 90981        | 87515         | 89273        |
| 8    | 82859   | 82942   | 83531        | 77743         | 76767        |
| 9    | 88686   | 99902   | 109225       | 109228        | 113755       |
| Mean | 93174   | 95887   | 97628        | 92958         | 93315        |
| STD  | 5601    | 4810    | 6607         | 8231          | 10026        |
| %RSD | 6.0     | 5.0     | 6.8          | 8.9           | 10.7         |

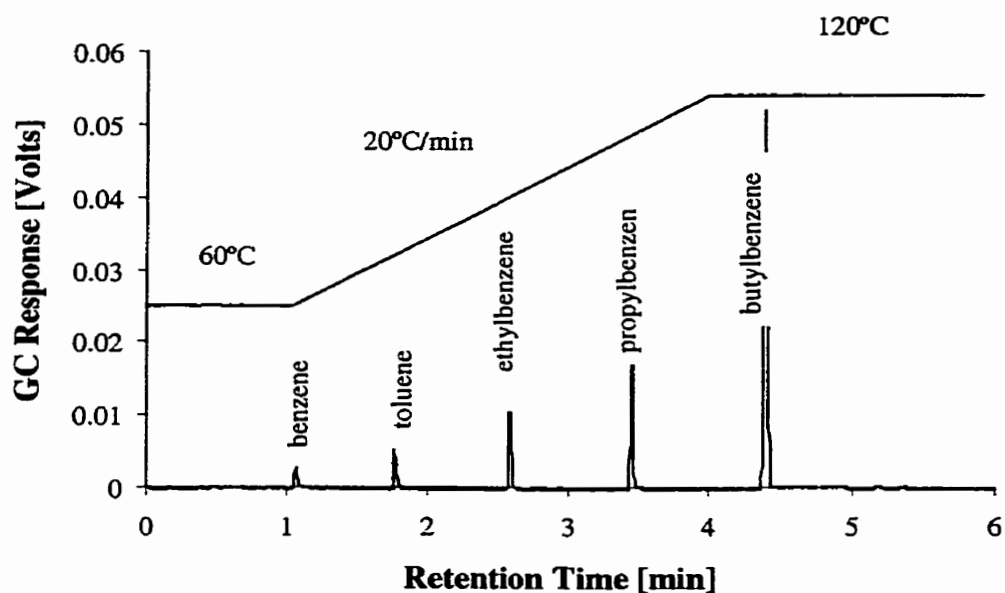


**Figure 2.3:** Gas chromatogram of alkylbenzenes.

*Calibration.* A sample chromatogram of the selected alkylbenzene compounds analysis, along with the temperature programming, is illustrated in Figure 2.3. The five compounds were very well separated.

The calibration curve of the area count of fiber injection of various concentrations analysis of each compound vs. the nominal concentration of each compound in the solution was first obtained and illustrated in Figure 2.4. The calibration curves were based on 6-point measurement from 50 ng/mL to 2000 ng/mL. For each concentration, three replicates were performed. As described in the theory section 2.2.2, this

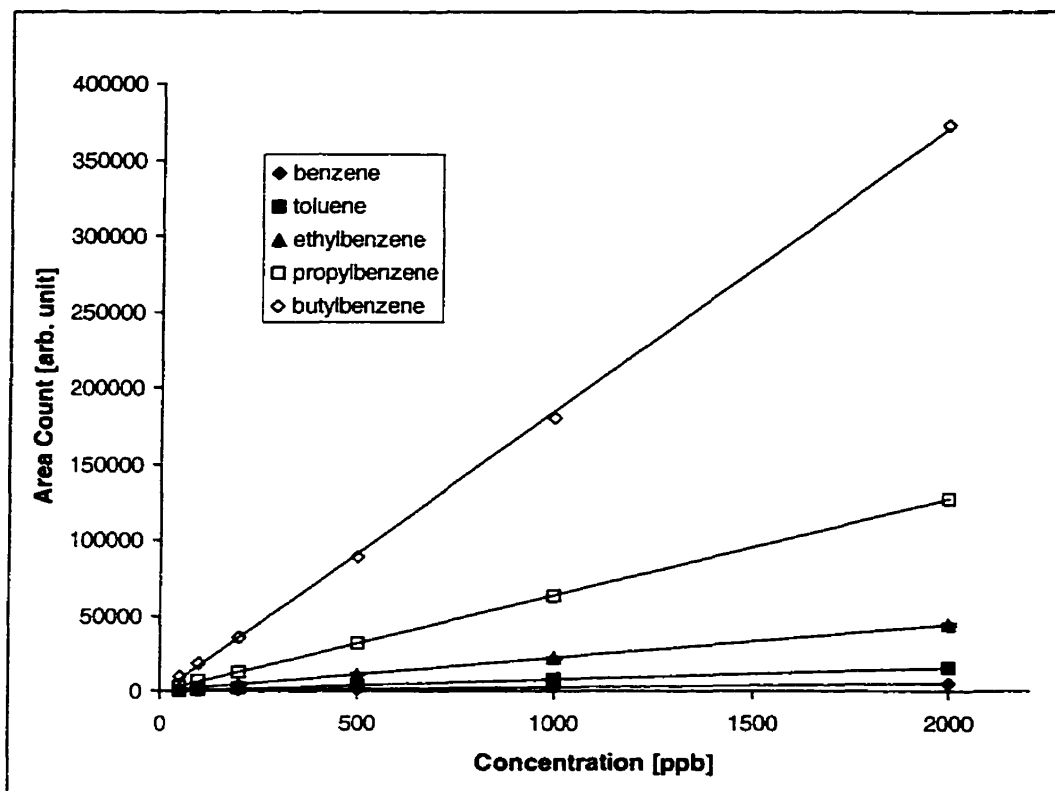


**Figure 2.4:** The calibration curves of the area count of fiber injection vs. the spiked concentration of the analyte in the buffer solution.

**Table 2.3:** Regression coefficients of the calibration curves shown in Figure 2.4.

| Compound      | Regression Equation               |
|---------------|-----------------------------------|
| Benzene       | $y = 2.54x - 0.72, R^2 = 1$       |
| Toluene       | $y = 7.75x - 23.9, R^2 = 1$       |
| Ethylbenzene  | $y = 21.9x - 106, R^2 = 0.9999$   |
| Propylbenzene | $y = 63.5x - 233, R^2 = 1$        |
| Butylbenzene  | $y = 186x - 2.04E3, R^2 = 0.9997$ |

calibration cannot be directly employed as the calibration curve to calculate the free concentration in the protein binding study since the nominal concentration is not the true free concentration in the solution. The nominal concentration is the summation of the compound partitioned in the solution, headspace and on the fiber. The absolute amount of the analyte extracted by the fiber can be measured from the response factor.

The  $K_{fh}$  values of SPME/PDMS data are listed in Table 2.4 (11). The volume of the polymer coating for 30  $\mu\text{m}$  PDMS fiber is 0.132  $\mu\text{L}$ . Since the true volume of the vial was 15.8 mL, the volume of the headspace was 7.8 mL. Since  $K_{fh} = C_f / C_h$ , The amount of the analyte in the headspace can be calculated according to the following equation:

$$n_h = \frac{n_f V_h}{K_{fh} V_f} \quad \text{Equation 2.16}$$

Therefore, the true free concentration of the analyte in the buffer solution can be calculated by the following equation:

$$C_s = \frac{n_s}{V_s} = \frac{n_{total} - n_f - n_h}{V_s} \quad \text{Equation 2.17}$$

The calculation results are listed in Table 2.5.

**Table 2.4:** Summary of  $K_{fh}$  and  $K_{fs}$  SPME/PDMS data for selected alkylbenzene compounds.

| Compound      | $K_{fh}$ (25°C) | $K_{fs}$ (22°C) |
|---------------|-----------------|-----------------|
| Benzene       | 301             | 58              |
| Toluene       | 818             | 189             |
| Ethylbenzene  | 2070            | 566             |
| Propylbenzene | 5040            | 1664            |
| Butylbenzene  | 8590            | 4011            |

**Table 2.5:** Summary of the data obtained from the calibration of alkylbenzenes.

| Benzene $V_s = 8mL$ , $V_h = 7.8mL$ , $V_f = 0.132\mu L$ , $K_{fh} = 301$ , $K_{fs} = 58$          |                  |            |            |            |             |
|--|------------------|------------|------------|------------|-------------|
| $C_{spike}$  | $n_{total}$ (ng) | Area Count | $n_f$ (ng) | $n_h$ (ng) | $C_s$ (ppb) |
| 50   | 400              | 129        | 0.72       | 62.5       | 42.1        |
| 100  | 800              | 256        | 1.43       | 125        | 84.2        |
| 200  | 1600             | 502        | 2.80       | 245        | 169         |
| 500  | 4000             | 1276       | 7.11       | 625        | 421         |
| 1000   | 8000             | 2539       | 14.16      | 1250       | 842         |
| 2000   | 16000            | 5090       | 28.38      | 2500       | 1684        |
| Toluene $V_s = 8mL$ , $V_h = 7.8mL$ , $V_f = 0.132\mu L$ , $K_{fh} = 818$ , $K_{fs} = 189$         |                  |            |            |            |             |
| 50   | 400              | 391        | 2.11       | 73.1       | 40.6        |
| 100  | 800              | 766        | 4.13       | 145        | 81.3        |
| 200  | 1600             | 1492       | 8.05       | 288        | 163         |
| 500  | 4000             | 3862       | 20.83      | 731        | 406         |
| 1000   | 8000             | 7696       | 41.51      | 1454       | 813         |
| 2000   | 16000            | 15498      | 93.60      | 2906       | 1625        |
| Ethylbenzene $V_s = 8mL$ , $V_h = 7.8mL$ , $V_f = 0.132\mu L$ , $K_{fh} = 2070$ , $K_{fs} = 566$   |                  |            |            |            |             |
| 50   | 400              | 1039       | 5.49       | 82.5       | 39.0        |
| 100  | 800              | 2146       | 11.33      | 165        | 78.0        |
| 200  | 1600             | 4242       | 22.40      | 330        | 156         |
| 500  | 4000             | 10857      | 57.34      | 823        | 390         |
| 1000   | 8000             | 21637      | 114.3      | 1646       | 780         |
| 2000   | 16000            | 43904      | 232.0      | 3288       | 1560        |
| Propylbenzene $V_s = 8mL$ , $V_h = 7.8mL$ , $V_f = 0.132\mu L$ , $K_{fh} = 5040$ , $K_{fs} = 1664$ |                  |            |            |            |             |
| 50   | 400              | 3181       | 17.62      | 92.8       | 36.2        |
| 100  | 800              | 6282       | 34.80      | 186        | 72.4        |
| 200  | 1600             | 12346      | 68.39      | 372        | 145         |
| 500  | 4000             | 31480      | 174.4      | 930        | 362         |
| 1000   | 8000             | 62676      | 347.2      | 1861       | 724         |
| 2000   | 16000            | 126980     | 703.4      | 3721       | 1447        |
| Butylbenzene $V_s = 8mL$ , $V_h = 7.8mL$ , $V_f = 0.132\mu L$ , $K_{fh} = 8590$ , $K_{fs} = 4011$  |                  |            |            |            |             |
| 50   | 400              | 9213       | 50.84      | 110        | 29.9        |
| 100  | 800              | 18.96      | 99.86      | 220        | 60.0        |
| 200  | 1600             | 35358      | 195.1      | 445        | 120         |
| 500  | 4000             | 89035      | 491.3      | 1101       | 301         |
| 1000   | 8000             | 180220     | 994.5      | 2198       | 601         |
| 2000   | 16000            | 372667     | 2057       | 4383       | 1195        |

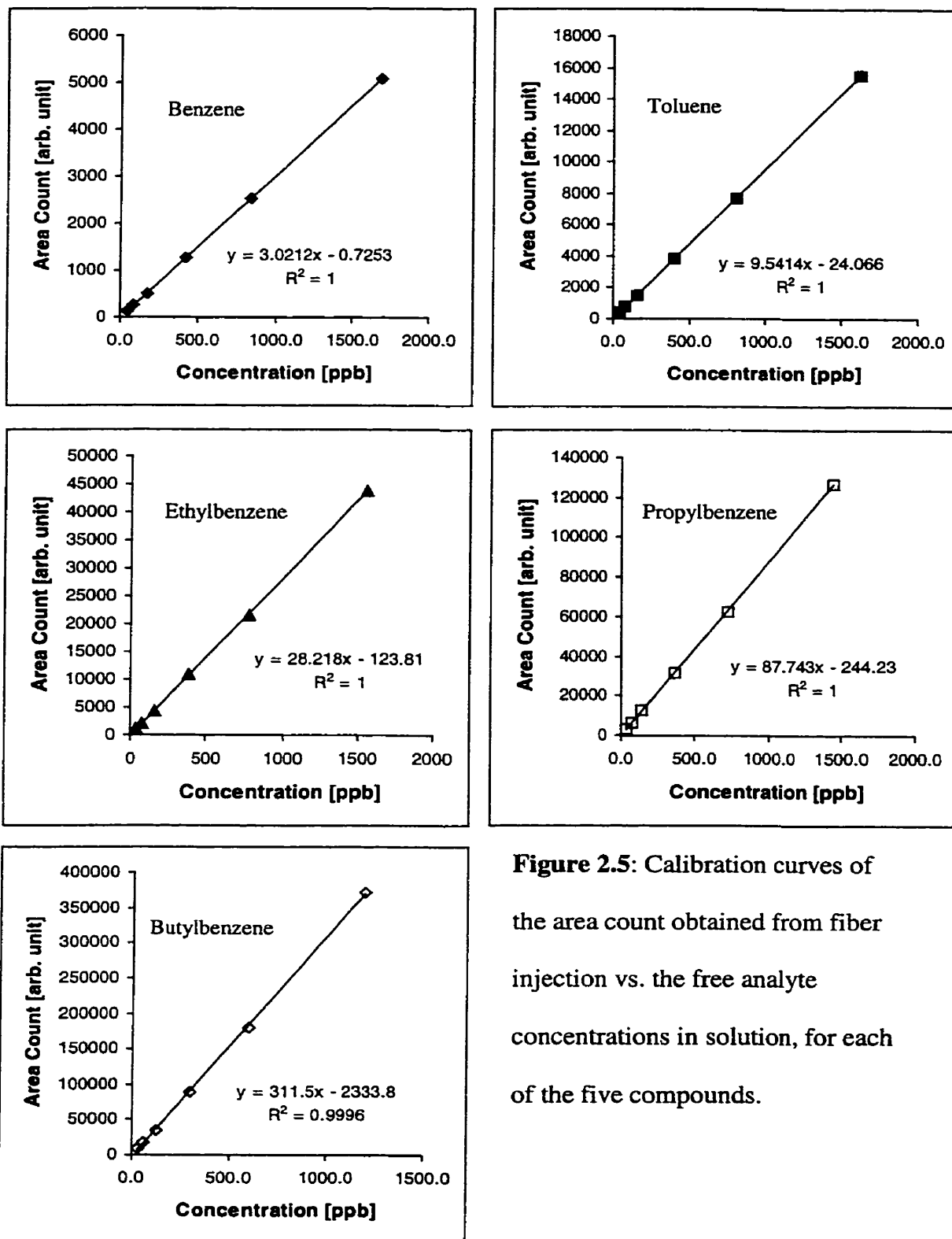


**Figure 2.5:** Calibration curves of the area count obtained from fiber injection vs. the free analyte concentrations in solution, for each of the five compounds.



The calibration curves of the area counts vs. the accurate free concentrations in the solution of each compound are illustrated in Figure 2.5. These calibration curves are employed for the determination of the free concentration in the protein binding study.

*Determination of Protein Binding Parameters.* The experimental setup for the determination of the protein binding parameters was the same as described in the calibration step, except that a 1 mg/mL BSA buffer solution was used instead of the pure buffer solution. Three concentrations of the total amount of the analyte (100 ng/mL, 200 ng/mL and 500 ng/mL) were investigated by spiking 800 ng, 1600ng or 4000 ng into the protein solution. For each of the concentrations, three replicates were performed. The free analyte concentrations can be determined with the calibration curve obtained in the previous section. The bound analyte concentration can be calculated by the following equation.

$$C_b = \frac{n_{total} - n_f}{V_s} - \left[ 1 + \frac{K_{hs} V_h}{V_s} \right] C_s \quad \text{Equation 2.18}$$

This equation was derived from Equation 2.9. Since the molar concentration of bound analyte equals the molar bound concentration of the protein, the K value can be easily calculated from Equation 2.2. The experimental results are listed in Table 2.6.

**Table 2.6:** Summary of the experimental results of alkylbenzenes binding to BSA.

| $C_{spike}$ (ppb)  | $n_{total}$ (ng) | Area Count | $n_f$ (ng) | $C_s$ (ppb) | $C_b$ (ppb) | $K / \log K$ ( $M^{-1}$ ) |
|--|------------------|------------|------------|-------------|-------------|---------------------------|
| Benzene, $V_s = 8mL$ , $V_h = 7.8mL$ , $V_f = 0.132\mu L$ , $K_{fh} = 301$ , $K_{fs} = 58$         |                  |            |            |             |             |                           |
| 100  | 800              | 132        | 0.74       | 44          | 48          | 18196 /4.26               |
| 200  | 1600             | 464        | 2.59       | 154         | 17          | 1818 /3.26                |
| 500  | 4000             | 1203       | 6.71       | 398         | 25          | 1056 /3.02                |
| Mean value of $\log K$ 3.51  |                  |            |            |             |             |                           |
| Toluene $V_s = 8mL$ , $V_h = 7.8mL$ , $V_f = 0.132\mu L$ , $K_{fh} = 818$ , $K_{fs} = 189$         |                  |            |            |             |             |                           |
| 100  | 800              | 546        | 2.95       | 60          | 26          | 7318 /3.86                |
| 200  | 1600             | 1116       | 6.02       | 120         | 52          | 7323 /3.86                |
| 500  | 4000             | 2824       | 15.2       | 299         | 131         | 7347 /3.87                |
| Mean value of $\log K$ 3.87  |                  |            |            |             |             |                           |
| Ethylbenzene $V_s = 8mL$ , $V_h = 7.8mL$ , $V_f = 0.132\mu L$ , $K_{fh} = 2070$ , $K_{fs} = 566$   |                  |            |            |             |             |                           |
| 100  | 800              | 1090       | 5.76       | 43          | 44          | 17275 /4.24               |
| 200  | 1600             | 2204       | 11.6       | 83          | 94          | 18936 /4.28               |
| 500  | 4000             | 5645       | 29.8       | 205         | 236         | 19289 /4.29               |
| Mean value of $\log K$ 4.27  |                  |            |            |             |             |                           |
| Propylbenzene $V_s = 8mL$ , $V_h = 7.8mL$ , $V_f = 0.132\mu L$ , $K_{fh} = 5040$ , $K_{fs} = 1664$ |                  |            |            |             |             |                           |
| 100  | 800              | 2226       | 12.33      | 28          | 61          | 36247 /4.56               |
| 200  | 1600             | 4472       | 24.77      | 54          | 125         | 39061 /4.59               |
| 500  | 4000             | 11431      | 63.32      | 133         | 315         | 39659 /4.60               |
| Mean value of $\log K$ 4.58  |                  |            |            |             |             |                           |
| Butylbenzene $V_s = 8mL$ , $V_h = 7.8mL$ , $V_f = 0.132\mu L$ , $K_{fh} = 8590$ , $K_{fs} = 4011$  |                  |            |            |             |             |                           |
| 100  | 800              | 2394       | 13.21      | 15          | 56          | 62208 /4.79               |
| 200  | 1600             | 4753       | 26.23      | 23          | 116         | 86330 /4.94               |
| 500  | 4000             | 12295      | 67.85      | 46          | 292         | 105763 /5.02              |
| Mean value of $\log K$ 4.92  |                  |            |            |             |             |                           |
| * Molecular weight of BSA: 67,000 Dalton   |                  |            |            |             |             |                           |

The results have been compared with the experimental results obtained by headspace GC method (by Carr, P. (8) unpublished). Table 2.7 is the comparison of the results obtained from the two methods independently. The similar results obtained by the two independent methods indicate that SPME is a valid method for protein binding study.

**Table 2.7:** Comparison of  $\log K$  values obtained from the SPME method and from headspace GC analysis.

| Chemicals     | $\text{Log}K_{\text{SPME}}$ | $\text{Log}K_{\text{headspace GC}}$ | Relative Difference (%)* |
|---------------|-----------------------------|-------------------------------------|--------------------------|
| Benzene       | 3.51                        | 3.53                                | 0.57                     |
| Toluene       | 3.71                        | 3.83                                | 3.23                     |
| Ethylbenzene  | 4.15                        | 4.16                                | 0.24                     |
| Propylbenzene | 4.49                        | 4.42                                | 1.55                     |
| butylbenzene  | 4.87                        | -                                   | -                        |

\* Relative Difference (%) =  $\text{abs}[(\log K_{\text{SPME}} - \log K_{\text{headspace GC}}) / \log K_{\text{SPME}}] \times 100$

*Further Discussions.* As shown in Table 2.8, the volume of the polymer coating of the fiber was very small. Even for the PDMS 100  $\mu\text{m}$  fiber, which has the biggest volume of polymer of the phases commercially available, the volume was still much smaller than 1  $\mu\text{L}$ . Since 8 mL of solution was used in the experiment, the analyte concentration was about 500 ng/mL, and the total mass of the analyte in the solution was 4  $\mu\text{g}$ . In order to have 10% of the free analyte to be extracted, the  $K_{fs}$ , would need to be greater than 1,000,000. According to the available published data, this condition is hard to satisfy even for the highly hydrophobic PAHs (10). In fact, the  $K_{fs}$  values for most of

**Table 2.8:** The geometric dimensions of selected fibers.

| Type of the fiber | D of core (mm) | Core volume (mm <sup>3</sup> ) | Total D (mm) | Total volume (mm <sup>3</sup> ) | Phase volume (mm <sup>3</sup> ) |
|-------------------|----------------|--------------------------------|--------------|---------------------------------|---------------------------------|
| PDMS 100μm        | 0.110          | 0.095                          | 0.300        | 0.707                           | 0.612                           |
| PDMS 65 μm        | 0.110          | 0.095                          | 0.240        | 0.452                           | 0.357                           |
| PDMS 30 μm        | 0.110          | 0.095                          | 0.170        | 0.227                           | 0.132                           |
| PDMS 7 μm         | 0.110          | 0.095                          | 0.124        | 0.121                           | 0.026                           |
| PA 85 μm          | 0.110          | 0.095                          | 0.280        | 0.615                           | 0.520                           |

Total volume – Core volume = Phase volume  
Length of the fiber = 10 mm; D = Diameter

the volatile organic compounds are below 100,000 (11). This means that in most cases, the analyte extracted by the fiber is less than 10% of the total amount of the free analyte. This value could be neglected without producing a significant error if we are only interested in determination of the free analyte concentration. However, for the calculation of bound analyte concentration, the partitioning on the fiber must be considered since it may be comparable to the bound concentration.

The amount of analyte partitioned in the headspace, however, could be significant compared with the total amount of the analyte in the system. The percentage of the analyte partitioned in the headspace can be evaluated by the Henry's law constant. By using 500 ng/mL solution with  $V_s = 8$  mL and  $V_h = 7.8$  mL as an example, the total amount of the analyte spiked into the system, the amount of the analyte extracted by the

SPME fiber and the amount of the analyte partitioned into the headspace obtained from the calibration step are listed in Table 2.9. The Henry's law constant ( $K_H$ ) for each compound is also listed.

**Table 2.9:** Summary of the experimental data of total amount of analyte spiked into the system, on the fiber and in the headspace. Henry's law constant (12) is also listed.

| compound      | Log $K_H$<br>L·atm·mol <sup>-1</sup> | $n_{total}$<br>ng | $n_f$<br>ng | $(n_f/n_{total})\%$ | $n_h$<br>ng | $(n_h/n_{total})\%$ |
|---------------|--------------------------------------|-------------------|-------------|---------------------|-------------|---------------------|
| Benzene       | 5.62                                 | 4000              | 7.11        | 0.180               | 625         | 15.6                |
| Toluene       | 6.76                                 | 4000              | 20.8        | 0.520               | 731         | 18.3                |
| Ethylbenzene  | 8.51                                 | 4000              | 57.3        | 1.43                | 823         | 20.5                |
| Propylbenzene | 9.77                                 | 4000              | 174         | 4.36                | 930         | 23.3                |
| Butylbenzene  | 13.5                                 | 4000              | 491         | 12.3                | 1100        | 27.5                |

From Table 2.9, we can see that for volatile compounds like alkylbenzenes, the amount of the analyte partitioned into the headspace was too large to be ignored. Therefore, it must be considered in the construction of the calibration curves. On the other hand, the partitioning to fiber coating is also not negligible in some cases.

For equilibrium constant measurement, equations are derived to describe the freely available analyte concentration in different systems. In a two-phase system (sample-dissolved protein, without headspace), the mass balance is:

$$n_{total} = n_s^{(0)} + n_b^{(0)} \quad \text{Equation 2.19}$$

Since  $C_p^{(0)} = C_{p,total} - C_b^{(0)}$ , where  $C_{p,total}$  is the initial protein concentration. A few simple rearrangements of Equation 2.2 will yield the expression describing the bound concentration at equilibrium:

$$C_b^{(0)} = \frac{KC_s^{(0)}}{1 + KC_s^{(0)}} \cdot C_{p,total} \quad \text{Equation 2.20}$$

The expression of the concentration of freely available analyte can be subsequently obtained by substituting Equation 2.20 into Equation 2.19:

$$C_s^{(0)} = \frac{n_{total}}{V_s + KC_{p,total}V_s / (1 + KC_s^{(0)})} \quad \text{Equation 2.21}$$

Note that Equation 2.21 is a quadratic equation of  $C_s^{(0)}$ .

In a three-phase system (headspace-buffer solution-dissolved protein), the mass balance is:

$$n_{total} = n_s^{(1)} + n_h^{(1)} + n_b^{(1)} = (V_s + K_{hs}V_h)C_s^{(1)} + C_b^{(1)}V_s \quad \text{Equation 2.22}$$

Similarly, an equation describing the freely dissolved analyte concentration in such a system can be obtained. The term in the denominator ( $K_{hs}V_h$ ) shows the presence of headspace.

$$C_s^{(1)} = \frac{n_{total}}{(V_s + K_{hs}V_h) + KC_{p,total}V_s / (1 + KC_s^{(1)})} \quad \text{Equation 2.23}$$

The four-phase system was established after the fiber was introduced into the system, the mass balance for such a system is:

$$n_{total} = n_f + (V_s + K_{hs}V_h)C_s^{(2)} + C_b^{(2)}V_s \quad \text{Equation 2.24}$$

The equation to describe the freely dissolved analyte concentration at equilibrium is:

$$C_s^{(2)} = \frac{n_{total}}{(V_s + K_{hs}V_h + K_{fs}V_f) + KC_{p,total}V_s / (1 + KC_s^{(2)})} \quad \text{Equation 2.25}$$

It is obvious from Equation 2.21, Equation 2.23 and Equation 2.25 that the concentrations of the freely dissolved analyte depend on the different systems due to the distribution of the analyte into the headspace and/or fiber. However, the difference can be represented by replacing the sample volume  $V_s$  in the first term of denominator by  $V_s + K_{hs}V_h + K_{fs}V_f$  (for equation 2.25). This also provides the conditions when the partition to the fiber and headspace can be neglected for the calculation of free analyte concentration:

$$V_s \gg K_{hs}V_h \text{ and } V_s \gg K_{fs}V_f,$$

which is similar to the condition for headspace GC analysis.

Figure 2.6 illustrates this phenomenon. Toluene was used as the example to plot these curves. The following parameters have been employed.  $K = 7329 \text{ mol}^{-1} \cdot L$ ,  $K_{hs} = 0.23$ ,  $K_{fs} = 189$ ,  $V_s = 8 \text{ mL}$ ,  $V_h = 7.8 \text{ mL}$ ,  $C_{p,total} = 5.97 \times 10^{-5} \text{ mol} \cdot L^{-1}$ . Curves (a), (b) and (c) correspond to Equation 2.21, Equation 2.23 and Equation 2.25, respectively.

The term  $K_{fs}V_f$  represents the effect of the fiber extraction, which is usually very small. For volatile compounds,  $K_{hs}$  is usually no larger than 1, which means that headspace effect can be neglected only if it is very small with respect to the sample volume. Semi-volatile compounds have much smaller  $K_{hs}$ , the  $K_{hs}V_h$  term may be negligibly small. However, such assumptions should always be verified before being applied.

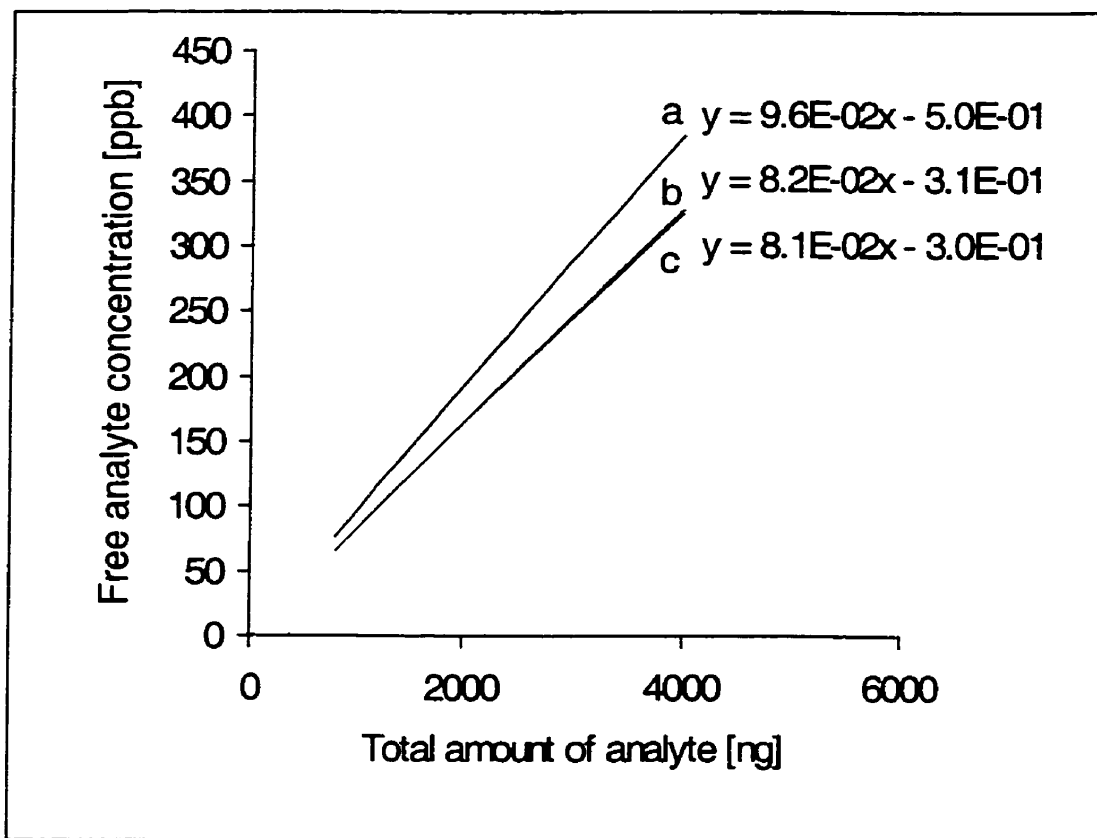


**Figure 2.6:** The free toluene concentration curves of a. two-phase system (buffer-dissolved protein), b. three-phase system (buffer-dissolved protein-headspace) and c. four-phase system (buffer-dissolved protein-headspace-fiber).

Comparison with the calibration system, where there is no protein added,

Equation 2.21 and 2.25 can be converted into:

$$C_s^{c(0)} = \frac{n_{total}^c}{V_s^c} \quad \text{Equation 2.21.c}$$

$$C_s^{c(2)} = \frac{n_{total}^c}{V_s^c + K_{hs}V_h^c + K_{fs}V_f} = \frac{V_s^c}{V_s^c + K_{hs}V_h^c + K_{fs}V_f} C_s^{c(0)} \quad \text{Equation 2.25.c}$$



where the symbol 'c' stands for calibration system.

From Equation 2.25.c, it is clear that  $C_s^{c(2)}$  and  $C_s^{c(0)}$  are linearly dependent.

However, comparing with Equation 2.21 and Equation 2.25, there is no such linear relationship between  $C_s^{(2)}$  and  $C_s^{(0)}$ . Since the value of  $C_s^{(2)}$  and  $C_s^{c(2)}$  are proportional to the fiber extraction amount  $n_f$  and  $n_f^c$ , respectively, we can draw the conclusion that, unlike in the calibration step, there is no linear dependence between fiber extraction amount  $n_f$  and the original free drug concentration  $C_s^{(0)}$ . Therefore, it is impossible to directly estimate the original free analyte concentration  $C_s^{(0)}$  (with protein presence, no headspace, no fiber) only from the calibration curve.  $C_s^{(0)}$  can only be calculated with the extra information such as the total protein concentration ( $C_{p,total}$ ) and binding equilibrium constant  $K$ .

The only solution was to plot the calibration curve of equilibrium analyte concentration in aqueous solution ( $C_s^{c(2)}$ ) vs. the amount of the analyte extracted by the fiber ( $n_f^c$ ), which was used in this study. This plot can be used to determine the free analyte concentration ( $C_s^{(2)}$ ) which is in equilibrium with the protein, fiber and headspace, after the measurement of the fiber extraction amount ( $n_f$ ).

It is interesting to pay close attention to the relationship between  $C_s^{(0)}$  and  $C_s^{(2)}$ .

The change of the analyte concentrations can be analogous to the drug elimination process in a pharmacology study (13). After the solution (with initial concentration  $C_s^{(0)}$ ) was introduced into the vial, some portion of the free analyte in the solution would

be transferred into headspace and fiber coating until equilibrium is attained. However, the decrease of free analyte concentration in the solution due to the binding to protein will cause a certain portion of the bound analyte to become dissociated and released as free analyte into the solution. If  $KC_{p,total} / (1 + KC_s^{(0)}) \gg 1$ , then  $C_s^{(0)} \approx C_s^{(2)}$ , which means that the free concentration will change very little. In such a case, the protein-bound analyte acts like a buffer. The analyte partitioned into the headspace and fiber comes from the dissociation of protein-bound analyte, even though the analyte amount in headspace can be comparable to the free analyte amount in the solution. If

$KC_{p,total} / (1 + KC_s^{(0)}) \ll 1$  and  $KC_{p,total} / (1 + KC_s^{(2)}) \ll \frac{K_{hs}V_h}{V_s}$ , the dependence between  $C_s^{(0)}$  and  $C_s^{(2)}$  will be the same as  $C_s^{c(0)}$  and  $C_s^{c(2)}$ . Only under such circumstance, can the calibration curve of  $n_f^c$  vs.  $C_s^{c(0)}$  be used to estimate the free analyte concentration  $C_s^{(0)}$ .

## 2.2.6 Determination of the Equilibrium Constant without the Calibration

Discussion now switches back to the headspace GC analysis. The effect of headspace should be similar to the SPME case. If the headspace cannot be ignored, equation 2.12 should be modified as

$$\begin{aligned}
 A^0 / A^f &= C_h^0 / C_h^f \\
 &= \frac{V_h + V_s / K_{hs} + C_p V_s K / K_{hs}}{V_h + V_s / K_{hs}} \\
 &= 1 + \frac{V_s}{V_s + K_{hs} V_h} K \cdot C_p
 \end{aligned}
 \tag{Equation 2.12.a}$$

Compared with equation 2.12, the effect of the headspace will contribute a multiplier of

$\frac{V_s}{V_s + K_{hs}V_h}$ . This equation can be easily adapted to the SPME analysis, where:

$$\begin{aligned} A^0 / A^f &= C_h^0 / C_h^f \\ &= 1 + \frac{V_s}{V_s + K_{hs}V_h + K_{fs}V_f} K \cdot C_p \end{aligned} \quad \text{Equation 2.12.b}$$

$A^0$  and  $A^f$  are the analyte peak areas with protein absence or presence, respectively.

Unbound protein concentration  $C_p$  can be calculated from equation 2.13 <sup>(1)</sup>:

$$C_p = C_{p,total} - (1 - A^f / A^0) \cdot C_s^0$$

where  $C_{p,total}$  is the total protein concentration;  $C_s^0$  is the total analyte concentration.

Therefore, the plot of  $A^f / A^0$  vs.  $C_p$  should be a line with slope of  $\frac{KV_s}{V_s + K_{hs}V_h + K_{fs}V_f}$ .

---

<sup>(1)</sup> Note: Although Equation 2.13 is derived when analytes partition on fiber and headspace are ignored, it still holds when the amount of analyte on fiber and headspace are significant. When protein is not present,

$$n_{total} = n_s^0 + n_h^0 + n_f^0 = n_f^0 \cdot \left(1 + \frac{V_h}{K_{\beta h}V_f} + \frac{V_s}{K_{\beta s}V_f}\right);$$

When protein is added,

$$\begin{aligned} n_{total} &= n_s^f + n_h^f + n_f^f + n_b = n_f^f \cdot \left(1 + \frac{V_h}{K_{\beta h}V_f} + \frac{V_s}{K_{\beta s}V_f}\right) + n_b \\ &= \frac{n_f^f}{n_f^0} \cdot n_{total} + n_b \end{aligned}$$

Therefore, the bound protein concentration can be expressed as:

$$C_b = \frac{n_b}{V_s} = \left(1 - \frac{n_f^f}{n_f^0}\right) \cdot \frac{n_{total}}{V_s} = \left(1 - \frac{A^f}{A^0}\right) \cdot C_s^0$$

**Table 2.10:** Summary of the data of the direct equilibrium constant measurement.

| Compound      | Slope | $\frac{V_s}{V_s + K_{hs}V_h + K_{fs}V_f}$ | $\log K$ |
|---------------|-------|---|----------|
| Benzene       | 3500  | 0.842                                     | 3.60     |
| Toluene       | 5380  | 0.816                                     | 3.88     |
| Ethylbenzene  | 12710 | 0.789                                     | 4.20     |
| Propylbenzene | 47900 | 0.756                                     | 4.59     |
| Butylbenzene  | 57350 | 0.687                                     | 4.90     |

Figure 2.7 and Table 2.10 illustrate the estimation of binding constant utilizing equation 2.12.b. In this experiment, the total protein concentration ( $C_{p,total}$ ) of 0.25 mg/mL, 1.00 mg/mL, 2.00 mg/mL and 4.00 mg/mL were used. The sample solution volume  $V_s$  and headspace volume  $V_h$  were 8.0 mL and 7.8 mL, respectively. The total analyte concentration  $C_s^0$  was 500 ppb. The estimated result demonstrates that it is compatible to the previous methods.

The advantage of this method is that only the relative ratio ( $A_0 / A_f$ ), total analyte concentration  $C_s^0$  and total protein concentration ( $C_{p,total}$ ) are required to calculate the first order binding equilibrium constant. There is no need to know the exact fiber extraction amount and the GC response factor. The only assumption was that the response of fiber and GC should be linear, which was satisfied in this experiment. Inherently, this method introduces less measurement error.

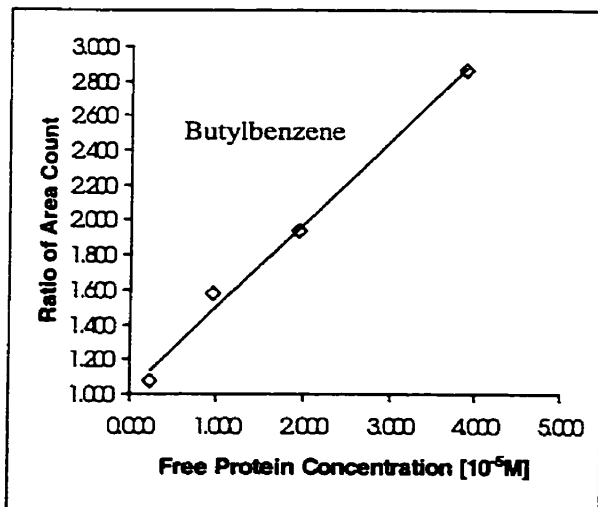
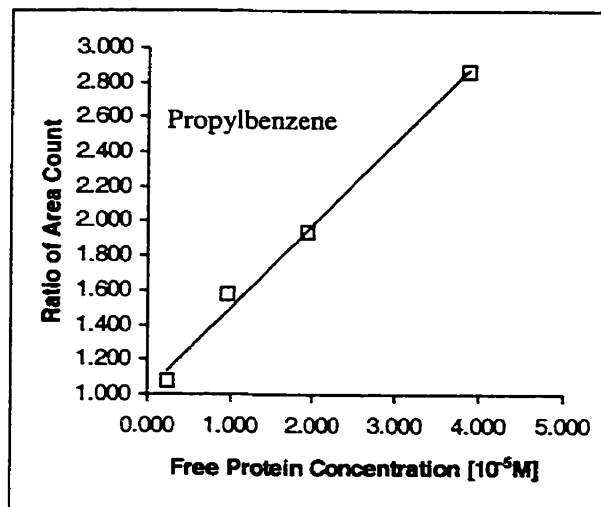
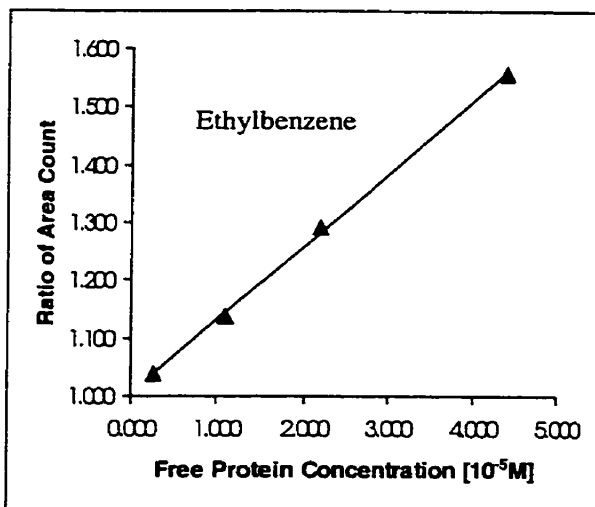
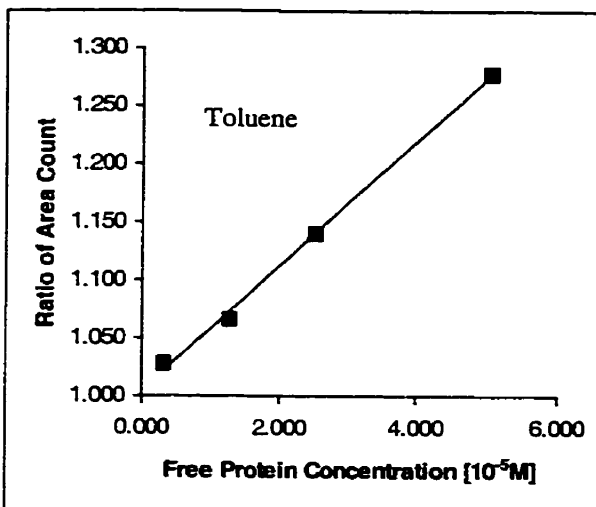
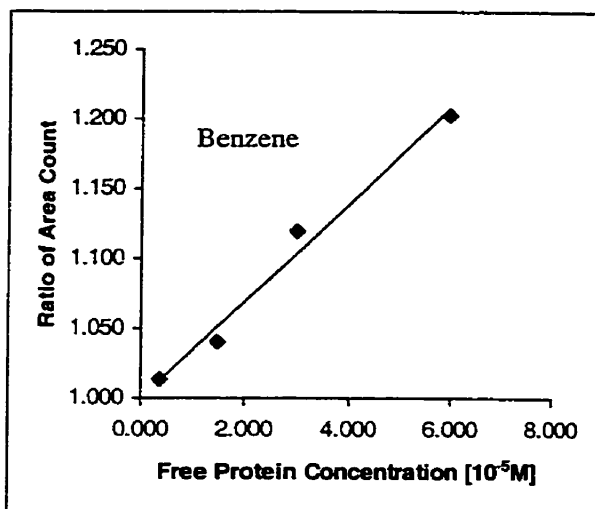


**Figure 2.7:** Curves to directly calculate the equilibrium constant.

### **2.2.7 Conclusion**

This work demonstrated that SPME is an effective and accurate method to determine the binding parameter of volatile organic compounds to protein, which is difficult for most conventional methods. Compared with headspace GC, SPME is simpler in operation and no expensive apparatus required. Another important factor of SPME is that it does not have theoretical reservations. Several approaches to measure the protein binding constant have been investigated, including one which only utilizes the relative peak area ratios.

However, to measure the free analyte concentration with protein presence correctly, special consideration should be exercised in the building up the calibration curve. While the amount of the analyte on the fiber could be neglected in most cases, the amount of analyte in the headspace is normally too large to be ignored for volatile organic compounds. Therefore, it is necessary always to validate the assumptions made to simplify the problem.

## 2.3 Study of Diazepam Binding to Human Serum Albumin by SPME

### 2.3.1 Background

The postulated structure of human serum albumin (HSA) and the possible locations of drug binding sites are illustrated in Figure 2.8 (3). The complete primary structure of human serum albumin has been known since 1975 (14, 15). It consists of a single peptide chain containing 585 amino acid residues, which is formed into nine double loops or subdomains by paired disulfide bonds (14, 15). As proposed by Behrens *et al.* (14), the tertiary structure of HSA consists of three domains, each formed by three loops. Several similarities exist among the three domains with respect to amino acid composition and sequence (15).

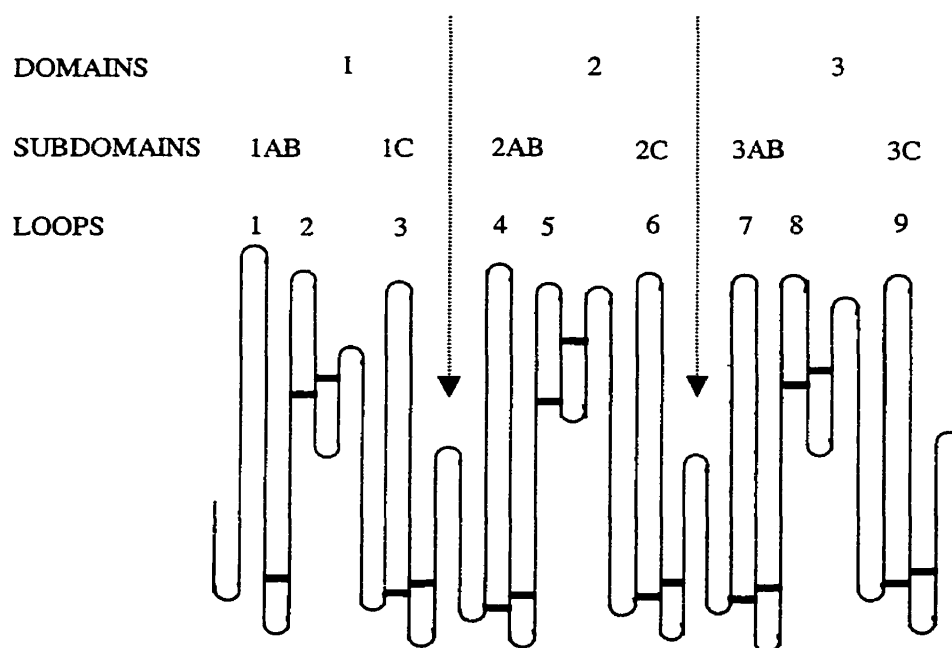


**Figure 2.8:** Loop structure of HSA indicating disulphide bonds forming loops, subdomains and domains. (Adapted from (3)). —: disulfide bond).

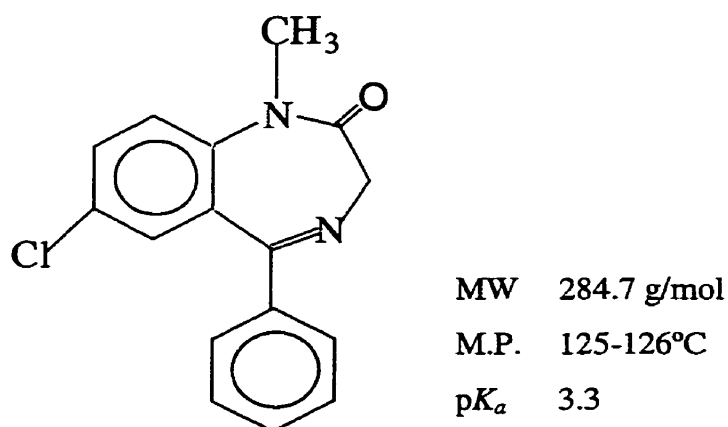


**Figure 2.9:** Structure and some of the physical properties of diazepam.

Brown and Shockley (16) developed a 3-dimensional model of HSA using restrictions imposed by helices, disulphide bridges, hydrophobic areas and the proline residues at the tip of each loop. Within each domain, subdomains consisting of loop A and B (large and small) and loop C were constructed. Further work with space-filling models suggested that the hydrophobic faces of the AB and C subdomains fitted together leaving a hydrophobic channel through the domain and a large indentation on each side of the molecule.

This space-filling model suggests two binding sites for fatty acids and /or drugs in each domain, making a total of six sites. Fatty acid binding studies generally show 6 sites in agreement with this model (17, 18). Drug binding site II is located in subdomain 3AB and the likely location of site I is subdomain AB.



Diazepam (7-chloro-1,3-dihydro-1-methyl-5-phenyl-3H-1,4-benzodiazepin-2-one) was used in this thesis as the target compound to illustrate the effectiveness of SPME as an alternative way to investigate the interaction between drug and protein. Diazepam is one member of the benzodiazepine drug family widely used as tranquilizers, hypnotics, muscle relaxants, and anticonvulsants (19, 20). The structure of diazepam and some of its physical properties are illustrated in Figure 2.9.

It is well known that diazepam binds to serum albumin. Various authors (21) have proven the presence of one specific binding site. The binding constants, the thermodynamic parameters, and their variation with pH have also been determined (22, 23).

The details of the molecular aspect of ligand binding to HSA is beyond the scope of this thesis. However, it is believed that diazepam binding to HSA occurs at binding site II, which is also called the “indole and benzodiazepine binding site” (24-26). The site binds several indole derivatives and benzodiazepines with a high degree of structural specificity (21, 27-29). In fact, diazepam is one of the specific marker ligands for this site (26).

### **2.3.2 Theory**

Since diazepam is a non-volatile, relatively polar organic compound, it is more likely to be hydrophilic than the alkylbenzenes studied in the previous section. In addition, it is expected that a very small amount of the diazepam will be partitioned in the headspace since it is very non-volatile by nature. For these types of compounds, direct

SPME, in which the extraction step is performed directly in the sample solution instead of in headspace, is employed.

To avoid possible experimental error introduced by the slight diazepam partitioning into the headspace, the headspace is totally eliminated in the experimental configuration. Employing the same methods that have been demonstrated in the previous section on alkylbenzenes binding to HSA, accurate results could be obtained even with the presence of the headspace by using the correct calculation method. Since it will increase the complexity of the data processing and the direct extraction method can be used, the vial was totally filled with sample solution leaving no headspace, as shown in Figure 2.10. In this configuration, diazepam binding to HSA was a three-phase system, which is buffer-dissolved protein-fiber coating. During the calibration step, it was a two-phase system (buffer-fiber coating).

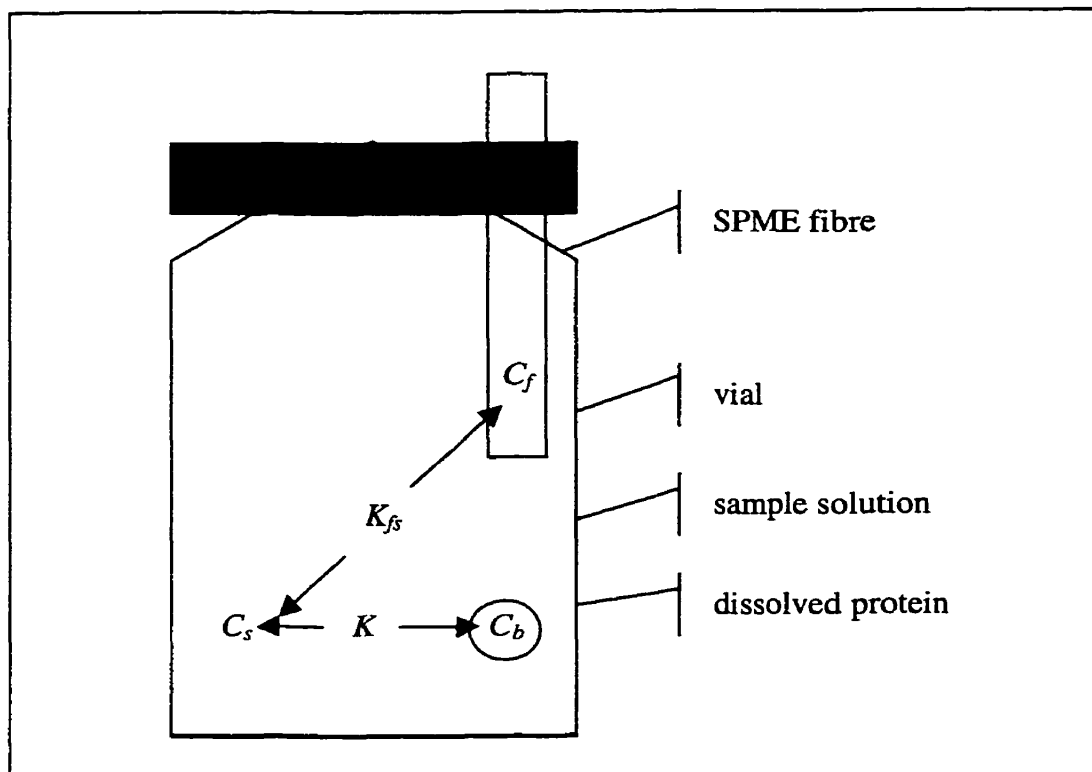


**Figure 2.10:** Schematic of equilibrium in three-phase system (sample solution-dissolved protein-fiber coating).

In the calibration step, the mass balance is:

$$n_{total} = n_f + n_s \quad \text{Equation 2.26}$$

A simple derivation yields:

$$C_s = \frac{n_{total} - n_f}{V_s} \quad \text{Equation 2.27}$$

If  $n_f$  is negligible, we have:

$$C_s = C_0 = \frac{n_{total}}{V_s} \quad \text{Equation 2.28}$$

This means that when the amount of the analyte on the fiber can be neglected, the calibration curve of initial concentration ( $C_0$ ) vs. the amount of the analyte on the fiber can be employed to calculate the free analyte concentration in protein binding study. However, if the compound has a large partition coefficient towards the fiber, the amount of the analyte partitioned onto the fiber has to be taken into consideration. In this situation, Equation 2.27 should be employed to calculate the free concentration, which will be used in the calibration curve to determine the free concentration in the protein binding study. The amount of the analyte on the fiber can be measured from the response factor of diazepam on GC, which can be obtained from syringe injection.

The mass balance for system with dissolved protein is:

$$n_{total} = n_f + n_s + n_b \quad \text{Equation 2.29}$$

Once the free concentration ( $C_s$ ) is known from the calibration curve corresponding to the fiber injection amount  $n_f$ , The bound concentration  $C_b$  can be calculated from the following equation.

$$C_b = \frac{n_{total} - n_f - C_s V_s}{V_s} \quad \text{Equation 2.30}$$

Since the molar bound drug concentration equals the molar bound concentration of protein, the equilibrium constant can be calculated from Equation 2.2.

### 2.3.3 Experimental

*Chemicals and Materials.* Diazepam was purchased from Radian (Austin, TX) as a 1 mg/mL methanol solution. This solution was diluted with methanol into 0.1 mg/mL, 0.01 mg/mL, 0.001 mg/mL solutions for experimental convenience. All these stock solutions were stored at  $-10^{\circ}\text{C}$ . The human serum albumin (HSA, 96% purity, no fatty acid) was purchased from Sigma (Mississauga, ON, Canada). SPME devices and fibers [100  $\mu\text{m}$  poly(dimethylsiloxane) (PDMS)] and all the vials used in the experiments were purchased from Supelco (Bellefonte, PA).

The pH 7.4 buffer solution was prepared by combining 200 mM disodium hydrogen orthophosphate and 200 mM sodium dihydrogen orthophosphate solution at a certain ratio under the monitoring of a pH meter. This buffer solution was diluted to form a 0.067 M pH 7.4 buffer solution. The calibration and protein binding measurements were performed in this buffer solution.

*Instrumentation and Analytical Conditions.* All analyses were performed on a Varian (Sunnyvale, CA) 3500 gas chromatograph equipped with a 10 m  $\times$  0.25 mm id  $\times$  0.25  $\mu\text{m}$  SPB-5 column (Sigma, Mississauga, ON, Canada), a septum-equipped programmable injector (SPI) with SPME insert and a FID. The carrier gas was helium (25 psi head pressure). The temperature program used for the fiber injection was 120  $^{\circ}\text{C}$ , held for 1 min, increased at 10  $^{\circ}\text{C min}^{-1}$  to 300  $^{\circ}\text{C}$ , held for 5 min. During the whole analysis, the injector and detector temperatures were kept at 250  $^{\circ}\text{C}$  and 300  $^{\circ}\text{C}$ , respectively.

The detector response factor was determined by a syringe injection of a 1 mg/mL standard diazepam solution in methanol (0.5  $\mu\text{L}$ ) using the same column temperature

program. The SPI injector was temperature programmed as follows: 50 °C held for 0.5 min, increased at 250 °C/min to 250 °C, held for 22 min. Liquid CO<sub>2</sub> was used to cool the injector before all injections. All the extractions were carried out at 23 °C. A 7 mm × 2 mm stirrer bar was used in each of the extraction vial (2 mL clear vial from Supelco).

*Method.* Since diazepam is a non-volatile and relatively polar compound, direct SPME, in which the extraction was performed direct in the sample matrix instead of the headspace, was used in this experiment. A 2 mL vial was used in the experiment to save the protein solution. A stirrer bar was first put into the vial and then 1.9 mL buffer or protein solution was added to completely fill the vial. This process leaves no headspace in the vial, so that the analyte partitioning to the headspace was eliminated. This vial was mounted on the plate/stirrer to start the agitation. The agitation speed was kept at 800 rpm. After the agitation was stable, a PDMS fiber was inserted into the vial for the extraction. The extraction time was optimized at 45 min. After the extraction, the fiber was transferred to the GC injector for analysis with a desorption time of 3 min. No carryover of analytes was observed. An extraction profile and calibration curve of diazepam were first investigated in 0.067 M phosphate buffer solution (pH = 7.4). For the protein binding study, 1 mg/mL HSA solution was prepared in the same buffer solution and used for the extraction. The free drug concentration was calculated from the GC response factor and the calibration curve. The equilibrium constant was then obtained from the Scatchard method.

### 2.3.4 Results and Discussion

*Decomposition of Diazepam.* Like most of the benzodiazepines, diazepam is a thermally labile compound, which is likely to be decomposed in the GC system if the temperature is sufficiently high. It was found that diazepam decomposed when a 30-meter column was used, since, on that column, the compound takes more time and higher temperature to elute. The problem was eliminated when a 10 meter column was used.

*Extraction Profile.* All the extractions in this study were carried out at 23°C. The extraction profile was first investigated to determine the equilibrium time. The equilibrium profile is presented in Figure 2.11. From the extraction profile, we can see

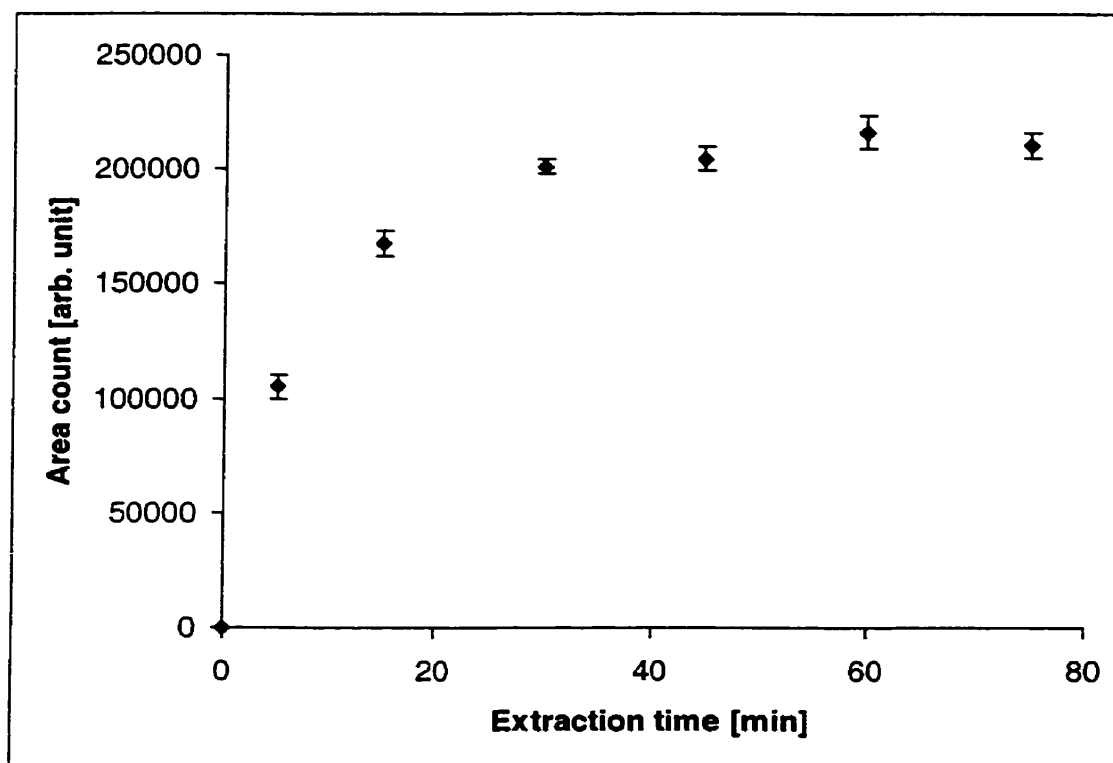


**Figure 2.11:** Extraction profile of diazepam by a PDMS 100  $\mu\text{m}$  fiber in 0.067 M pH = 7.4 phosphate buffer. Agitation speed was 800 rpm.

that the equilibrium is reached after 35 min. Therefore, 45 min was used as the extraction time for all experiments.

*GC Response Factor.* The GC response factor was determined by syringe injection an aliquot of 0.6  $\mu\text{L}$  of 0.1 mg/mL (total mass = 60 ng) diazepam methanol solution into the GC system. The “sandwich” method was used for the syringe injection. The response factor was determined as 3602 area counts per ng diazepam.

*Calibration Curve.* The calibration curve (Figure 2.12) was performed in 0.067 M phosphate buffer (pH = 7.4) solution with diazepam concentration varying from 0.25  $\mu\text{g/mL}$  to 10  $\mu\text{g/mL}$ . A diazepam standard methanol solution was spiked into the buffer solution to obtain the sample solution with a certain concentration. It was found that the trace amount of methanol could affect the precision of analysis by swelling the fiber

**Table 2.11:** Summary of the data for diazepam analysis in buffer solution.

| $C_{total}$ (ng/mL) | Area   | $n_{total}$ (ng) | $n_f$ (ng) | $(n_f/n_{total})\%$ | $C_s$ (ng/mL) |
|---------------------|--------|------------------|------------|---------------------|---------------|
| 100                 | 17124  | 200              | 4.75       | 2.38                | 97.6          |
| 200                 | 32818  | 400              | 9.11       | 2.28                | 195           |
| 300                 | 47621  | 600              | 13.2       | 2.20                | 294           |
| 400                 | 60318  | 800              | 16.7       | 2.09                | 392           |
| 500                 | 71144  | 1000             | 19.8       | 1.97                | 490           |
| 600                 | 86088  | 1200             | 23.9       | 1.99                | 588           |
| 700                 | 102845 | 1400             | 28.6       | 2.04                | 686           |
| 800                 | 111570 | 1600             | 31.0       | 1.94                | 785           |
| 900                 | 124120 | 1800             | 34.5       | 1.91                | 883           |
| 1000                | 135109 | 2000             | 37.5       | 1.88                | 981           |

The response factor is 3062 area count units/ng of diazepam.



coating. Therefore, during the calibration, as well as the protein binding analysis, methanol was added to the solution to keep methanol concentration the same in each analytical vial for all the concentrations of diazepam.

The amount of the analyte partitioned onto the fiber coating can be calculated from the response factor and the area count of the fiber injection. The results are shown in Table 2.11.

Column 5 in Table 2.11 shows that the amount of the analyte extracted by the

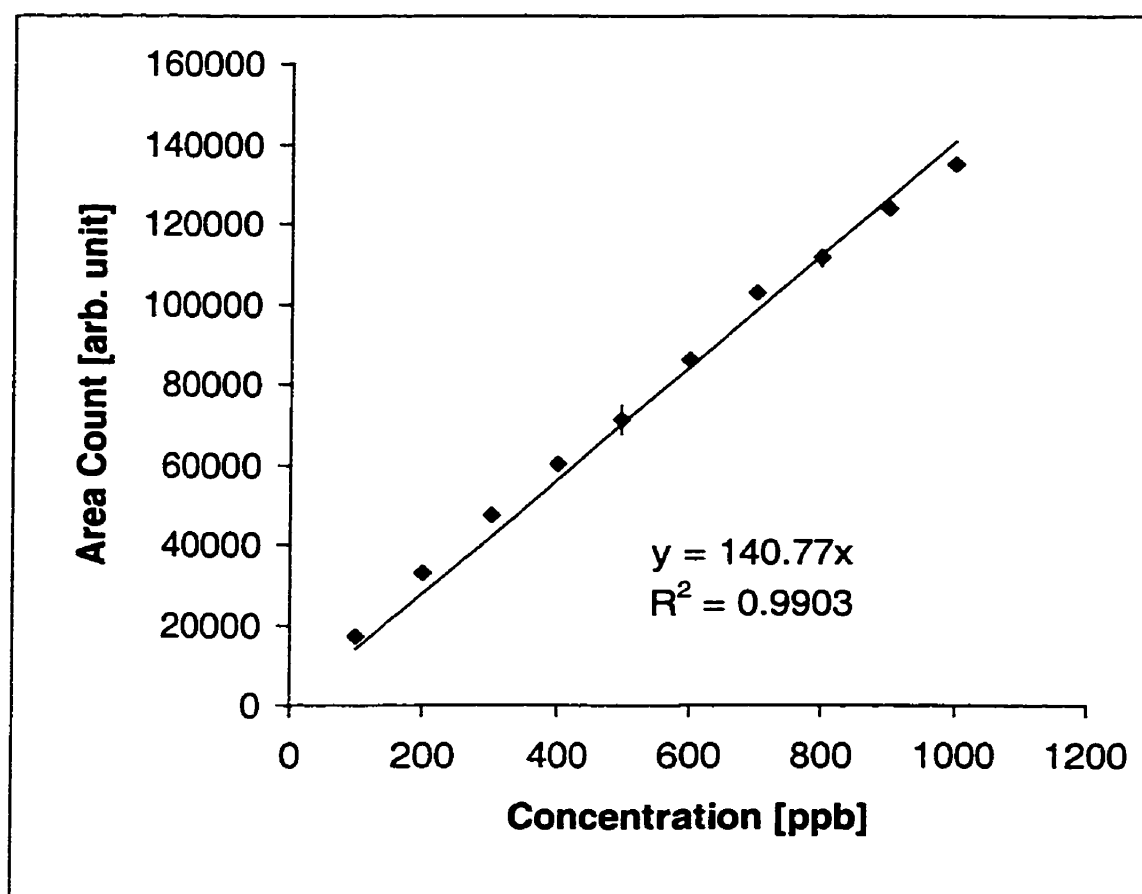


**Figure 2.12:** Calibration curve of diazepam. The x-axis is the total concentration of diazepam.

fiber is less than 3% of the total amount of the analyte in the solution. This amount is so small that it can be neglected in plotting the calibration curve. Therefore, the calibration curve of the total concentration  $C_{total}$  vs. the area count can be used as the calibration curve to determine the free drug concentration in the protein binding study. The calibration curve is presented in Figure 2.12. The measurements were performed in 3 replicates. The regression parameters are shown in the chart area.

The calibration curve is linear with regression equation of  $y = 140.77x$  and a square of regression coefficient ( $R^2$ ) of 0.9903.

*Determination of the Binding Parameters.* The moles of drug bound per moles of protein ( $r$ ), the molar free concentration ( $[D]$ ) and the value of  $r/[D]$  have been calculated and summarized in Table 2.12. A Scatchard plot was employed to calculate the equilibrium constant and the number of binding sites in this study.

The concentration of HSA used in this study was 1mg/mL, which is  $1.45 \times 10^{-5}$  M (molecular weight of HSA is 69,000 g/mol). Since the analyte concentration loaded on the SPME fiber only reached equilibrium with the free analyte concentration in the solution, the concentration obtained from the calibration curve was the free diazepam concentration in the solution. The amount of the analyte loaded on the SPME fiber can be calculated through the GC response factor. Therefore, the bound drug concentration in the solution could be easily obtained from Equation 2.30.

**Table 2.12:** Summary of the experimental data of diazepam binding to HSA.

| $C_{total}$<br>(ng/mL) | Area<br>count | $C_s$<br>(ng/mL) | Percentage<br>drug bound | $r$   | [D]<br>(mol·L <sup>-1</sup> ) | $r/[D]$<br>(L·mol <sup>-1</sup> ) |
|------------------------|---------------|------------------|--------------------------|-------|-------------------------------|-----------------------------------|
| 1000                   | 11304         | 80.3             | 92.0                     | 0.223 | 2.82E-07                      | 7.90E+05                          |
| 2000                   | 18814         | 134              | 91.1                     | 0.331 | 4.69E-07                      | 7.05E+05                          |
| 3000                   | 29395         | 209              | 89.6                     | 0.434 | 7.33E-07                      | 5.92E+05                          |
| 4000                   | 65777         | 467              | 84.4                     | 0.614 | 1.64E-06                      | 3.74E+05                          |
| 5000                   | 123885        | 880              | 78.0                     | 0.756 | 3.09E-06                      | 2.44E+05                          |
| 6000                   | 205805        | 1462             | 70.8                     | 0.857 | 5.14E-06                      | 1.67E+05                          |

The Scatchard plot is presented in Figure 2.13. From the regression equation of the Scatchard plot, the slope was equal to  $1.02 \times 10^6$ , y-intercept equal to  $1.03 \times 10^6$ , x-intercept equal to 1.0. Therefore, the equilibrium constant  $K = 1.02 \times 10^6 \text{ L}\cdot\text{mol}^{-1}$  and the  $\log K$  value was 6.01. The number of binding sites per protein molecule was 1.0.

The apparent equilibrium constant and the total binding constant are reported as  $1.159 \times 10^6 \text{ L}\cdot\text{mol}^{-1}$  and  $4.919 \times 10^5 \text{ L}\cdot\text{mol}^{-1}$  (23). This is the only value of equilibrium constant that is published about diazepam binding to HSA. Compared with the result in this study, which is  $1.02 \times 10^6 \text{ L}\cdot\text{mol}^{-1}$ , the two results are very comparable with the relative difference of their log value being less than 1%.

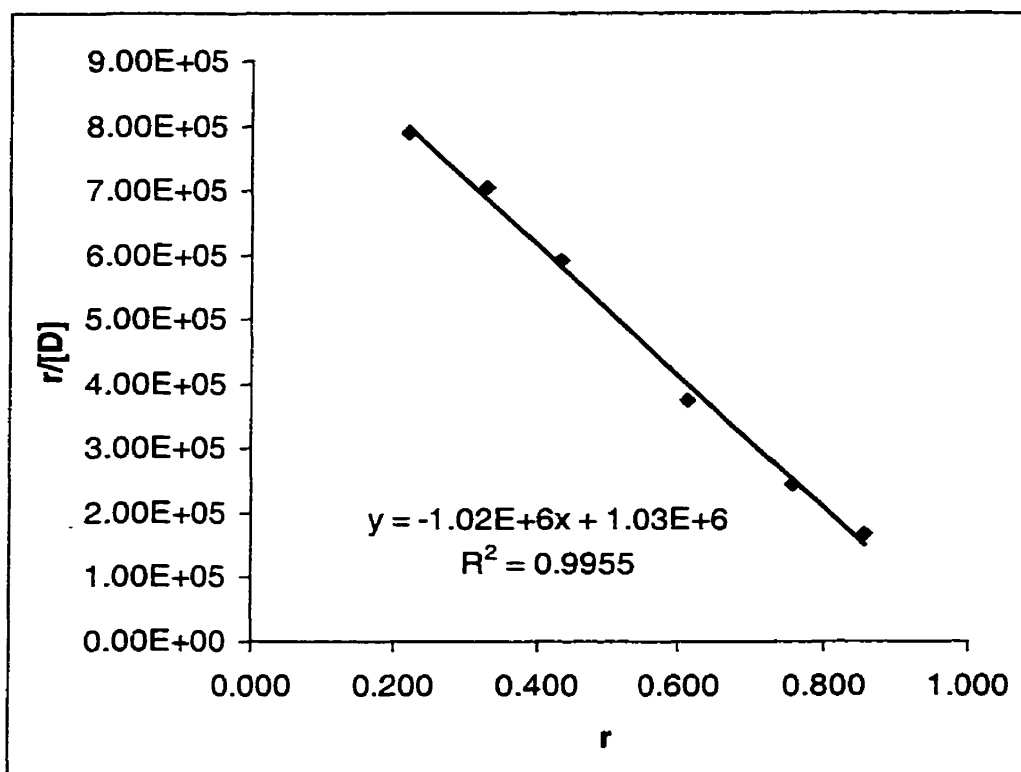


**Figure 2.13:** Scatchard plot for diazepam binding to HSA.

### 2.3.5 Determination of the Equilibrium Constant without Calibration

The direct equilibrium constant measurement method developed for alkylbenzene binding analysis can be modified for diazepam binding analysis. Since no headspace is involved and the effect of fiber extraction amount is negligible (about 3%), the mass balance for the system with protein in present can be written as:

$$\begin{aligned}
 n_{total}^{(1)} &= n_f^{(1)} + n_s^{(1)} + n_b^{(1)} \\
 &= C_s^{(1)}(V_f / K_{sf} + V_s + KC_p^{(1)}V_s) \\
 &\approx C_s^{(1)}V_s(1 + KC_p^{(1)})
 \end{aligned}
 \tag{Equation 2.31}$$

For this experiment, the total protein concentration was constant and the diazepam concentration was varied. Choosing the solution with diazepam concentration of  $C_s^{(0)}$  without protein present as the reference system, then:

$$n_{total}^{(0)} = C_s^{(0)} \cdot V_s .$$

Therefore, for systems with protein and different diazepam concentrations, using the fact

that  $\frac{C_s^{(0)}}{C_s^{(1)}} = \frac{A^{(0)}}{A^{(1)}}$  and  $C_{total}^{(1)} = \frac{n_{total}^{(1)}}{V_s}$ , the following expression holds:

$$\frac{n_{total}^{(1)}}{n_{total}^{(0)}} \cdot \frac{A^{(0)}}{A^{(1)}} = \frac{C_{total}^{(1)}}{C_s^{(0)}} \cdot \frac{A^{(0)}}{A^{(1)}} = 1 + KC_p^{(1)} \quad \text{Equation 2.32}$$

where the superscript '(1)', and '(0)', stand for system with protein, and reference system without protein, respectively;  $C_p^{(1)}$  is the unbound protein concentrations, which can be determined from following equations:

$$\begin{aligned} C_p^{(1)} &= C_{p,total} - C_b^{(1)} = C_{p,total} - (C_{total}^{(1)} - C_s^{(1)}) \\ &= C_{p,total} - (C_{total}^{(1)} - C_s^{(0)} \cdot \frac{A^{(1)}}{A^{(0)}}) \end{aligned} \quad \text{Equation 2.33}$$

Table 2.13 and Figure 2.14 shows the plot of  $\frac{C_{total}^{(1)}}{C_s^{(0)}} \cdot \frac{A^{(0)}}{A^{(1)}}$  vs.  $C_p^{(1)}$ . From the plot

we obtain an equilibrium constant of  $9.77 \times 10^5 \text{ L} \cdot \text{mol}^{-1}$ , which agreed with the value attained from previous Scatchard plot.

**Table 2.13:** Experimental data of diazepam binding to HSA for direct equilibrium constant measurement. Note that for reference system,  $C_s^{(0)}$  was 1000 ppb without protein, with a corresponding area count  $A^{(0)}$  being 135,109.

| $C_{total}^{(1)}$<br>(ng/mL) | Area count | $\frac{C_{total}^{(1)} A^{(0)}}{C_s^{(0)} A^{(1)}}$ | $C_p^{(1)}$<br>(mol/L) |
|------------------------------|------------|---|------------------------|
| 1000                         | 11304      | 11.95   | 11.28E-6               |
| 1500                         | 18814      | 10.77   | 9.73E-6                |
| 2000                         | 29395      | 9.19  | 8.24E-6                |
| 3000                         | 65777      | 6.16  | 5.66E-6                |
| 4000                         | 123885     | 4.36  | 3.68E-6                |
| 5000                         | 205805     | 3.28  | 2.30E-6                |

$C_{total}^{(1)}$  is total diazepam concentration.  $C_p^{(1)}$  is unbound protein concentration.

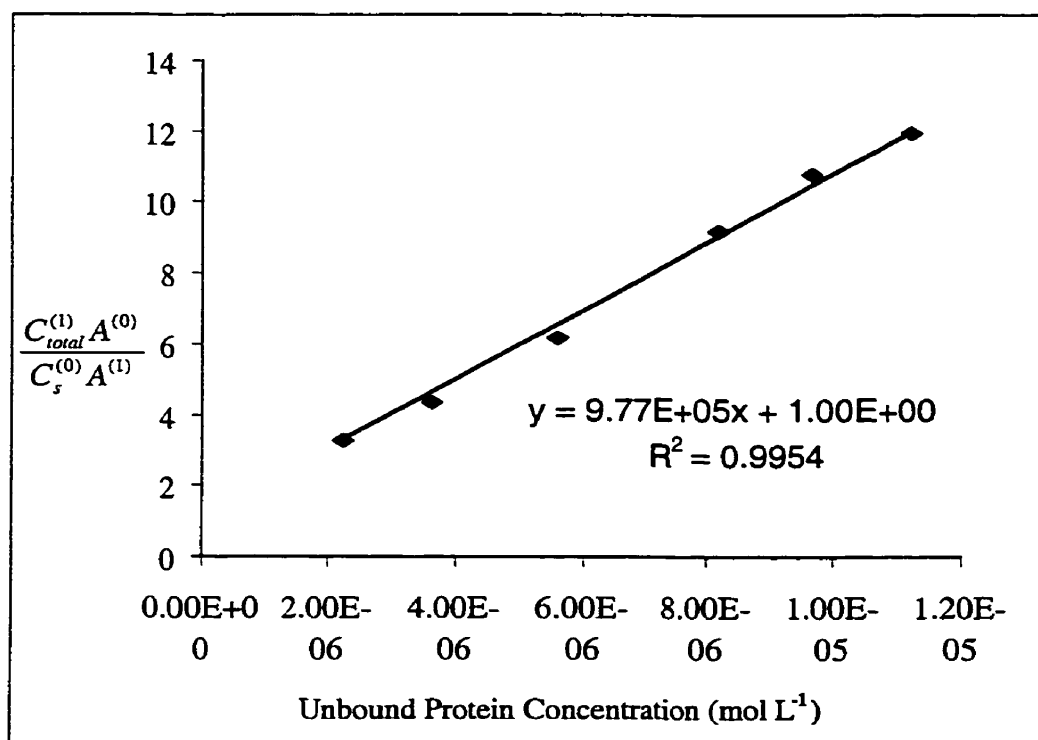


**Figure 2.14:** Direct measurement of diazepam-HSA binding equilibrium constant.

### **2.3.6 Conclusion**

SPME is an equilibrium process between the amount of drug partitioned onto the SPME fiber, the concentration of free drug and the concentration of bound drug in the solution. The portion of the drug analysed in a GC system through fiber injection represents the true amount of the drug that had reached equilibrium with the solution. Therefore, the equilibrium between the drug-protein binding process was not affected. In most cases this value is so small that it could be neglected without influencing the equilibrium system. However, the verification should be always performed before the assumption is exercised.

In this research, both the Scatchard plot and direct measurement were employed to determine the binding parameters of diazepam binding to HSA. In the direct measurement approach, no calibration and GC response factor was needed. Both the results are compared with the value obtained by different methods from the literature. The experiment demonstrates that SPME is a viable alternative approach to study protein-binding phenomena.

## **2.4 Diazepam Binding to HSA – Small Volume Analysis by SPME**

In the previous section, it was demonstrated that diazepam binding to HSA can be successfully studied by SPME. However, this application has been performed in a 2 mL vial. Although this volume is already fairly small, for some expensive or hard-to-obtain protein samples, it is desirable to further decrease the protein solution volume. In this section, the parameters of diazepam binding to protein have been measured in a small volume of protein solution (150  $\mu\text{L}$ ).

It is important to mention that the method described in Section 2.3 is perfectly suitable for the small volume analysis. The neglect of the amount of analyte on the fiber in the calibration step should always be verified, especially for small volume analysis.

### **2.4.1 Theory and Description of the Method**

In this method, a known amount of the analyte was first loaded onto to the fiber from a buffer solution with a known concentration of the analyte. For the ease of the experiment, it is better to load the analyte from a solution with a large volume so that each load can have the same amount of analyte extracted. The GC response factor has to be determined in order to know the exact amount of the analyte on the fiber. A calibration curve of amount of the analyte on the fiber vs. the free analyte concentration in the solution is constructed. This calibration curve is employed to determine the free concentration in the protein binding study.

The fiber loaded with diazepam compound is then inserted into the solution of known protein concentration, for desorption. There is no headspace for this protein solution. After equilibrium has been reached, the fiber is withdrawn from the solution and



analyzed by GC with fiber injection. The amount of the analyte left on the fiber can be determined by the GC response factor.

The drug desorbed into the protein solution consists of two phases: freely dissolved in the buffer solution or bound to protein. The free concentration of the analyte is an important parameter that needs to be determined.

The amount of the analyte initially loaded onto the fiber is the total amount of the analyte in the protein binding process. So it is termed as “ $n_{total}$ ”. When equilibrium with protein solution has been obtained,  $n_{total}$  is equal to:

$$n_{total} = n_b + n_s + n_f = C_b V_s + C_s V_s + n_f \quad \text{Equation 2.31}$$

The amount of the analyte on the fiber after the desorption to the protein solution ( $n_f$ ) can be determined from the GC response factor. Given  $n_f$ , the freely dissolved drug concentration ( $C_s$ ) can be determined from the calibration curve. Since the volume of the protein ( $V_s$ ) and the amount of the analyte loaded onto the fiber ( $n_{total}$ ) are known values, the bound concentration ( $C_b$ ) was easily calculated. The Scatchard method was finally applied to determine the equilibrium constant.

## 2.4.2 Experimental

*Chemicals, Materials and Instrumentation.* The chemicals, materials and instrumentation were used as described in Section 2.3 with the following exceptions. A polyethylene insert (Supelco, Bellefonte, PA; Catalogue number: 24798) was positioned in the 2 mL vial for the small volume analysis. The volume of the small insert was 150  $\mu\text{L}$ . The configuration of the experiment is shown in Figure 2.15.

The analytical conditions for the GC analysis were also the same as described in Section 2.3. The methods of preparing the standard sample solutions, buffer solutions, and protein solutions were kept the same.

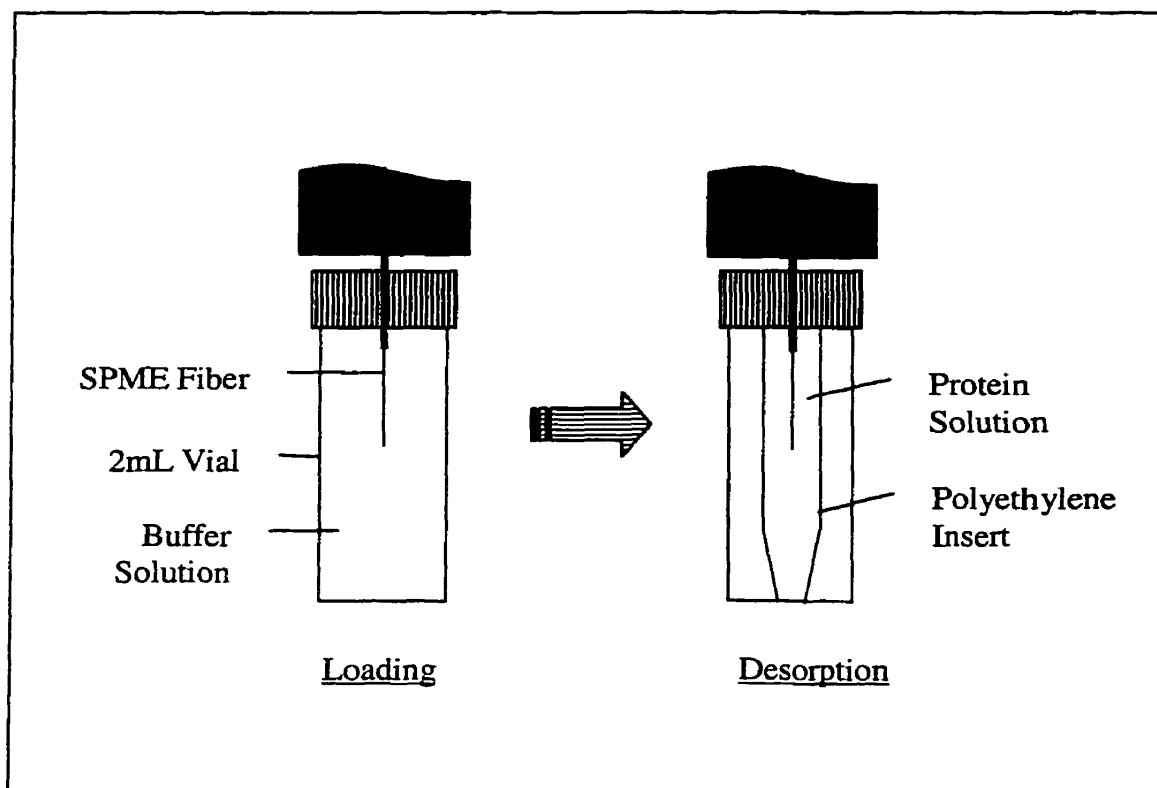


**Figure 2.15:** Experiment configurations for diazepam binding to HSA in small volume analysis.

### 2.4.3 Results and Discussion

*Drug Loading and Calibration.* The same calibration curve was obtained as illustrated in Figure 2.12. The amount of the drug loaded on the fiber was determined from this curve using the area count obtained from GC analysis. The absolute mass of the analyte loaded on to the fiber was calculated from the GC response factor, which comes from the previous analysis: 3062 per ng. This calibration curve was also employed in the protein binding study to determine the free analyte concentration.

*Determination of the Binding Parameters.* During the protein binding analysis, three concentrations were investigated. The diazepam was loaded from 500 ng/mL, 1000 ng/mL and 2000 ng/mL 2 mL buffer solutions, respectively. For each of the concentrations, 3 replicates were measured. The extraction time in the drug loading step and the desorption time in the protein solution were controlled to be 45 min. The protein concentration in this study was 0.05 mg/mL ( $7.25 \times 10^{-7}$  M). The molecular weight of HSA is 69,000 g/mol. Table 2.14 summarizes the experimental results.

The Scatchard plot is presented in Figure 2.16. From the regression equation of the Scatchard plot, the slope equals  $1.25 \times 10^6$ , y-intercept equals  $1.17 \times 10^6$ , x-intercept equals 0.93. Therefore, the binding equilibrium constant K was  $1.25 \times 10^6 \text{ M}^{-1}$  and the logK value was 6.10. The number of binding sites per protein molecule was 0.93, which is close to 1.

In this study, the protein concentration used was  $7.25 \times 10^{-7}$  M (50 ppm) instead of  $1.45 \times 10^{-5}$  M as in the last experiment. The total drug concentration introduced by the amount of the analyte loaded on the fiber was  $4.53 \times 10^{-7}$  M (128.9 ng/mL for the analyte loaded from 1000 ng/mL buffer solution). Therefore, the molar concentration of total

**Table 2.14:** Summary of the experimental data of diazepam binding to HSA in small volume analysis. The protein concentration was 0.05 mg/mL.

| $C_{load}$<br>(ng/mL) | $n_{total}$<br>(ng) | area<br>count | $n_f$<br>(ng) | $C_s$<br>(ng/mL) | $n_b$<br>(ng) | bound drug<br>percentage | $r$   | $r/[D]^*$ |
|-----------------------|---------------------|---------------|---------------|------------------|---------------|--------------------------|-------|-----------|
| 500                   | 19.8                | 8970          | 4.2           | 62.3             | 6.28          | 40.2                     | 0.203 | 926773    |
| 1000                  | 37.5                | 18566         | 7.9           | 128.9            | 10.27         | 34.7                     | 0.332 | 733083    |
| 2000                  | 68.4                | 37042         | 14.4          | 257.1            | 15.45         | 15.5                     | 0.499 | 552710    |

\*molar concentration is used.

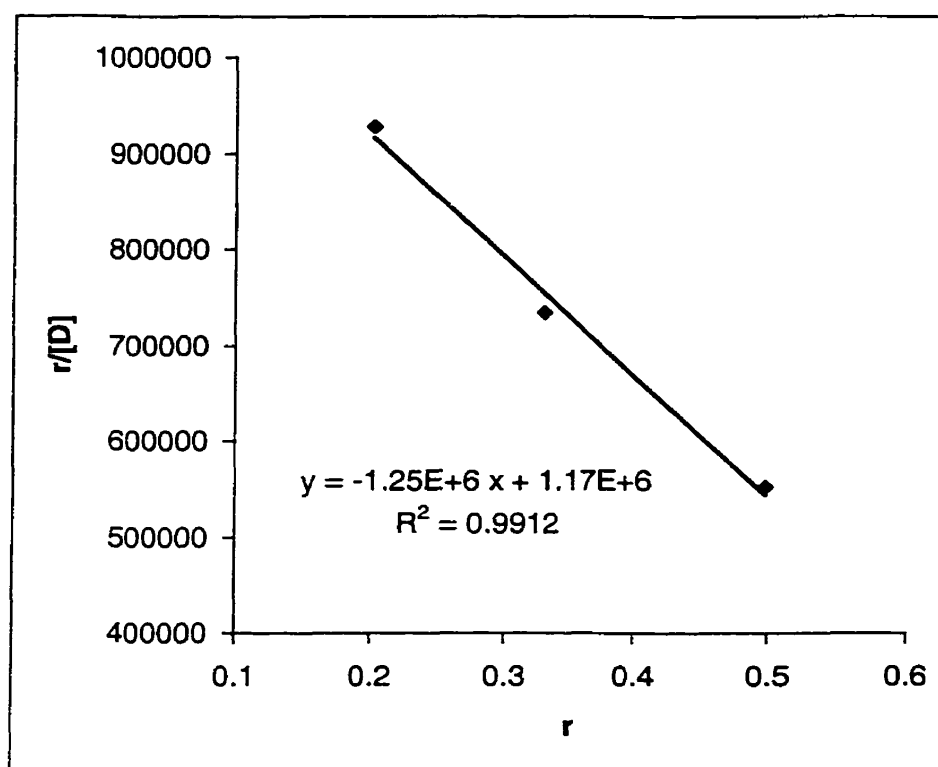


**Figure 2.16:** Scatchard plot for small volume diazepam-HSA binding analysis.

drug and protein were in the same order of magnitude. This was an important consideration in the experimental design to minimize the error for both bound and free concentration calculations.

#### 2.4.4 Direct Measurement for Small Volume Binding Study

It is possible to directly determine the diazepam binding constant without using the GC response factor. Using the same method as described in section 3.1, the fiber extraction amount (area count  $A^0$  and  $A^f$ ) without and with protein was measured. From Equation 2.12 and Equation 2.13, the binding constant could be determined.

Then how would one to calculate the total diazepam concentration  $C_s^0$  in Equation 2.13? When the fiber reached equilibrium with buffer solution without protein, the amount of diazepam left on fiber was  $n_f^0$ , the amount desorbed into the solution was  $n_{total} - n_f$ , where  $n_{total}$  is the amount of diazepam loaded on the fiber from large volume solution with diazepam concentration of  $C_{load}$ . Therefore, the equilibrium diazepam concentration without protein was  $C_s = \frac{n_f^0}{n_{total}} C_{load} = \frac{A^0}{A_{load}} \cdot C_{load}$ . The total diazepam concentration for the small volume system can be expressed as:

$$C_s^0 = \frac{n_{total}}{n_{total} - n_f^0} C_s = \frac{A^0}{A_{load} - A^0} \cdot C_{load} \quad \text{Equation 2.32}$$

Substitute Equation 2.32 into Equation 2.13, the unbound protein concentration ( $C_p$ ) was:

$$C_p = C_{p,total} - (1 - A^f / A^0) \cdot \frac{A^0}{A_{load} - A^0} \cdot C_{load} \quad \text{Equation 2.13a}$$

Table 2.15 and Figure 2.17 shows the plot of  $\frac{A^0}{A^f}$  vs.  $C_p$ . In this experiment, protein concentration of 0.05 mg/mL was used. From the plot, the diazepam to HSA binding constant was determined as  $0.995 \times 10^6 \text{ M}^{-1}$ , which agrees with the result from section 2.3.

Table 2.15: Experimental data for diazepam binding to HSA (small volume) for direct equilibrium constant measurement.

| $C_{\text{load}}$ (ng/mL) | $A_{\text{load}}$ | $A^0$ | $A^f$ | $A^f/A^0$ | $C_p$ ( $10^{-7}\text{M}$ ) |
|---------------------------|-------------------|-------|-------|-----------|-----------------------------|
| 500                       | 71140             | 13958 | 8920  | 1.564     | 5.70                        |
| 1000                      | 135109            | 27017 | 18566 | 1.454     | 4.51                        |
| 2000                      | 246424            | 48633 | 37042 | 1.310     | 3.14                        |

#### 2.4.5 Conclusion

In summary, this section provides another method to determine the drug-protein binding affinity. This method was best suited for the small volume analysis since the amount of the analyte loaded on the fiber was normally very small. Theoretically, this method provides an accurate and economical approach. But the experimental error could possibly be larger than the method described in section 2.3 due to two factors. First, it is hard to agitate the protein solution in such a small volume. In this experiment, both mechanical and manual agitation methods were applied simultaneously. Furthermore, the amount of the drug loaded by the fiber cannot be determined exactly since it involves GC

response factors. This error will be amplified since all the concentrations used for calculation of  $K$  are directly related to it.

Direct measurement method for diazepam binding constant measurement was investigated for small volume analysis. Although this method successfully avoids the determination of GC response factor, it is more prone to the error from GC measurement since it needs a complicated formula (Equation 2.13a) to calculate the unbound protein concentration.

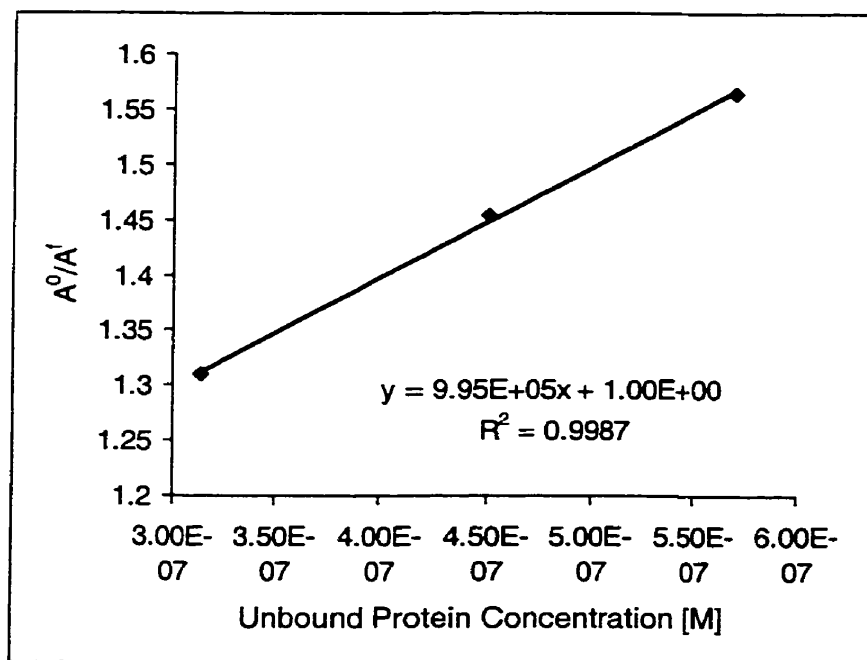


**Figure 2.17:** Direct measurement of diazepam HSA binding equilibrium constant (small volume).

## **2.5 Conclusions of Protein Binding Analysis by SPME**

Drug binding to protein has a significant meaning in drug metabolism studies and other pharmacokinetic applications. The protein binding study by SPME for volatile organic compounds, e.g. alkylbenzenes, binding to BSA, and then a common drug, diazepam, binding to HSA, have been investigated in this chapter.

Binding of volatile organic compounds to BSA, which is difficult for conventional methods, has been analyzed by SPME. The theory was discussed and possible confusions were clarified.

Normally, for protein binding study, a calibration curve is first constructed employing the solution without protein present. This calibration curve is then used to calculate the free ligand concentration in the protein solution. Special care should be exercised, especially for the binding of volatile organic compound to protein where headspace SPME is utilized.

In this chapter, a method that can directly measure the equilibrium constant without constructing a calibration curve and utilizing GC response factor was initiated. The method has been successfully applied to alkylbenzenes, diazepam and small volume diazepam binding studies. This method is suitable for the systems with first-order binding.

In conclusion, the work done in this chapter demonstrated that SPME is an accurate and very applicable method for drug-protein binding study.



## 2.6 References

---

1. La Du, B. N.; Mandel, H. G.; Way, E. L. *Fundamentals of Drug Metabolism and Drug Disposition*, The William & Wilkins Company, **1971**, 67.
2. Seydel, J. K.; Schaper, K.-J. *Pharmacol. Ther.*, **1982**, 15, 131.
3. Tillement, J.-P.; Lindenlaub, E (ed). *Protein Binding and Drug Transport*, F. K. Schattauer Verlag - Stuttgart, New York, **1986**, pp 5-7.
4. Potter, G. D.; Guy, J. L. *Proc. Soc. Exp. Bio. Med.*, **1964**, 116, 658-660.
5. Scatchard, G. *J. Am. Chem. Soc.*, **1949**, 51, 660-692.
6. Fletcher, J. E.; Spector, A. A. *Comp. and Biomed. Res.*, **1968**, 2, 164-175.
7. Nozaki, Y.; Gurd, F. R. N.; Chen, R. F.; Edsall, J. T. *J. Am. Chem. Soc.* **1957**, 79: 2123-2129.
8. Li, J.; Carr, P. *Anal. Chem.*, **1993**, 65, 1443-1450.
9. Veas, W. H. J.; Ramos, E. U.; Legierse, K. C. H. M.; Hermens, J. L. M. in Pawliszyn, J. (ed.), *Applications of Solid Phase Microextraction*, The Royal Society of Chemistry, UK, **1999**, pp129 – 139.
10. Langenfeld, J. J.; Hawthorne, S. B.; Miller, D. J. *Anal. Chem.*, **1996**, 68, 144-155.
11. Pawliszyn, J. *Solid Phase Microextraction: Theory and Practice*, Wiley-VCH, Inc., **1997**, p146, p156.
12. Schwarzenbach, R. P.; Gschwend, P. M.; Imboden, D. M. *Environmental Organic Chemistry*, John Wiley & Sons, Inc., Appendix.
13. Martin, B. K. *Nature*, **1965**, 207, 274-276.
14. Behrens, P. Q., Spiekerman, A. M., Brown, J. R., *Fedn Proc.* **1975**, 34, 591

15. Meloun, B., Moravek, L., Kostka, V., *FEBS Lett.* **1975**, *58*, 134-137.
16. Brown, J. R.; Shockley, P. Serum albumin: structure and characterization of its ligand binding sites. In: Jost, P. C.; Griffith, O. H. (eds.). *Lipid-protein interactions*, Vol. 1, pp25-68, John Wiley and Sons Inc., New York, **1982**.
17. Ashbrook, J. D.; Spector, A. A.; Santos, E. C.; Fletcher, J. E. *J. Biol. Chem.*, **1975**, *250*, 2333-2338.
18. Goodman, D. S. *J. Biol. Chem.*, **1958**, *80*, 3892-3898.
19. Mulé, S. J.; Casella, G. A. *J. Anal. Toxicol.*, **1989**, *13*, 179-184.
20. Drouet-Coassolo, C.; Aubert, C.; Coassolo, P.; Cana, J. *J. Chromatogr.* **1989**, *487*, 295-311.
21. Müller, W. E.; Wollert, U. *Naunyn-Schmiedeberg's Arch. Pharmacol.* **1973**, *280*, 229-237.
22. Müller, W. E., Wollert, U., *Naunyn-Schmiedeberg's Arch. Pharmacol.* **1974**, *283*, 67-82.
23. Coassolo, P., Sarrazin, M., Sari, J. C., and Briand, C., *Biochem. Pharmac.* **1978**, *27*, 2787-2791.
24. Müller, W. E., Wollert, U., *Pharmacology*, **1979**, *19*, 59
25. Sudlow, G., Birkett, D. J., Wade, D. N., *Molec. Pharmac.* **1976**, *12*, 1052
26. Sjöholm, I., Ekman, B., Kober, A., Ljungstedt-Pahlman, I., Seiving, B., Sjödin, T., *Molec. Pharmac.* **1979**, *16*, p. 767
27. Müller, W. E., Wollert, U., *Naunyn-Schmiedeberg's Arch. Pharmacol.* **1975**, *288*, 17
28. Müller, W. E., Wollert, U., *Molec. Pharmac.* **1975**, *11*, 52-
29. Sjödin, T., Roosdorp, N., Sjöholm, I., *Biochem. Pharmac.* **1978**, *25*, 2131-2140.

## **CHAPTER 3**

### **DETERMINATION OF THEOPHYLLINE BY IMMUNOAFFINITY**

#### **SPME AND IN-TUBE SPME IN SERUM**

### **3.1. Introduction**

#### **3.1.1 Background**

Taking advantage of the extraordinary molecular recognition ability of antibodies, the immobilization of an antibody on a solid surface plays an important role in modern biotechnology for the development of rapid and sensitive analytical methods. This technique is especially crucial for the analysis of the complex matrices, such as biological samples, which often contain many different components contributing to some level of interference.

From the first adsorption immobilization of invertase onto charcoal and alumina by Nelson and Griffin in 1916 (1), through the intense research activities in the 1960s, immobilization of enzymes emerged in the 1970s as a major commercially viable technology for food and drug processing.

From the base technology derived from enzyme immobilization, immobilization methods of other proteins, such as antibodies, have been developed. Immobilized antibodies have been used in established immunoassays such as enzyme-linked immunoassay, radioimmunoassay, fluoroimmunoassay (2, 3). They also form the basis of modern clinical diagnostics and are widely applied to new detection and diagnostic devices, such as biosensors (bioaffinity sensors), for applications in medicine, food and drug processing and environmental monitoring (4). Immobilized antibodies and binding

proteins also serve as the basis for biospecific separations, such as affinity chromatography and filtration, which are applied to the production of new genetically engineered products, such as drugs and hormones (5-11). An antibody-coated immunosorbent has also been used for extremely sensitive (part per trillion (ppt) level) pesticides analysis by coupling on-line with liquid chromatography/atmospheric pressure chemical ionization/mass spectrometry (LC/APCI/MS) (12).

The objective of the study presented in this chapter is to develop a viable method to perform immunoaffinity SPME extraction for the analysis of complex biomatrices based on antibody immobilization techniques.

### **3.1.2 Antibody and Antigen**

Antibodies (Ab) are an important subclass of proteins. Ab are highly selective molecules (glycoproteins) produced by mammalian immunological systems following exposure to a foreign molecule, i.e. an antigen. Of the many antibodies employed as the recognition element, immunoglobulin antibodies, and in particular immunoglobulin G (IgG), are among the most frequently used.

IgG is a globular, Y-shaped protein with dimensions of approximately  $10 \times 14 \times 5$  nm as determined by X-ray crystallography (13). The IgG antibody is composed of four polypeptide chains, two heavy and two light chains linked via disulfide groups (14); it bears two receptor sites, Fab (fragment antigen binding), and a carbohydrate Fc (fragment crystallizable) portion located at the base of the Y (Figure 3.1). The variable regions of the Fab fragments are the location of the binding site for the specific antigen. There are two binding sites per IgG.

Immunoglobulins can be cleaved at the middle of their H chains by various proteases (15). For example, papain cleaves chains at the N-terminal side of the disulphide bridges that keep the H chains together, thereby generating two Fab fragments and one Fc fragment.

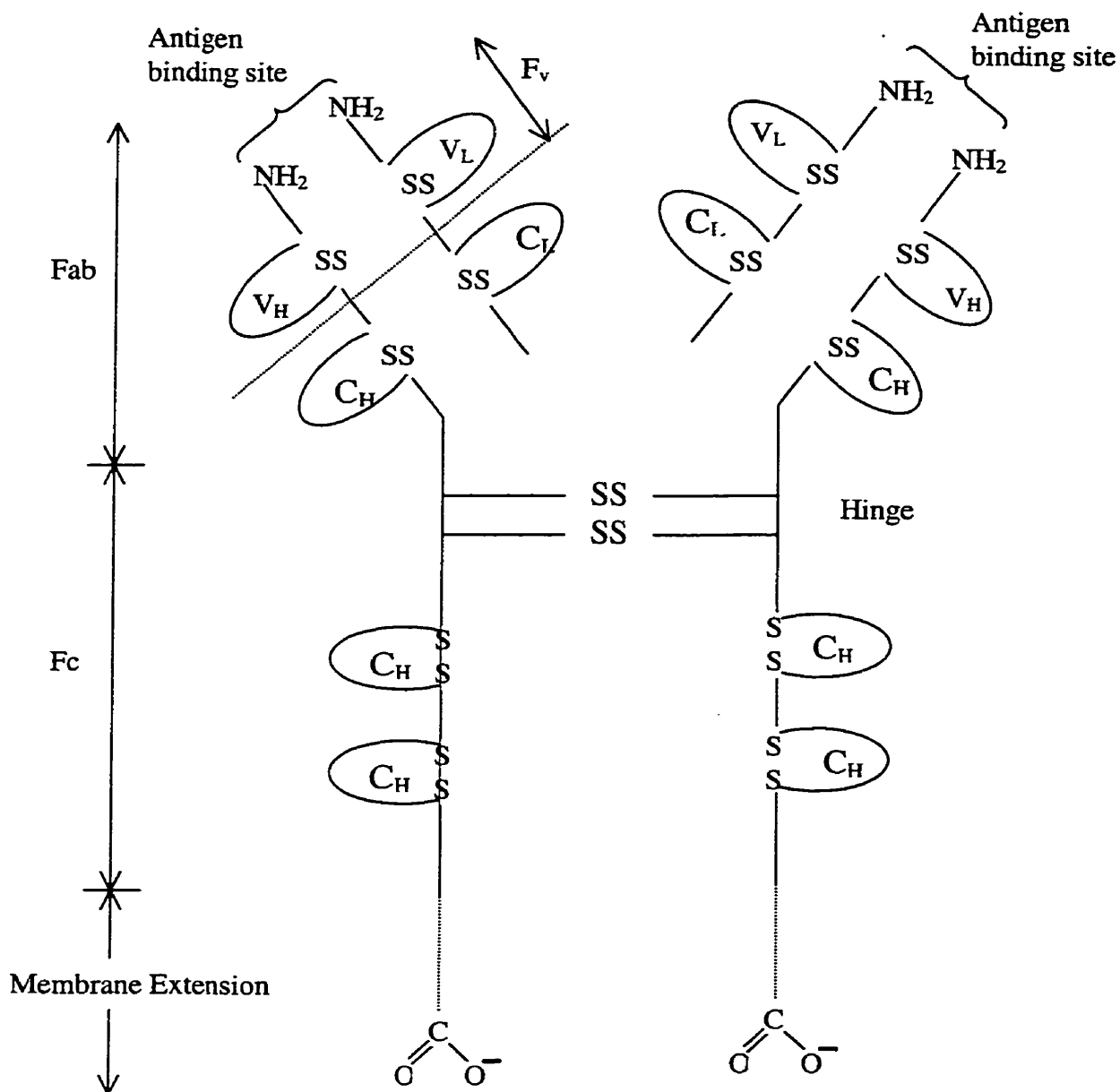


**Figure 3.1:** Schematic of the structure of IgG antibody molecule. The four polypeptide chains, two heavy and two light chains, are linked via disulfide groups. The number of these disulfide groups can vary, depending on the source of the antibody.

### 3.1.3 Antibody Immobilization

*Selection of the Support and Immobilization of Antibody.* An ideal support for antibody immobilization should have the following characteristics: 1) be rigid and porous to allow more attachment of samples; 2) providing functional groups to enable appropriate coupling with a sufficient amount of antibodies; and 3) be hydrophobic, to avoid nonspecific interactions with the analytes and the sample matrix (16).

Many types of insoluble supporting materials have been utilized for antibody immobilization. However, few materials can satisfy all of these criteria. Cyanogen bromide-activated Sepharose has been mostly used in immunoaffinity applications (17). This support has very few nonspecific interactions, which is ideal for complex samples. But its positively charged groups at neutral pH and the toxicity of CNBr make it unsuitable for biological sample analysis. Rigid synthetic polymers are another group of support that is widely used. In general, these supports allow a good orientation of the antibodies, which are covalently bonded to the functional groups of the support material. However, nonspecific interactions may occur between the polymer matrix and the analyte (18).

At present, aldehyde-activated silica support is the best in terms of the performance for its very low level of nonspecific interactions, its high stability over a wide pH range and its resistance to high pressure. Possible disadvantages include low binding capacity and poor orientation of the antibody sites (18). However, these drawbacks can be overcome by choosing proper immobilization methods.

*Preparation of the Silica Surfaces.* The preparation of the silica surface is very important for the antibody immobilization. The purpose of the surface preparation is to clean the surface free of grease and other contamination and to hydroxylate the surface for exposure of more silanol groups (-Si-OH). The silanol group allows the modification of the surface with a variety of functional groups, through the covalent attachment of silane molecules.

The experimental procedure used for the preparation of surfaces can be summarized as follows (19, 20):

Glass/quartz supports with chemically polished surfaces should be sonicated subsequently in a detergent solution, rinsed with large amount of distilled water, wiped with an acetone-soaked cotton swab, and sonicated again in dichloromethane to remove the traces of polishing agent (usually it is an epoxy resin) from the surface.

Normally there are two methods that can be used to perform the further cleaning and activation. a). Precleaned supports can be placed in a freshly prepared 'piranha' solution, 70:30 (v/v) concentrated sulfuric acid : 30% hydrogen peroxide, for 1 h at 60-70°C or under ultrasound. (Caution: Piranha solution is extremely corrosive and can react violently with organic compounds.) b). Alternatively, the supports can be treated with sulfochromic solution for 30 min at 70-80 °C. In both of the methods, the supports are subsequently rinsed with a large amount of distilled water, dried under a nitrogen stream, and used immediately.



*Modification of the Surfaces with Siloxane Polymers.* The first class of compounds that can be used for the covalent immobilization of proteins to both silicone and silicone dioxide surfaces is functionalized silanes. The surface of silica is formed by silanol (-Si-OH) and siloxane (-Si-O-Si-) groups. The surface concentration of silanol groups typically ranges between 1 and 3  $\mu\text{mol}/\text{m}^2$  (21, 22). The purpose of the chemical modification is to form a cross-linked siloxane monolayer on the surface and to provide a high concentration of functional groups that can be further activated for binding with proteins.

Silanes used for surface modification can be classified under two main groups: alkyltrichlorosilanes with the general formula  $\text{Cl}_3\text{-Si-(CH}_2)_n\text{-X}$  (where X is -CH<sub>3</sub>, -CF<sub>3</sub>, -CH=CH<sub>2</sub>) and alkoxy silanes with the general formula  $\text{R}_3\text{-Si-(CH}_2)_n\text{-X}$  (where R is -OMe, -OEt, -CH<sub>3</sub>, and X is -NH<sub>2</sub>, -SH, -glycidyl, etc.).

Functional groups on the silica surface formed from silane monomers (-NH<sub>2</sub>, -SH, -OH) can be chemically modified to form the active intermediates that can react with protein. There are two main types of functional groups on protein molecules that can be employed to attach the protein molecule onto the chemically modified silica surface: the primary amine group of the lysine residues on the external surface of the globular molecular and the sulfhydryl groups on the free cysteine residues. Many methods, including the types and the conditions of the reaction, have been investigated. Detailed reviews of protein immobilization methods can be found in references 23 and 24.

In this thesis, the silica surface was first activated with (3-aminopropyl) triethoxysilane (APTES), leaving a primary amine group on the surface. Then glutaraldehyde was subsequently used to modify the surface, yielding an aldehyde that

can form an imine linkage with the primary amines on the protein. The antibody molecules were finally attached on the silica surface through the reaction between the amine group on the protein and the aldehyde group on the surface.

### **3.1.4 Immunoassay**

Immunoassay (IA) is an analytical method that employs antibodies for the determination of sample components. Because of the extraordinary affinity, specificity, and variety of antibody-antigen binding reactions, immunoassays have become essential routine and research tools throughout the biological sciences, particular in clinical analysis. Currently, with the development and wide application of protein immobilization techniques, most of the immunoassays, especially nonisotopic immunoassays, rely on immobilized antibody (25, 26). The immunoassay method has been used in this thesis to test the applicability of the antibody immobilized silica surface for SPME immunoaffinity extraction.

There are numerous forms of immunoassays, each classified according to a range of criteria such as sample type, the nature of the analyte, assay conditions, etc. Based on the detection methods, immunoassay can be categorized as enzyme-linked immunosorbent assay (ELISA), radioimmunoassay (RIA) and fluoroimmunoassay (FIA) (2, 3). In ELISA, the analyte is measured with an enzyme-conjugated antibody and the enzyme substrate. In RIA, the radioactivity of the radiolabeled analyte is measured to indicate the amount of the bound analyte. In FIA, the bound analyte is quantitated by the fluorescence intensity.

Based on the mechanism of the assay, the immunoassay can be subdivided into two categories: non-competitive solid-phase immunoassays and competitive solid-phase immunoassays. A general approach of non-competitive, solid-phase immunoassay is illustrated in Figure 3.2 (a) by employing radiolabeled antigen (RIA) as an example. The antibody was first immobilized onto the silica surface and then these antibody molecules extract the corresponding antigens (analytes) from the sample solution. The extracted analytes are finally detected by their radioactivities. In this analysis, the radioactivity is normally proportional to the free antigen concentration, if it is far below the antibody saturation level.

Figure 3.2 (b) illustrates the principle of the competitive, solid-phase immunoassay. In this method, the assay is based on the competition of antigen (analyte) with radiolabeled analogue of the analyte for the limited number of antibody binding sites. The immobilized antibodies are employed to extract the mixture of radiolabeled and non-radiolabeled antigen samples. The concentration of the hot (radiolabeled) analyte is kept constant and the concentration of cold (non-radiolabeled) antigen is varied. The concentration of the cold analyte is therefore inversely proportional to the amount of labeled analyte bound to the antibody.

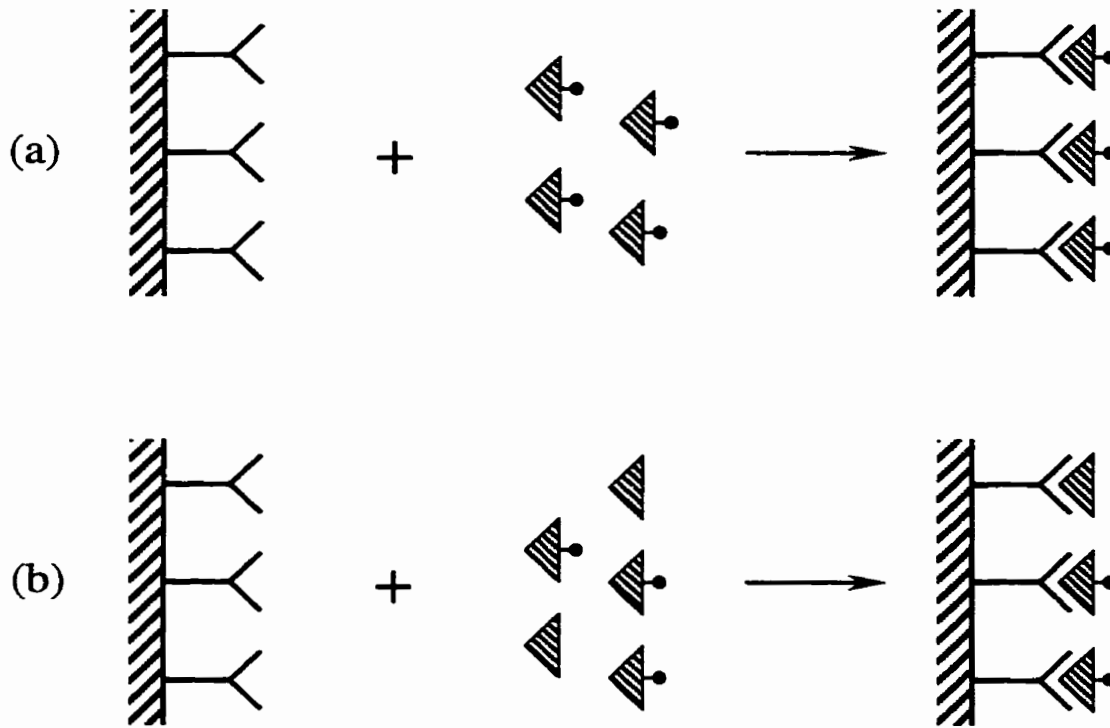


**Figure 3.2:** Non-competitive (a) and competitive (b) solid-phase radioimmunoassay.

▴: Antigen (analyte); ▴•: Radiolabeled antigen; —Y: Antibody molecule;

▨—Y: Immobilized antibody.

### 3.1.5 Scintillation Detection

In RIA, the radioactivity of the radiolabeled antigen is detected by a liquid scintillation counter. Scintillation detection has certain distinct advantages such as introducing labels that induce only very minor changes to the structure of the labeled antigen, and also high sensitivity. A tritiated molecule has the same molecular size as the non-radioactive antigen, making the usage of these materials very convenient to study binding reactions of small molecules. However, sometimes the regulatory constraints in their usage and clean up costs make radioactivity a poor choice for a convenient immunoassay.

The first commercial model of liquid scintillation counter became available in 1954, soon after the basic principles of liquid scintillation were discovered in 1950 (27). As shown in Figure 3.3, the process of liquid scintillation counting is relatively simple. The beta decay electron emitted by the radioactive isotope in the sample excites a solvent molecule, which in turn transfers the energy to the solute, or fluor. The energy emission of the solute (the light photon) is converted into an electrical signal by a photomultiplier tube (PMT).

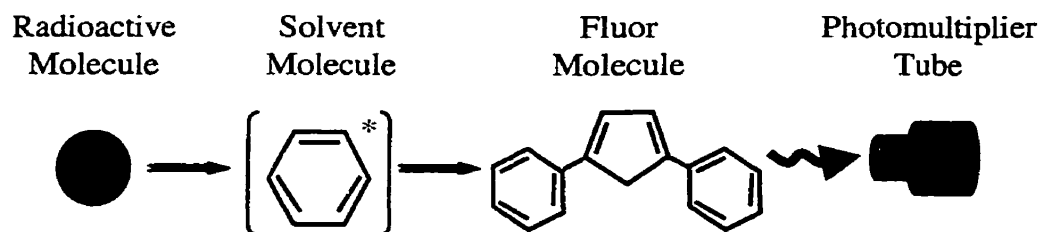


**Figure 3.3:** The scintillation process.

The mixture of organic solvents and solutes is referred to as the scintillation cocktail. The main components of solvents include benzene, fluorobenzene and m-, p-, o-xylene. This mixture is designed to capture the beta emission and transform it into a photon emission, which can be detected via a photomultiplier tube within a scintillation counter. The cocktail must also act as a solubilizing agent, keeping a uniform suspension of the sample.

Several physical processes may interfere with the efficiency of liquid scintillation counting: chemiluminescence, photoluminescence, and other processes that are generally referred to as background. Chemiluminescence is the spurious generation of light emissions as a result of chemical reactions between additives or specimens and the components of liquid scintillation. These photon emissions are the result of chemical energy converted into molecular excitation energy, which in turn undergoes electronic decay with the emission of a photon detected by the PMTs. To reduce the effects of this phenomenon, samples should be equilibrated for a certain period of time in the scintillation counter. Photoluminescence is simply the emission of photons from an excited molecular species. This may occur in vial walls, caps, and other material activated by light. Photoluminescence can be reduced by acidification of the solubilized sample, but can be best eliminated by dark-adaptation of samples several hours before counting. The numerous processes grouped under the heading of background include chance coincidence, Cherenkov radiation, cross-talk between PMTs, and some existing form of natural radioactivity such as thorium, potassium-40, and uranium.

### 3.2 Experimental

*Chemicals and Materials.* All chemicals were used as purchased. Theophylline antiserum (developed in rabbit, product number: T-2524),  $^3\text{H}$ -theophylline (specific activity 14.5 Ci/mmol, concentration 12.4  $\mu\text{g}/\text{mL}$ , product number: T4924), theophylline, caffeine, (3-aminopropyl)triethoxysilane (APTES), glutaraldehyde (25% aqueous solution), ethanolamine, trifluoroacetic acid (TFA), sodium azide and the prepackaged phosphate buffered saline (PBS, pH = 7.4) were all purchased from Sigma-Aldrich (Mississauga, ON, Canada). Diazepam was purchased from Radian (Austin, TX) as a 1 mg/mL methanol solution. Water was obtained from a Barnstead/Thermodyne NANO-pure ultrapure water system (Dubuque, IA). Figure 3.4 shows the chemical structures of theophylline and caffeine.

The fused silica fibers (1800  $\mu\text{m}$  diameter, no cladding, no buffer, part number: FSnn1800) and fused silica capillaries (i.d. = 347  $\mu\text{m}$ ) were all purchased from Polymicro Technologies Inc. (Phoenix, AZ).

Ecolume liquid scintillation cocktail and 20 mL polyethylene scintillation vials were purchased from ICN Pharmaceuticals (Costa Mesa, CA). The dispenser for the scintillation cocktail was purchased from VWR Scientific, Canada. A Beckman-Coulter liquid scintillation counter, model LS1701 (Fullerton, CA) was used for radioisotope counting. Culture tubes (13  $\times$  75 mm) were purchased from Fisher Scientific (Nepean, ON, Canada).

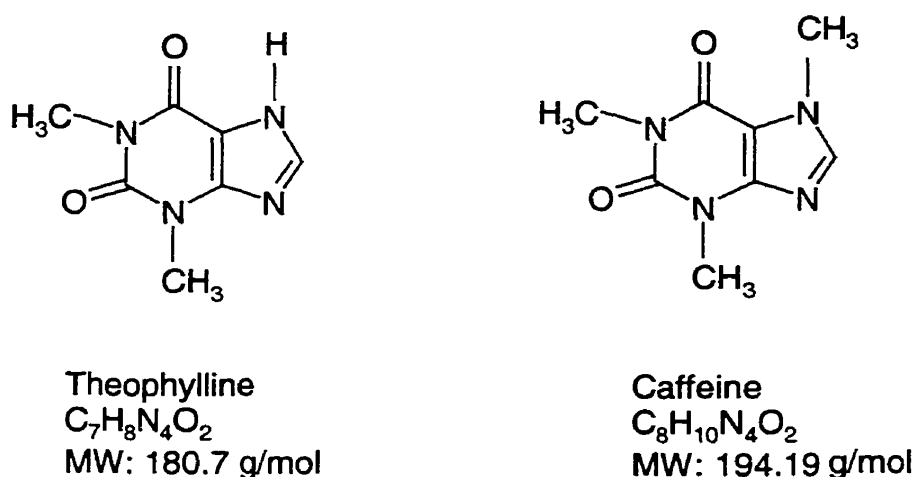


**Figure 3.4:** Chemical structures of theophylline and caffeine.

*Preparation of Standard Mixtures.* The theophylline and caffeine 1 mg/mL ethanol solutions were prepared by measuring the desired amount of the compounds into a certain amount of ethanol. The 0.1 mg/mL, 0.01 mg/mL, 0.001 mg/mL theophylline and caffeine solutions were prepared by subsequently diluting the stock solution with ethanol and PBS. The  $^3H$ -theophylline solution was diluted with ethanol 100-, 1000-, 10,000- fold to provide 124 ng/mL, 12.4 ng/mL and 1.24ng/mL standard solutions, respectively.

The 1 mg/mL of diazepam solution was diluted with methanol into 0.1mg/mL, 0.01mg/mL, 0.001mg/mL solutions for the convenience of the experiment. PBS solution was prepared by diluting one pack of prepackaged PBS powder with 1L NANO-pure water in volumetric flask according to the manufacturer's instruction. The pH 9.2 0.1 M carbonate buffer solution was prepared by mixing 0.1 M sodium carbonate and 0.1 M sodium bicarbonate under the monitoring of pH value with a pH meter. The 0.05%



sodium azide solution was prepared by measuring the desired amount of sodium azide into PBS solution. All the fused silica fibers and capillaries were stored in sodium azide (0.05%) PBS solution in the fridge (4°C) after coating with antibodies.

### 3.2.1 Method

#### 3.2.1.1 Preparation of the Antibody Immobilized Surface

*Preparation of the Fused Silica Surface.* The silica fibers were cut into 23 mm length pieces. This size of fiber can fit into a 13 × 75 mm culture tube, in which all the surface reactions for the fibers took place at room temperature. About 20 fibers were contained in the culture tube. The fused silica capillary was cut into 60 cm long pieces, coiled and put in a beaker.

The fused silica surfaces were cleaned with a 30:70 mixture of 30% hydrogen peroxide (H<sub>2</sub>O<sub>2</sub>) and concentrated sulfuric acid (H<sub>2</sub>SO<sub>4</sub>) with ultrasonication for 1 hour and then thoroughly rinsed in water, pure ethanol and water with ultrasonication respectively. The cleaning of the fiber was performed in the culture tube, while the cleaning solution was injected into the capillary when the inner surface of the capillary was cleaned. Special care should be exercised so that the surface of the fused silica was not touched with fingers to avoid any contamination (19, 22, 28).

*Silanization of Cleaned Silica Surfaces.* After the surface pretreatment, the capillary was interfaced to a Razel syringe pump, model A-99 (Stamford, CT) as shown in Figure 3.5. The connection was simply accomplished by inserting the affinity SPME capillary inlet and syringe outlet into a small piece of tight fitting teflon tubing. All the

reactions to the inner surface of the capillary were conducted with this device. The reactions to the surface with the fiber were performed in the same culture tube.

The silanization reaction scheme is shown in Figure 3.6 (a). APTES was used as the silanization reagent. For the silica fiber, the reaction was performed in the same culture tube as that in the cleaning step. For the silica capillary, the reaction was performed with the syringe pump assembly. A fresh ethanol solution of APTES was prepared with 5% of APTES, 5% of deionized water and 90% ethanol (v/v). The fibers/capillaries were allowed to react with this solution for 30 min at room temperature.

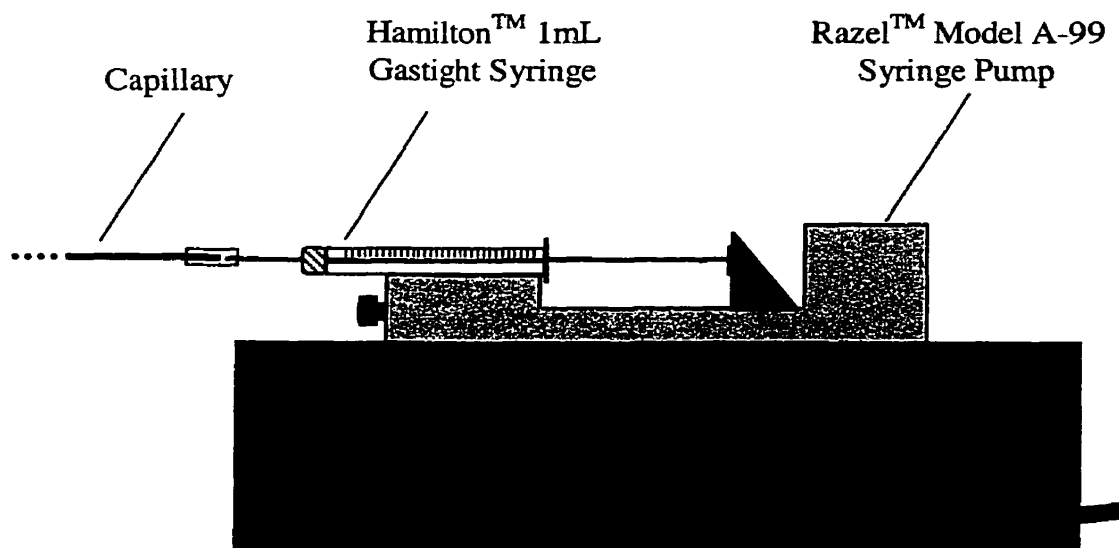


**Figure 3.5:** The schematic diagram represents the configuration of the capillary interfaced with the syringe pump for the inside-tube reactions.

In this reaction, the ethoxyl groups were first reacted with water in the solution to form silanol groups (-Si-OH). The hydrolysis of ethoxyl groups is followed by the formation of siloxane oligomers in the solution. These oligomers, as well as the monomers containing free silanol groups, diffuse onto the surface and physically adsorb on it. The final and slowest step is the film formation process, which forms -Si-O-Si- bond through the reaction with silanol groups on the surface (22).

After the reaction, the fibers/capillaries were rinsed with water ten times followed by rinsing with ethanol twice. They were then cured in a vacuum oven, which had been flushed with nitrogen three times, at 60°C for overnight (about 15 hours).

*Surface Modification with Glutaraldehyde.* The reaction scheme for the coupling of glutaraldehyde to the silanized overlayer step is illustrated in Figure 3.6 (b). Glutaraldehyde has two aldehyde groups on each end of the carbon chain. One end is reacted with the amino groups of APTES on the silica surface and the other end reacts with the amino groups (of lysine residue) on the antibody molecules.

Glutaraldehyde is the most commonly used reagent in protein immobilization since it is inexpensive, readily available, and easy to use. Detailed research shows that the commercial aqueous solutions of glutaraldehyde (25% or 70%) represent multi-component mixtures, which include free glutaraldehyde, mono- and dihydrate, a cyclic hemiacetal and oligomers (29). The pH of these aqueous solutions is 3.1. It is obvious that each of these components participates differently in cross-linking reactions. But they all exhibit the ability to react and cross-link with protein. Since the product of the reaction of glutaraldehyde to protein is very stable even without further reduction, it was suspected that the product is not through the formation of a Schiff base (29). The details

of the proposed reaction mechanism of the glutaraldehyde coupling can be found in reference 29.

The silanized fused silica surfaces were allowed to react with 2.5% of glutaraldehyde in PBS for 1.5 hour followed by thoroughly rinsing with PBS buffer.

*Immobilization of Antibody.* The glutaraldehyde activated surfaces were then reacted with an antibody solution for 10 hours. One vial of theophylline antiserum was diluted with 2 mL pH 9.2 carbonate buffer(0.1M) and added to the culture tube containing 20 fused silica fibers. A 0.6 mg/mL antibody solution (carbonate buffer at pH = 9.2) was prepared and allowed to react with the capillary inner surface by fully filling the capillary with the antibody solution.

After the reaction, the antibody-coupled fibers/capillary were rinsed with PBS and the remaining aldehyde groups on the surface were deactivated with ethanolamine (0.2M) in PBS for 1 hour. The fibers/capillary were then rinsed with PBS and stored in 0.05% solutions of sodium azide in PBS for future use.

*Binding and Desorption Conditions.* Once the antibodies have been immobilized on the silica surface, they are ready for direct extraction. Ionic attraction, hydrogen bonding, hydrophobic attraction and van der Waals forces are all involved in the antigen-antibody interaction. Therefore, the pH value of the sample solution is very important for the binding. Normally, the maximum bindings are obtained at pH about 7.4, which is the pH value of human blood (4). Therefore, in this experiment, the pH = 7.4 PBS solution was used.

While the antibody immobilized fibers were not designed for repeated usage, the antibody immobilized fused silica capillary was intended for repeated extraction and dissociation. The dissociation method should be carefully considered and chosen.

Theoretically, dissociation of the antibody-antigen complex can be accomplished by any solution that is able to disturb the binding forces mentioned above. Furthermore, the elution buffer must not denature the antibody to allow the antibody-immobilized surface to be regenerated.

The introduction of excess protons or hydroxyl ions by changing the pH of the elution buffer is one of the most widely used elution procedures. Alternatively, the ionic strength of the elution buffer can be altered by the addition of chaotropic salts such as sodium thiocyanate and sodium chloride (1.5 – 8 mol/L) (30). An antibody-antigen complex can also be dissociated by the addition of any solution that contains polarity-reducing agents (i.e. ethylene glycol, methanol, ethanol, and acetonitrile). These agents act by reducing the polarity of the solution surrounding the antibody-antigen complex and thus neutralizing the hydrophobic forces responsible for the attraction. Although it was thought that organic solvents would irreversibly denature antibodies, there are certain methods that use high concentrations of organic polarity modifier without the loss of antibody response (17, 31).

Considering the method developed in this thesis has the potential to be coupled to a highly sensitive HPLC system, methanol : water : TFA 70 : 29 : 1 (v/v) was employed for desorption.

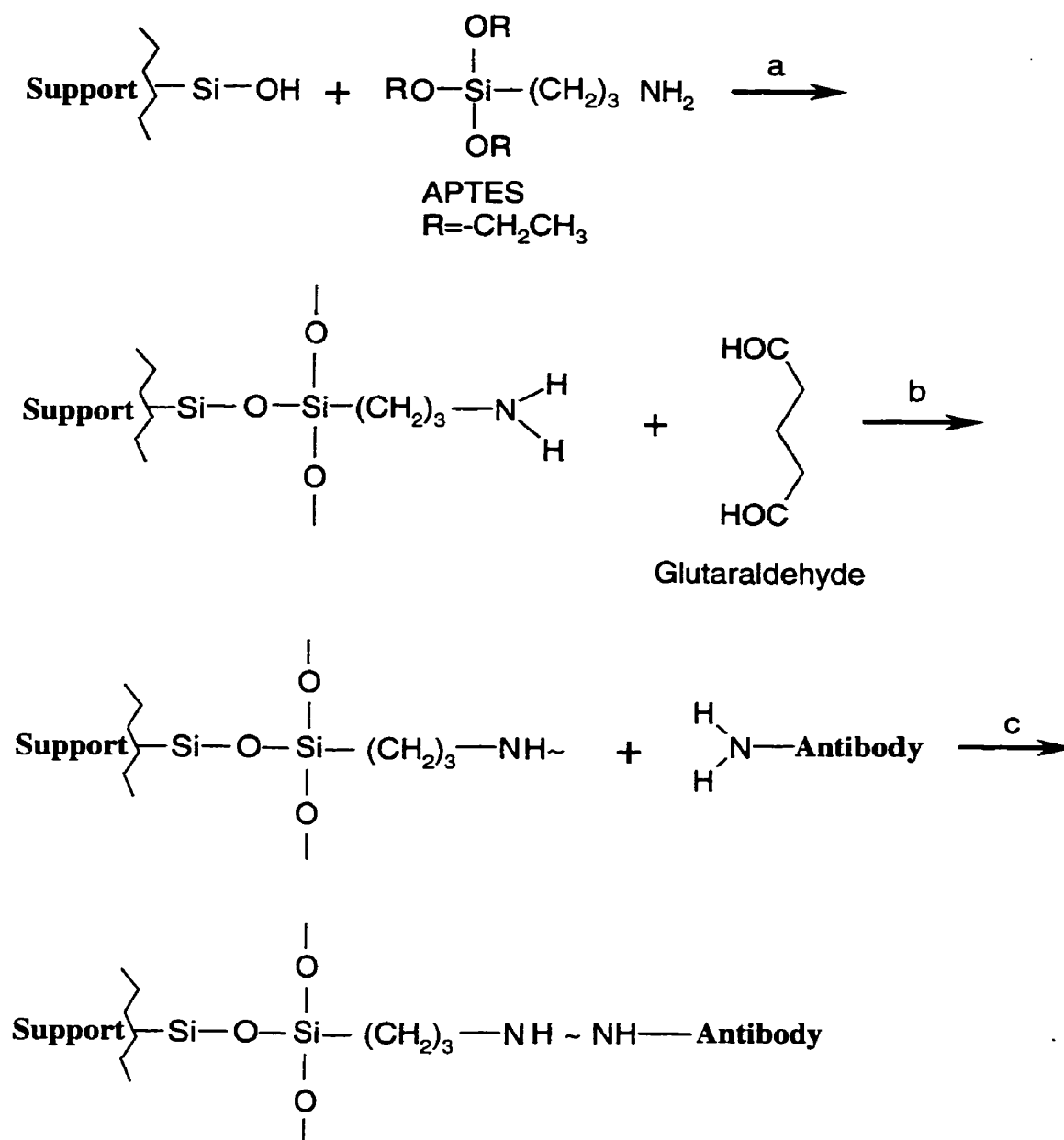


**Figure 3.6:** Reactions involved in the antibody immobilization. a. Silanization of silica surface with APTES; b. Surface modification with glutaraldehyde; c. Immobilization of antibody.

### 3.2.1.2 Test of the Antibody Immobilized Surface

*Antibody immobilized fiber.* Several experiments have been designed to test the performance of the antibody-coated surfaces. The basic procedure is described as follows by using analysis of antibody activity as an example. The fibers were removed from their storage solutions, and incubated in a freshly diluted,  $^3\text{H}$ -theophylline in PBS for 3 hours at room temperature on a shaking bed. The fibers were then removed from the solution, washed twice by totally immersion in PBS and then placed in scintillation vials containing 20 mL of scintillation cocktail. The vials were vigorously shaken and counted in duplicate with the liquid scintillation counter for 5 min. The average values of the two counts were considered as the final counting results. This completely removed the labeled theophylline from the fiber as determined by subsequent counting of the fiber in fresh scintillation cocktail.

The competitive binding was analyzed by incubating the antibody-coated fibers in a solution of  $^3\text{H}$ -theophylline and caffeine at different concentrations. The binding specificity was investigated by using a fixed concentration of  $^3\text{H}$ -theophylline together with various amounts of cold diazepam, which possesses no specific binding to anti-theophylline. In this analysis, the  $^3\text{H}$ -theophylline was kept at a concentration that can saturate the antibody-coated fiber and the concentrations of cold diazepam were varied.

A human serum sample was finally analyzed. Certain amount of the theophylline was first added into the serum sample. The serum sample was diluted 100 fold and then the same analysis was performed. **Safety cautions:** Human serum sample is a potential biohazard. Unused serum samples should be treated with Javex before disposal as hazardous waste.

*Antibody immobilized capillary.* For experiments with the capillary tubing, the similar scheme was used except that the experiment configuration was different. The capillary was mounted on the syringe pump as shown in Figure 3.5 for the ease of the experiment. Both plastic connecting tubing and syringe were disposed of after each sample to avoid cross-contamination. Unless otherwise specified, a flow rate of 14  $\mu\text{L}/\text{min}$  was used to introduce the analyte sample and 30  $\mu\text{L}/\text{min}$  for the wash and desorption solutions. The desorption solution was collected in a 20 mL polyethylene scintillation vial containing 20.0 mL Ecolume scintillation cocktail for scintillation counting. Prior to all injections, the affinity SPME capillary was conditioned with PBS for 10 min.

## **3.2.2 Results and Discussion**

### **3.2.2.1 Reaction of Antibody Immobilization**

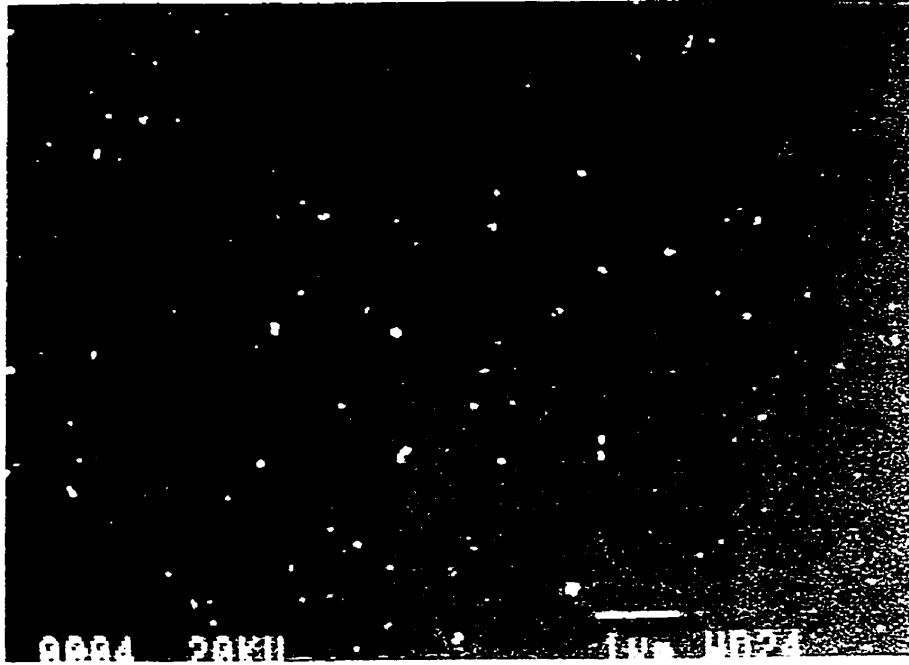
While there are many methods capable of immobilizing antibodies on a fused silica surface, it was found that the method used in this study is one of the most convenient, since the reaction conditions were very mild – the entire immobilization was performed at room temperature.

It was found that the surface cleaning is the most crucial step for the whole reaction. A relatively mild cleaning method, such as cleaning with pH 10  $\text{NH}_4\text{OH}$  solution results in no immobilization at all. This is either because of contamination from grease and other coating covering the surface or the hydroxylation with this method is not sufficient to expose silanol group on the surface. An alternative cleaning method, which

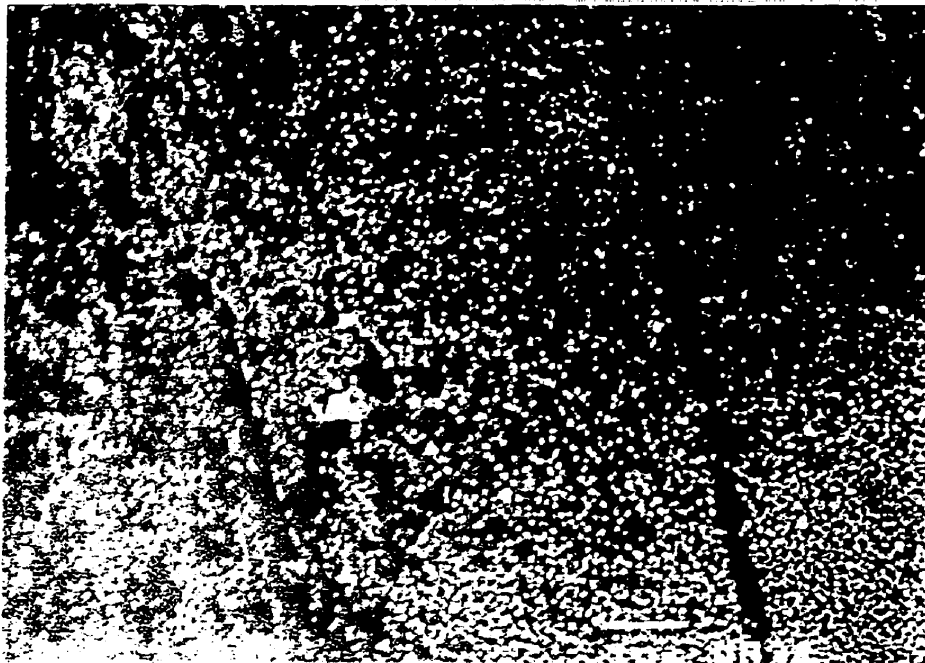


performed very well, is to immerse the silica surfaces in hot chromic acid at 80°C for 30 min and then to thoroughly rinse with water.

The scanning electron micrograph (SEM) of the cleaned silica surface before the reaction is shown in Figure 3.7 (a). The SEM pictures after reacting with glutaraldehyde and antibody are shown in Figure 3.7 (b) and Figure 3.7(c), respectively. It is can be seen from the difference in the micrographs that the silica surface was successfully modified using these reactions.



(a)



(b)



(c)

**Figure 3.7:** Scanning electron micrographs (SEM) of (a) cleaned fused silica surface; (b) glutaraldehyde activated surface; (c) antibody-immobilized surface.

### 3.2.2.2 Binding Studies with Immobilized Antibodies

#### 3.2.2.2.1 Antibody Immobilized Fiber Surface Analysis

*Specificity.* In this analysis, the concentration of  $^3\text{H}$ -theophylline was kept constant at 4 ng/mL, while the concentration of diazepam was varied from 1 to 500 ng/mL with 9 points investigated. Since the antibody does not specifically bind to diazepam, diazepam can only participate in non-specific binding. Therefore, if there is any non-specific binding of theophylline, the presence of the diazepam will cause a

decrease in scintillation response to  $^3\text{H}$ -theophylline. As presented in Figure 3.8, the regression line is horizontal, which means there is no significant non-specific binding of anti-theophylline observed for coated fused silica fiber. This result is consistent with what has been reported by other researchers (28, 30).

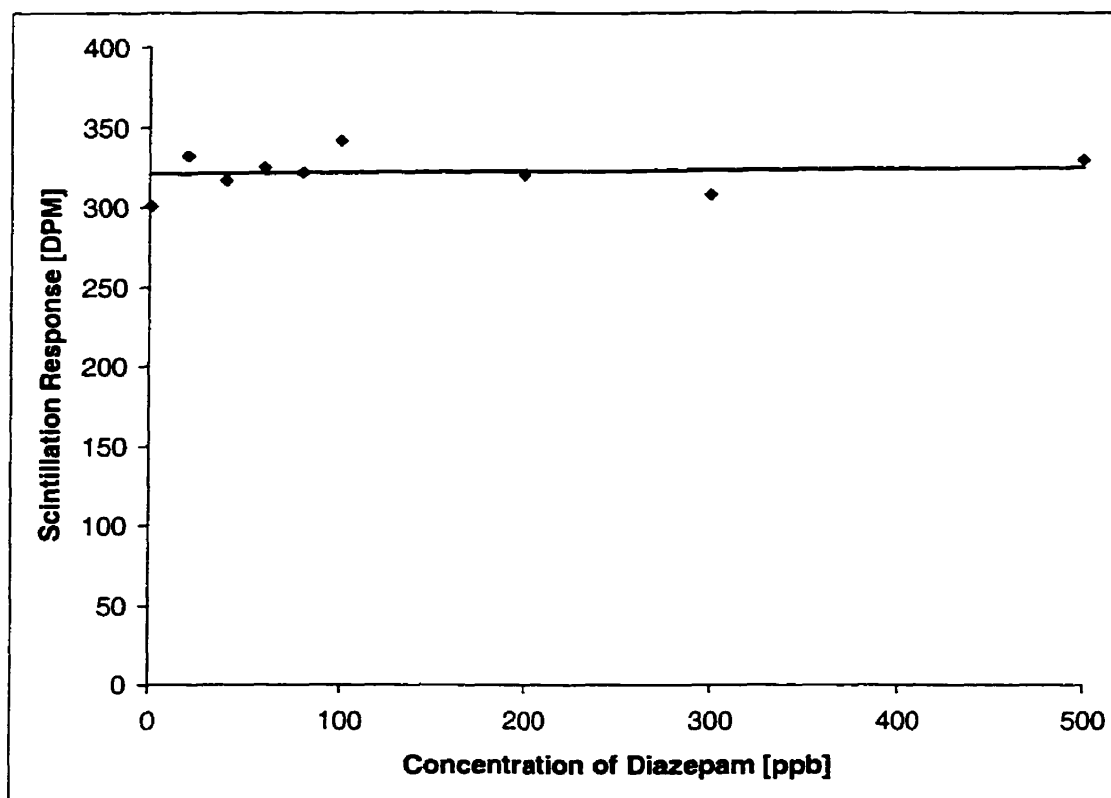


**Figure 3.8:** Binding of  $^3\text{H}$ -theophylline on the anti-theophylline immobilized silica fiber surface in the presence of various amounts of unlabeled diazepam.

*Binding Isotherm.* The  $^3\text{H}$ -theophylline binding isotherms (concentration range from 0 to 12 ng/mL) on the anti-theophylline coated fused silica fiber surface are presented in Figure 3.9.

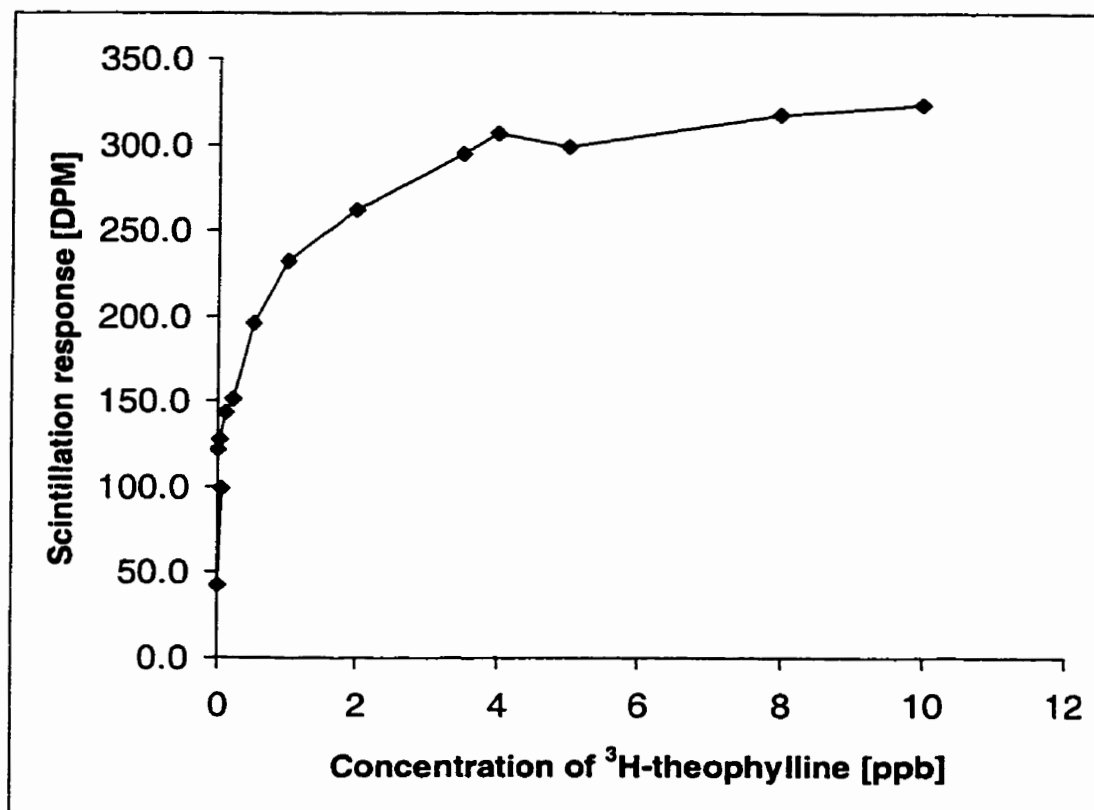


**Figure 3.9:** Binding isotherm of anti-theophylline immobilized fiber surface.

The maximum binding of  $^3\text{H}$ -theophylline at the plateau region shown in the figure started at about 4 ng/mL of theophylline, where the scintillation value is about 350 DPM.

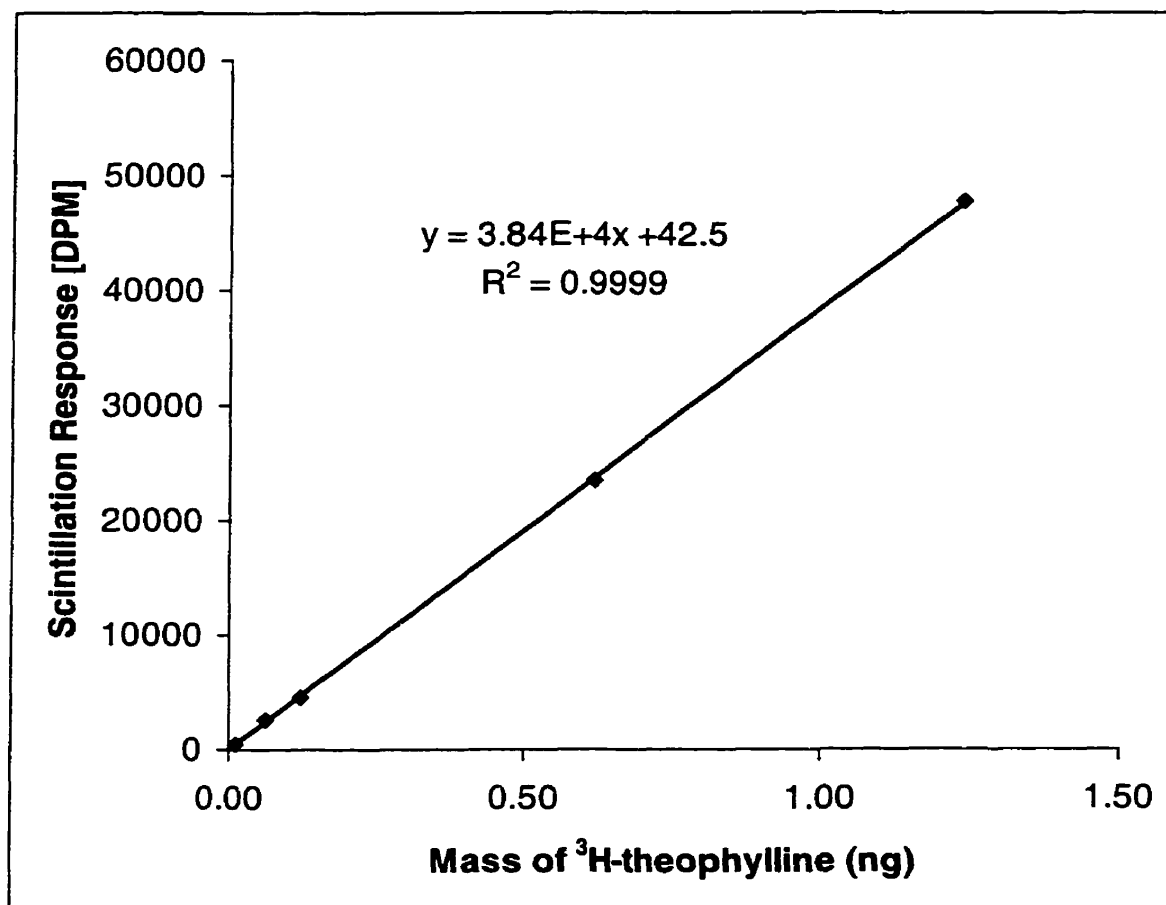


**Figure 3.10:** Calibration curve of mass of <sup>3</sup>H-theophylline on the fiber vs. the scintillation response.

From the scintillation response calibration curve (Figure 3.10), which was obtained from direct syringe injection to the scintillation cocktail, the absolute mass of theophylline to reach the saturated binding is about  $1.0 \times 10^{-3}$  ng. Since the surface area of each fiber is  $1.3 \text{ cm}^2$ , assuming the molecular weight of antibody is 150 KDa and each antibody molecule binds to exactly one theophylline molecule, the active surface density of antibody on the fused silica can be estimated as  $1 \text{ ng/cm}^2$ . This value is forth folds lower than the value reported in reference (32) (about  $40 \text{ ng/cm}^2$ ) and two orders of

magnitude lower than that reported in reference (28) (about 200 ng/cm<sup>3</sup>). The reason may come from different aspects. It could be the property of silica surface since the number of hydroxyl group is hard to compare. Quartz, which is more pure in terms of the SiO<sub>2</sub> component, was used in reference (32) and that could also explain the discrepancy.

*Cross Reactivity Study.* A competitive immunoassay was also performed. The competitive binding was measured by keeping the concentration of <sup>3</sup>H-theophylline at a fixed saturation value (4 ng/mL) and adding various concentrations of cold theophylline in the solution. The concentration of cold theophylline was varied from 0.005 ng/mL to 5 ng/mL. The binding curve is shown in Figure 3.11. The competitive binding from caffeine to <sup>3</sup>H-theophylline on the anti-theophylline immobilized surface is shown in Figure 3.12. The specificity (cross-reactivity) is defined as the ratio of antigen concentration to cross-reactant concentration at 50% inhibition of maximum binding (33). The cross-reactivity of theophylline to anti-theophylline is defined as 100%. From Figure 3.11, we can calculate that 0.4 ng/mL cold theophylline is needed to inhibit 50% of radiolabeled 4 ng/mL theophylline binding.

According to the manufacturer's information, the cross-reactivity of caffeine to anti-theophylline solution is 4%. This indicates that higher caffeine concentration is required to inhibit theophylline binding, which is demonstrated by the experimental results shown in Figure 3.12. From this figure, we can calculate that 400 ng/mL caffeine is needed to inhibit 50% of theophylline binding, which corresponds to a cross ratio of 0.1%. The possible reason is that since the immobilized antibody is highly orientated on the surface, the available surface area for possible non-specific binding becomes smaller

comparing with of the antibody in solution, which will result in lower cross reactivity value.

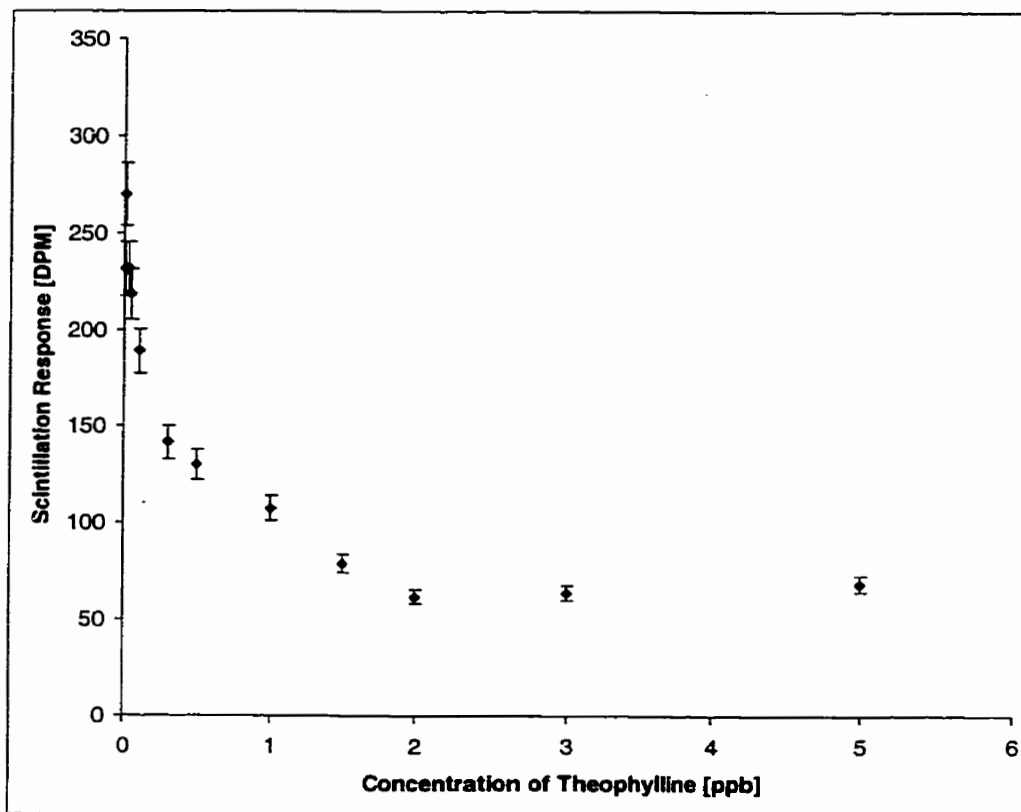


**Figure 3.11:** Competitive binding of cold theophylline with the  $^3\text{H}$ -theophylline to the anti-theophylline immobilized on a fused silica surface. The  $^3\text{H}$ -theophylline was kept at saturation value (4 ng/mL), while the cold theophylline concentration was varied. Duplicates were measured for each point.



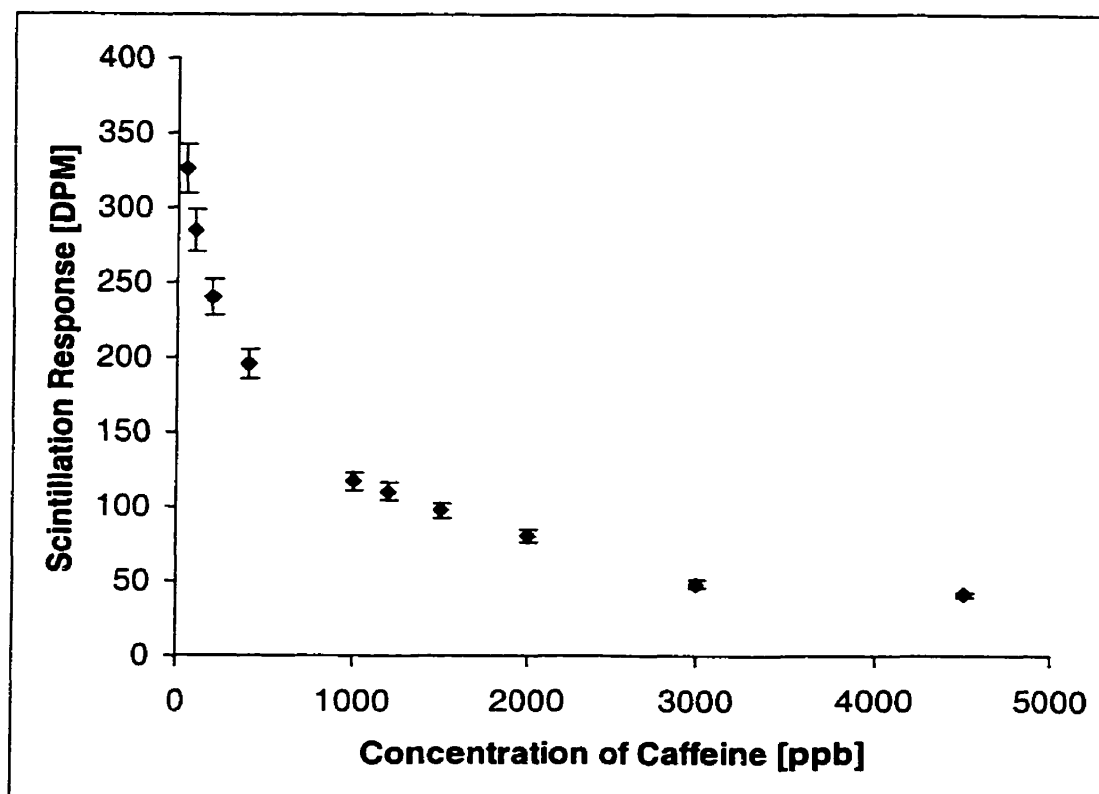


**Figure 3.12:** Competitive binding of caffeine with  $^3\text{H}$ -theophylline on anti-theophylline-coated fused silica fibers.

*Serum Sample Analysis.* The human serum was first spiked with theophylline. The concentrations were 10 ng/mL and 50 ng/mL respectively. This sample was diluted 100 fold with PBS. The diluted solution was spiked with 4 ng/mL  $^3\text{H}$ -theophylline. The anti-theophylline-coated fiber was put in the 1 mL vial containing this solution and incubated for 3 hours. After the incubation, the fiber was taken out of the solution, rinsed with PBS twice, and put in the scintillation vial for counting. The comparison of the serum sample results with the results of shown in Figure 3.11 is listed in Table 3.1.

**Table 3.1:** Analysis of theophylline in human serum sample with antibody immobilized silica fiber.

| Concentration (ng/mL)<br>(after dilution for serum )                         | Serum sample<br>[DPM] | From Figure 3.11<br>[DPM] | *Relative<br>Difference (%) |
|--|-----------------------|---------------------------|-----------------------------|
| 0.1  | 193.28                | 194.04                    | 0.4                         |
| 0.5  | 142.15                | 133.26                    | 6.8                         |
| *relative difference =[abs(serum sample-from figure 3.11)/from figure 3.11]% |                       |                           |                             |

#### 3.2.2.2.2 Binding Study of In-tube Immunoaffinity SPME

*Specificity.* The binding characteristics of the immunoaffinity SPME capillary were compared to a bare silica capillary of equal dimensions. A 1000 fold (12.4 ng/mL) dilution of  $^3\text{H}$ -theophylline stock was prepared in PBS and introduced to both capillaries over a time range of 3-25 min at 14  $\mu\text{L}/\text{min}$ . The extracted  $^3\text{H}$ -theophylline was desorbed from either capillary and counted by the scintillation method as already described. Desorption of the bound theophylline was accomplished with a 500  $\mu\text{L}$  solution of methanol : PBS : 1% TFA (70:29:1). It can be seen from Figure 3.13 that the binding of  $^3\text{H}$ -theophylline with the bare fused silica capillary was very low compared with the immunoaffinity capillary. From the same figure, it also can be seen that the bare silica capillary reaches equilibrium much faster than immunoaffinity capillary in the binding with  $^3\text{H}$ -theophylline.

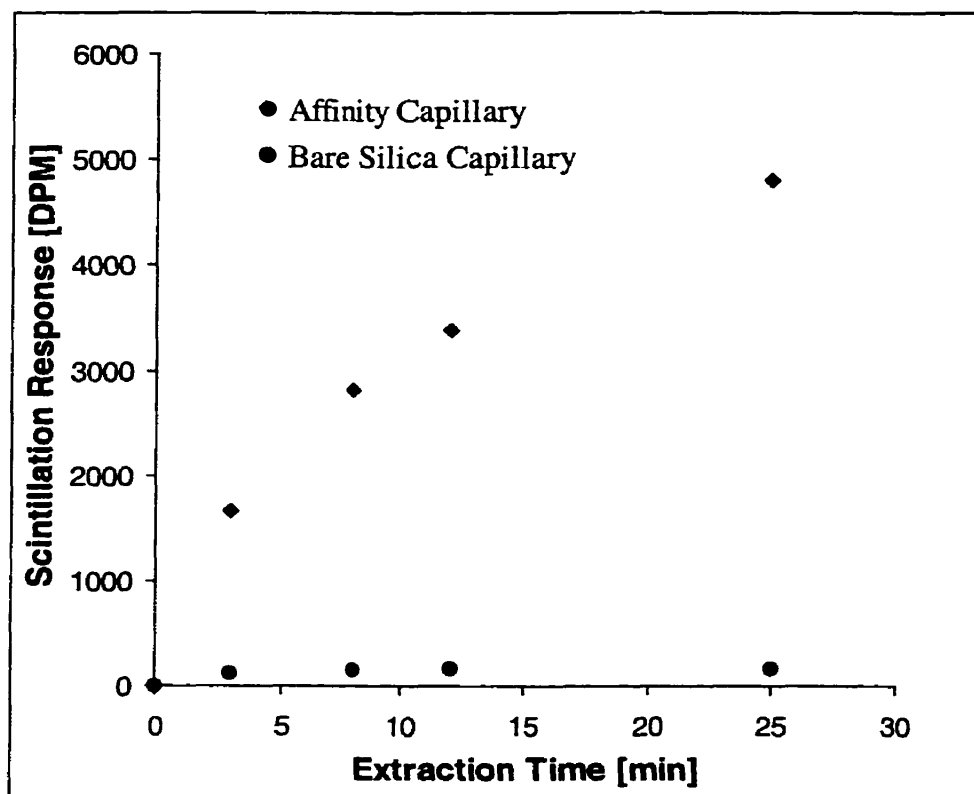


**Figure 3.13:** The comparison of the immunoaffinity capillary with the bare fused silica capillary in the binding to  $^3\text{H}$ -theophylline. The concentration of  $^3\text{H}$ -theophylline was 12.4 ng/mL.

*Cross Reactivity Study.* A binding isotherm for the in-tube immunoaffinity SPME approach was generated with PBS samples spiked with a mixture of 1000 fold diluted  $^3\text{H}$ -theophylline (12.4 ng/mL) and various concentration of cold theophylline (1.0-1000 ng/mL) (Figure 3.14). The samples were passed through the immunoaffinity capillary for

a period of one hour with the flow of 14  $\mu\text{L}/\text{min}$ , followed by flushing the capillary with 150  $\mu\text{L}$  of PBS buffer.

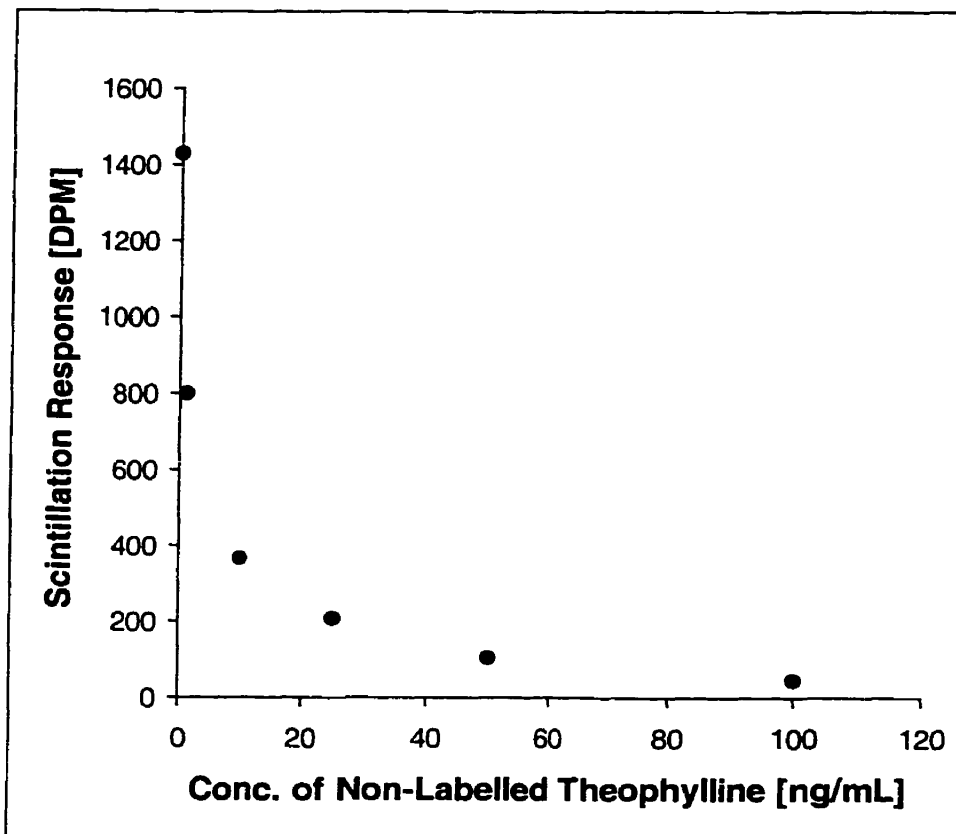


**Figure 3.14:** The competition of non-radiolabeled theophylline to  $^3\text{H}$ -theophylline in the binding with the anti-theophylline immobilized capillary. The concentration of  $^3\text{H}$ -theophylline was kept at 12.4 ng/mL.

The specificity of the theophylline immunoaffinity SPME capillary was investigated using a fixed concentration of  $^3\text{H}$ -theophylline together with concentrations

of caffeine that range over 1-10000 ng/mL (Figure 3.15). Comparing with Figure 3.14 and Figure 3.15, we can obtain a similar cross reactivity value for caffeine.

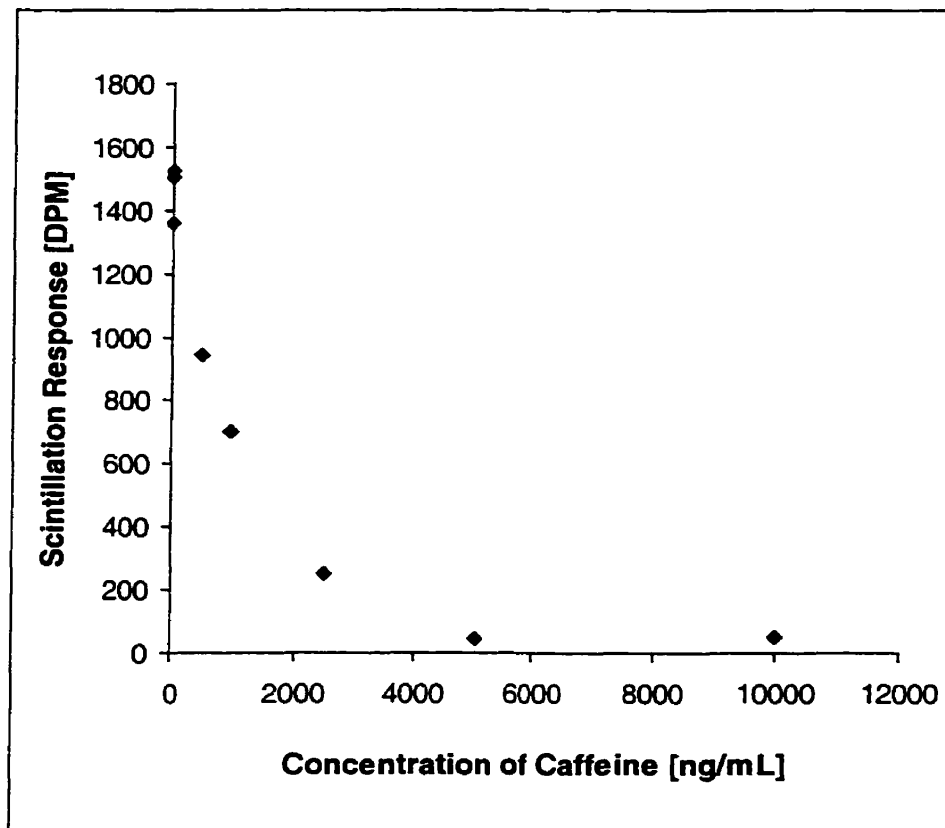


**Figure 3.15:** Cross reactivity study of caffeine to  $^3\text{H}$ -theophylline in the binding to anti-theophylline immobilized capillary.

*Serum Analysis.* A 1500  $\mu\text{L}$  aliquot of human serum sample was spiked with various amounts of theophylline (prepared in PBS) to provide a working concentration of 1.0-100 ng/mL. The  $^3\text{H}$ -theophylline stock was diluted 10 fold in PBS and a 10  $\mu\text{L}$  aliquot was added to the serum standards. The sample was transferred to a 1.0 mL

disposable plastic syringe. Extraction of the theophylline from the serum sample was accomplished by passing the sample through the immunoaffinity SPME capillary at a rate of 14.0  $\mu\text{l}/\text{min}$  for 1.0 h. The capillary was flushed with 150  $\mu\text{L}$  of PBS buffer and the desorption of the bound theophylline was accomplished with a 500  $\mu\text{L}$  aliquot of methanol : PBS : 1 TFA (70:29:1). The elute from the capillary was collected into a 20.0 mL polyethylene scintillation vial containing 20.0 mL of scintillation cocktail. The serum sample results were compared to previously obtained theophylline binding isotherm.

**Table 3.2:** Analysis of theophylline in human serum sample with antibody immobilized capillary.

| Concentration (ng/mL)<br>(after dilution for serum )       | Serum sample<br>[DPM] | From Figure 3.14<br>[DPM] | *Relative<br>Difference (%) |
|--|-----------------------|---------------------------|-----------------------------|
| 1  | 746                   | 800                       | 6.75                        |
| 10   | 346                   | 365                       | 5.21                        |
| 50   | 99                    | 104                       | 4.81                        |
| 100  | 49                    | 47                        | 4.26                        |
| *relative difference =[abs(serum sample-from figure 3.14)] |                       |                           |                             |

### 3.3 Conclusion

In this section, theophylline antiserum was immobilized on fused silica surfaces (on a fiber and the inner surface of the capillary) and used for solid phase immunoaffinity analysis. The methods for surface preparation and antibody immobilization have been reviewed. SEM images of silica fibers at each surface modification stage have been collected. Combined with the results of diazepam and caffeine competitive binding studies, conclusions can be made that active theophylline antibodies have been successfully immobilized on the silica surfaces.

Utilizing the high binding selectivity of immobilized anti-theophylline, the coated SPME fibers and capillaries were successfully employed to study the concentration of theophylline in human serum samples. The results demonstrated that antibody immobilized SPME and in-tube SPME can be used for drug analysis in complex biomatrices. Compared with traditional immunoassays, the antibody immobilized SPME approach is simple and convenient, only requiring little sample preparation. Scintillation detection method was employed because of the low capacity of the coated fiber/capillaries, which is due to the small surface areas and low antibody surface density. This is likely because of the different property of the silica (34) or the disorientation of the antibody (35). The immobilization technique could be further improved to enhance the density of active antibodies, which may enable the direct coupling of antibody immobilized in-tube SPME with LC/MS systems.

The stability of immobilized antibody was shown is that after one week of storage in a solution of sodium azide (5%) in PBS, no significant changes of fiber properties were noticed.

### 3.4 References

---

1. Aga, D. S.; Thurman, E. M. *Immunochemical Technology for Environmental Applications*, ACS Symposium Series 657, Washington, DC, **1996**.
2. Diamandis, E. P.; Christopoulos, T. K. *Immunoassay*, Academic Press, San Diego, **1996**.
3. Rogers, K. R.; Mulchandani, A.; Zhou, W. *Biosensor and Chemical Sensor Technology: Process Monitoring and Control*, ACS symposium Series 613, Washington, DC, **1995**.
4. Jones, V. W.; Kenseth, J. R.; Porter, M. D.; Mosher, C. L.; Henderson, E. *Anal. Chem.*, **1998**, 70, 1233-1241.
5. Scouten, W. H.; Luong, J. H. T.; Brown, R. S. *Trends Biotechnol.*, **1995**, 13, 178.
6. Boutelle, M. G.; Fellows, L. K.; Cook, C. *Anal. Chem.*, **1990**, 64, 1790.
7. Bhatia, S. K.; Hickman, J. J.; Ligler, F. S. *J. Am. Chem. Soc.*, **1992**, 114, 4432.
8. Jones, K. *Chromatographia*, **1991**, 32, 469.
9. Lin, S. H. *J. Chem. Technol. Biotechnol.*, **1991**, 50, 17.
10. Caruso, F.; Niikura, K.; Furlong, D. N.; Okahata, Y. *Langmuir*, **1997**, 13, 3427.
11. Ferrer, I.; Hennion, M.-C.; Barceló, D. *Anal. Chem.* **1997**, 69, 4508-4514.
12. Amit, A. G.; Mariuzza, R. A.; Phillips, S. E.; Poljak, R. J. *Science*, **1986**, 233, 747.
13. Lehninger, A. L.; *Biochemistry*, 2<sup>nd</sup> ed., Worth, New York, **1977**; Bagchi, P.; Birnbaum, S. M.; *J. Colloid Interface Sci.*, **1981**, 83, 460.
14. Price, C. P., *Clin. Chem. Lab. Med.* **1998**, 36, 341-347.



15. Martin-Esteban, A.; Fernandez, P.; Camara, C. *Fresenius J. Anal. Chem.*, **1997**, 357, 927-933.
16. De Boevere, C.; Van Peteghem, C. *Anal. Chim. Acta.*, **1993**, 275, 341-345.
17. Pichon, V.; Chen, L.; Hennion, M.-C.; Daniel R.; Martel, A.; Le Goffic, F.; Abian, J.; Barceló, D. *Anal. Chem.*, **1995**, 67, 2451-2460.
18. Falipou, S.; Chovelon, J. M.; Martelet, C.; Margonari, J.; Cathignol, D. *Sensors Actuators*, **1999**, 74, 81-85.
19. Qian, W.; Xu, B.; Wu, L.; Wang, C.; Song, Z.; Yao, D.; Lu, Z.; Wei, Y. *J. Inclusion Phen. Macrocy. Chem.*, **1999**, 35, 419-429.
20. Welsch, T.; Frank, H.; Vigh, G. *J. Chromatogr.*, **1990**, 506, 97.
21. Kohler, J.; Chase, D. B.; Farlee, R. D.; Vega, A. J.; Kirkland, J. J. *J. Chromatogr.*, **1986**, 352, 275.
22. Dubrovsky, T. B.; Lvov, Y. (ed.); Mohwald, H. (ed.), *Protein Architecture: Interfacing Molecular Assemblies and Immobilization Biotechnology*, Marcel Dekker, Inc., New York, **2000**. Chapter 2, 25-50.
23. William, R. A.; Blanch, H. W. *Biosensors & Bioelectronics*, **1994**, 9, 159-167.
24. Moore, D. *Anal. Chem.*, **1984**, 56, 920A.
25. Voller, A.; Bidwell, D. E.; Bartlett, A. *Enzyme Linked Immunosorbent Assay (ELISA)*, Dynatech Laboratories, Alexandria, VA, **1979**.
26. Tijssen, P. *Practice and Theory of Enzyme Immunoassays*. In Burdon, R. H.; Van Knippenberg, P. H. (ed.), *Laboratory Techniques in Biochemistry and Molecular Biology*, vol. 15. **1985**.

27. Bransome, E. D. Jr., *The Current Status of Liquid Scintillation Counting*. Grune & Stratton, Inc. New York, **1970**.
28. Lin, J.-N.; Herron, J.; Andrade, J. D.; Brizgys, M. *IEEE Transaction on Biomedical Engineering*, **1988**, 35, 466-471.
29. Walt, D. R.; Agayn, V. I. *Trend Anal. Chem.*, **1994**, 13, 425-430.
30. Pillips, T. -M.; In Giddiugs, J. -C.; Grushka, E.; Brown, P. R. (ed.), *Advances in Chromatography, Biotechnological Applications and Methods*, Dekker INC, New York, **1989**.
31. Van Ginkel, L. -A. *J. Chromatogr.* **1991**, 564, 363-366.
32. Williamson, M. L.; Atha, D. H.; Reeder, D. J.; Sundaram, P. V. *Anal. Lett.*, **1989**, 22, 803-816.
33. Sigma's instruction for product theophylline antiserum. Product number: T-2524.
34. Kohler, J.; Kirkland, J. J. *J. Chromatogr.*, **1987**, 305, 125-150.
35. Lu, B., Xie, J., Lu, C., Wu, C., Wei, Y., *Anal. Chem.*, **1995**, 67, 83-87.

## **CHAPTER 4**

# **APPLICATION OF MOLECULARLY IMPRINTED POLYMER IN SPME: A PRELIMINARY STUDY**

### **4.1 Introduction**

#### **4.1.1 Molecularly Imprinted Polymer (MIP)**

In Chapter 3, the application of the immobilization of an antibody, both on a fused silica fiber and in a fused silica capillary, for SPME analysis has been discussed. However, the major disadvantage of this approach is the supply and stability of biological antibodies. Their production can be uncertain and costly. However, once available, it has been shown in Chapter 3 that extraction procedures based almost entirely on antibody-antigen interactions can be obtained.

Starting with the first discovery of crown ethers by Pederson (1, 2), many researchers have been continuously trying to find artificial recognition materials. To date, the most successful approach for producing a synthetic recognition site has been the technique of molecular imprinting.

Molecular imprinting is a technique used for preparing polymers with synthetic recognition sites having a predetermined selectivity for an analyte(s) of interest (3). The imprint is obtained by arranging polymerisable functional monomers around a template (the analyte). Complexes are then formed through molecular interactions between the analyte and the monomer precursors. The complexes are assembled in the liquid phase and fixed by crosslinking polymerisation. Removal of the template from the resulting polymer matrix creates vacant recognition sites that exhibit affinity for the analyte.

#### **4.1.2 Preparation of MIPs**

There have been two main approaches to the synthesis of MIPs. Wulff (4) and co-workers produced MIPs by synthesizing specific sugar or amino acid derivatives, which contained a polymerizable function such as vinylphenylboronate. After polymerization they hydrolysed the sugar moiety and used the polymer for selective binding. This approach is usually referred to as covalent molecular imprinting.

Mosbach (5) and co-workers developed the so-called non-covalent approach. They used a monomer such as methacrylic acid (MAA) along with a cross-linker such as ethylene glycol dimethacrylate (EDMA) mixed with the template (the analyte molecule). After polymerization the analyte is washed out of the polymer leaving a cavity that can selectively bind the template.

#### **4.1.3 Advantages and Applications of MIP**

The potential applications of MIP are many (4-6), since they show physical robustness, high mechanical strength, resistance to elevated temperatures and pressures, and stability in the presence of extremes of acids, bases, metal ions, and organic solvents, features that are favorable for routine analysis (7).

To date, practical applications of MIPs for bio- and pharmaceutical analysis are still fairly limited. However, several possibilities for use in analytical methods have been extensively explored. These include the production of solid phase extraction (SPE) columns (8), HPLC columns for affinity separations (9-11), capillary electrochromatography media (12), selectively permeable membranes (13, 14), radioligand binding assays (15, 16), and sensors (17).

#### **4.1.4 Objective of This Study**

The objective of this study is to investigate the potential application of MIP, as an alternative molecular recognition material to antibody, for SPME analysis.

## **4.2 Theory**

### **4.2.1 Preparation of MIP for Diazepam**

The structure and physical properties of diazepam are presented in Figure 2.8. In this work, a MIP imprinted with diazepam was synthesized and used as the target material to be studied. The schematic representation of the preparation of MIP for diazepam is shown in Figure 4.1.

The functional MAA is first mixed with the diazepam print molecule, and crosslinking monomer, EDMA, in a suitable solvent. MAA is selected for its ability to form hydrogen bonds with a variety of chemical functionalities in the print molecule. The polymerization reaction was then started by addition of initiator (2,2'-azobis (2-isobutyronitrile), AIBN). A rigid insoluble polymer is formed. Finally, the print molecule is removed by solvent extraction. 'Imprints', which are complementary to the print molecule in both shape and chemical functionality, are now present within the polymeric network. The curve line in Figure 4.1 represents an idealized polymer structure but does not take into account the accessibility of the substrate to the recognition site.

The carboxylic acid function of MAA forms ionic interactions with amino groups and hydrogen bonds with polar functions of the print molecules. Dipole – dipole and hydrophobic interactions may also contribute in the formation of the specific binding sites for the imprinted molecule (18, 19). It is also these non-covalent intermolecular

interactions between the print molecule in a sample solution and the functional groups of the MIP that subsequently drive the specific molecular recognition binding process.

Of the imprinting strategies used, it has become evident that the use of non-covalent interactions between the print molecule and the functional monomers is the more versatile. The apparent weakness of these interaction types when considered individually may be overcome by allowing a multitude of interaction points simultaneously. The use of non-covalent interactions in the imprinting step closely resembles recognition processes observed in nature (20).

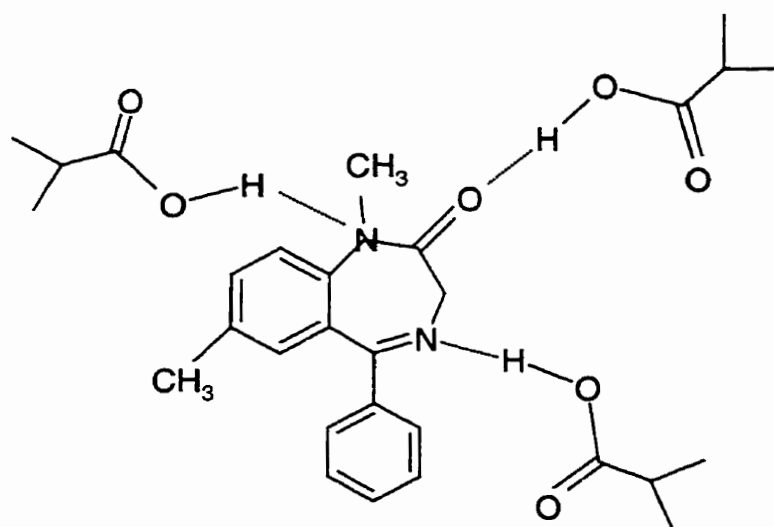


**Figure 4.1:** Typical hydrogen bond interactions between diazepam (target) and MIP binding site are depicted by broken lines (adapted from (20)).

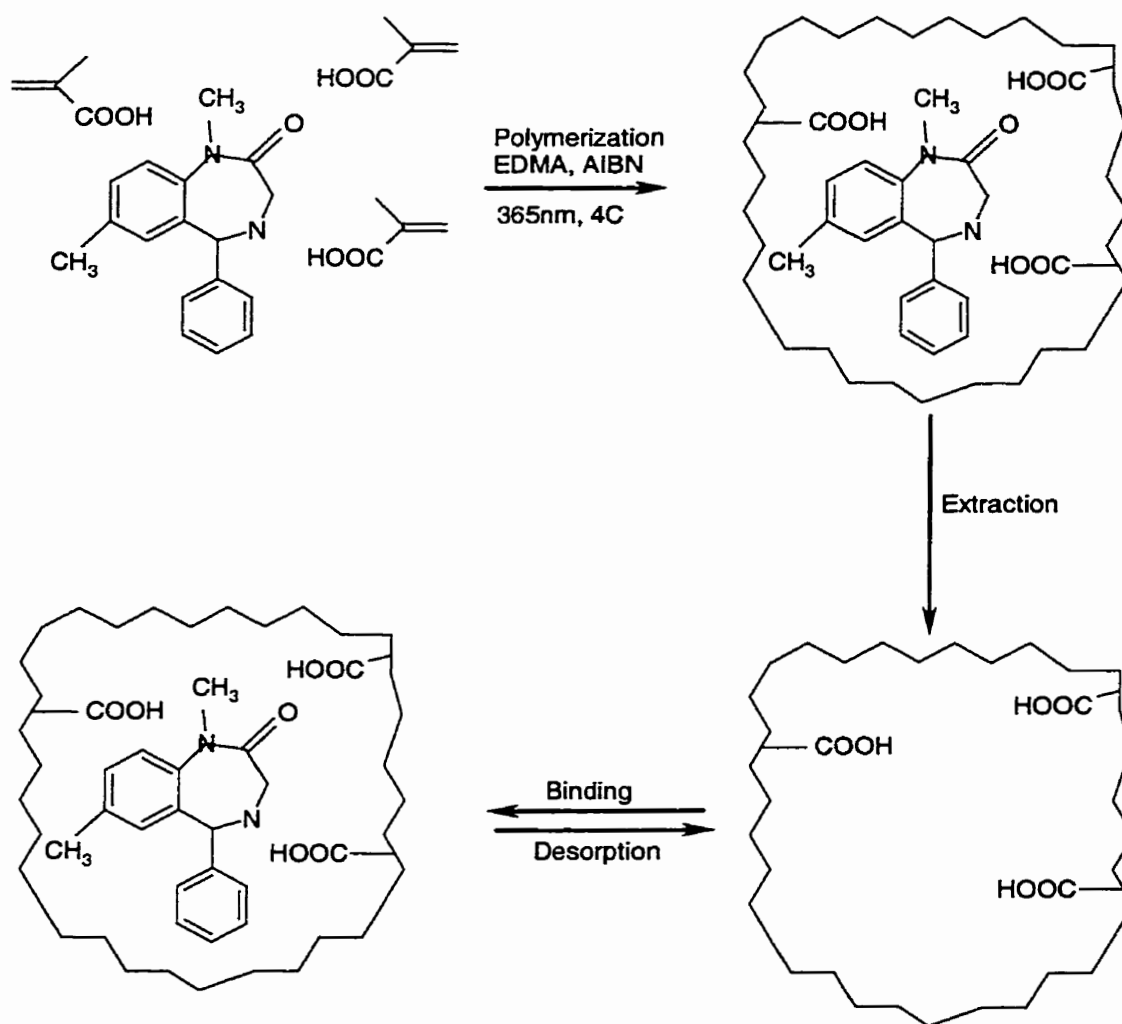


**Figure 4.2:** Preparation of a diazepam MIP and binding vs. desorption.



## 4.3 Experimental

### 4.3.1 Chemicals and Materials

The methacrylic acid (MAA), ethylene glycol dimethacrylic (EDMA), diazepam and 2,2'-azobis (2-isobutyronitrile) (AIBN) were purchased from Sigma-Aldrich (Mississauga, Ontario). The diazepam was purchased under a license from Health Canada since it is a controlled substance.

<sup>3</sup>H-Diazepam was purchased from NEN™ Life Science Products, Inc. (Boston, MA) as 3.454 µg/mL ethanol solution. The specific activity is 82.5 Ci/mmol.

### 4.3.2 Method

*Synthesis of MIPs.* To a glass 20 mL flask were added dichloromethane (6.2 mL), diazepam (0.2 g), MAA (0.36 g), EDMA (4.12 g) and AIBN (0.08g). The flask was capped with a rubber septum and vented with a syringe needle. The reaction mixture was sparged with nitrogen for 5 min while in a sonicating water bath before polymerization at 4°C for 16 hours. The reaction was initiated with ultraviolet light (366 nm). The reaction was protected by nitrogen during the whole reaction time.

After 30 min, a white, glassy polymer began to form in the flask. The reaction was carried out for 16 hours, at which time the solvent had evaporated. The flask was set in a vacuum oven, which has been flushed with nitrogen 3 times, at 60°C for a minimum 15 hours.

The polymer was removed from the flask and ground by hand with a mortar and pestle. The powder was sieved with water through a 25 µm sieve and recovered by filtration on No. 1 Whatman filter paper.

The polymer (< 25  $\mu\text{m}$ ) was sedimented several times in acetonitrile to remove the fine material. The coarse polymer was extracted by extensive washing of the particles with MeOH/acetic acid (9/1, v/v). Finally the polymer particles were dried under vacuum and stored in a desiccator at room temperature and ready for use.

A control polymer was synthesized using the same method except no imprint molecule was added (18).

*Synthesis of the MIPs on the Fused Silica Fiber.* Before the reaction was initiated, an ordinary fused silica SPME fiber (without coating, the fiber had been washed in the hot sulfuric acid for 5 min and then rinsed in water) was inserted into the reactant solution. After the polymerization was initiated and before the polymer becomes hard, the fiber was taken out from the viscous liquid. The polymerization reaction continued on the fiber.

The fiber was then extensively washed with MeOH/acetic acid (9/1, v/v) and dichloromethane.

*Immunoaffinity Analysis.* A 1 mL  $\text{CH}_2\text{Cl}_2$  solution containing the test compounds, in which the components are different according to the different assays, was first added in a 1 mL polyethylene tube. The fiber was then inserted into the solution. Special care was exercised to make sure that the fiber was properly labeled and the polyethylene tube was covered. The tube was then mounted on the shaking bed for 3 hours extraction. After the extraction, the fiber was then withdrawn from the tube, briefly dipped into water, and put into 1 mL methanol solution for 5 min desorption. The fiber was taken out of the methanol solution and 19 mL scintillation cocktail was added to the methanol solution for scintillation counting.

### 4.3.3 Results and Discussion

*Coating of the MIP on the Fiber.* One of the challenges of this study was to coat the MIP on the SPME fiber. Two approaches have been tried. The first one is direct synthesis of MIP on the fiber. The main disadvantage is the difficulty in removing the entire template analyte molecule. Even after extensive washing, it was proven that it is difficult to achieve this. Since the SPME technique, and especially SPME with a molecular recognition sorbent, is a very sensitive method, a trace amount of the analyte left on the fiber would be a vital impediment for the whole experiment.

The other method is to glue the fine polymer powder to the fused silica SPME fiber. The fiber was washed in hot sulfuric acid to clean the surface from grease and other coating before the gluing. A thin layer of glue was attached to the fused silica SPME bare fiber. The Silicon™ glue was identified as the optimum adhesive that was studied in this application. The fiber had a layer of MIP powder wrapped onto it by rolling the fiber in the powder. The fiber was then put in the oven at 60°C for overnight, and was then ready to use.

Since the print molecule is much easier to be washed out from MIP fine powder than from the layer of polymer on the fiber, this method is more practical. However, in this research stage, all the fibers are manually made. It is obvious that the reproducibility of the fiber preparation technique will be very poor and an experimental error is inherently introduced. Nevertheless, this coating method was employed with all experiments in this study. Figure 4.3 presents Scanning Electronic Micrographs (SEM) of the MIP coated fiber.

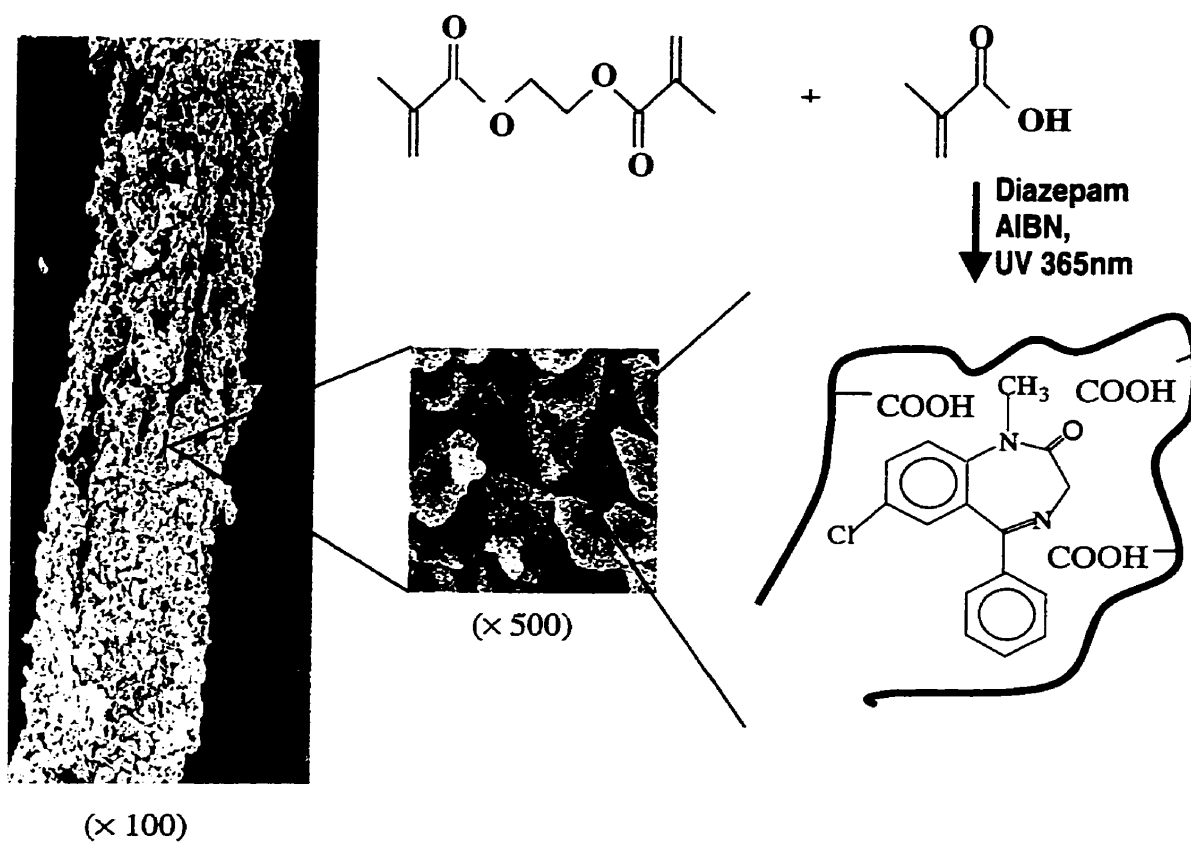


**Figure 4.3:** The schematic diagram representing the polymerization of MIP and SEM pictures showing the MIP powder after it is glued on the fiber surface.

*Immunoaffinity Analysis – Preliminary Results*. The comparison of anti-diazepam molecular imprinted polymer to the control polymer in binding  $^3\text{H}$ -diazepam was first performed. Figure 4.4 shows the comparison of the two fibers in extracting  $1\text{ ng/mL } ^3\text{H}$ -diazepam. The experiment was based on three duplicates of measurement. As mentioned earlier, due to the poor reproducibility of the 'home-made' fiber, the experimental error is fairly large.

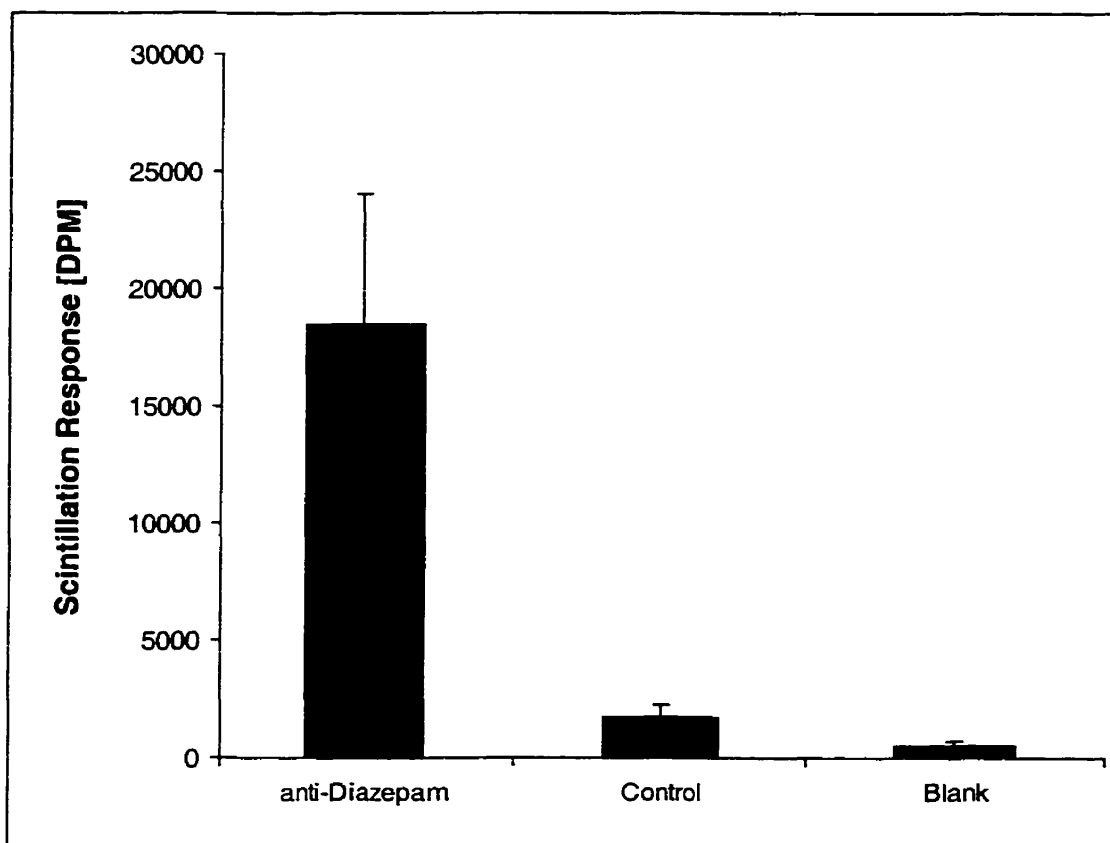


**Figure 4.4:** The comparison of anti-diazepam MIP and controlled polymer in binding the  $1\text{ ng/mL } ^3\text{H}$ -diazepam in  $\text{CH}_2\text{Cl}_2$  solution. The blank value is the blank test (extraction of blank solvent) of anti-diazepam fiber.

It is obvious from Figure 4.4 that the anti-diazepam binding is much higher than the control polymer. The blank test of the anti-diazepam fiber shows that the amount of the remaining diazepam on the MIP is very small.

Competitive binding of the cold diazepam to  $^3\text{H}$ -diazepam was also performed. The concentration of  $^3\text{H}$ -diazepam was kept at 1 ng/mL while the concentration of the cold diazepam was varied from 0.2 ng/mL to 3.0 ng/mL. The competitive curve showing these results is presented in Figure 4.4. The curve clearly shows the competitive binding trend with an increase in the cold-diazepam concentration.

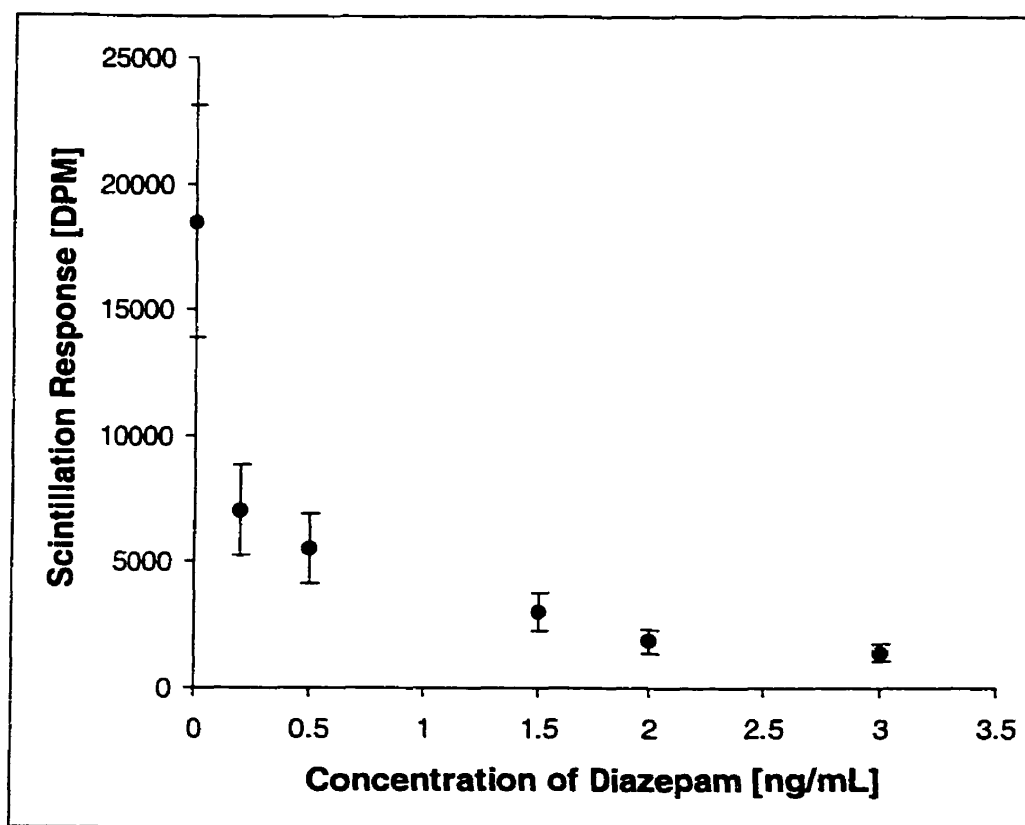


**Figure 4.5:** The competitive binding of cold diazepam with  $^3\text{H}$ -diazepam in the binding to anti-diazepam MIP fiber. The concentration of  $^3\text{H}$ -diazepam was 1 ng/mL.

The cross-reactivity from nordazepam, which is another important compound in the benzodiazepine compounds family, to the anti-diazepam MIP was also investigated with the same experimental method. The results are presented in Figure 4.6.

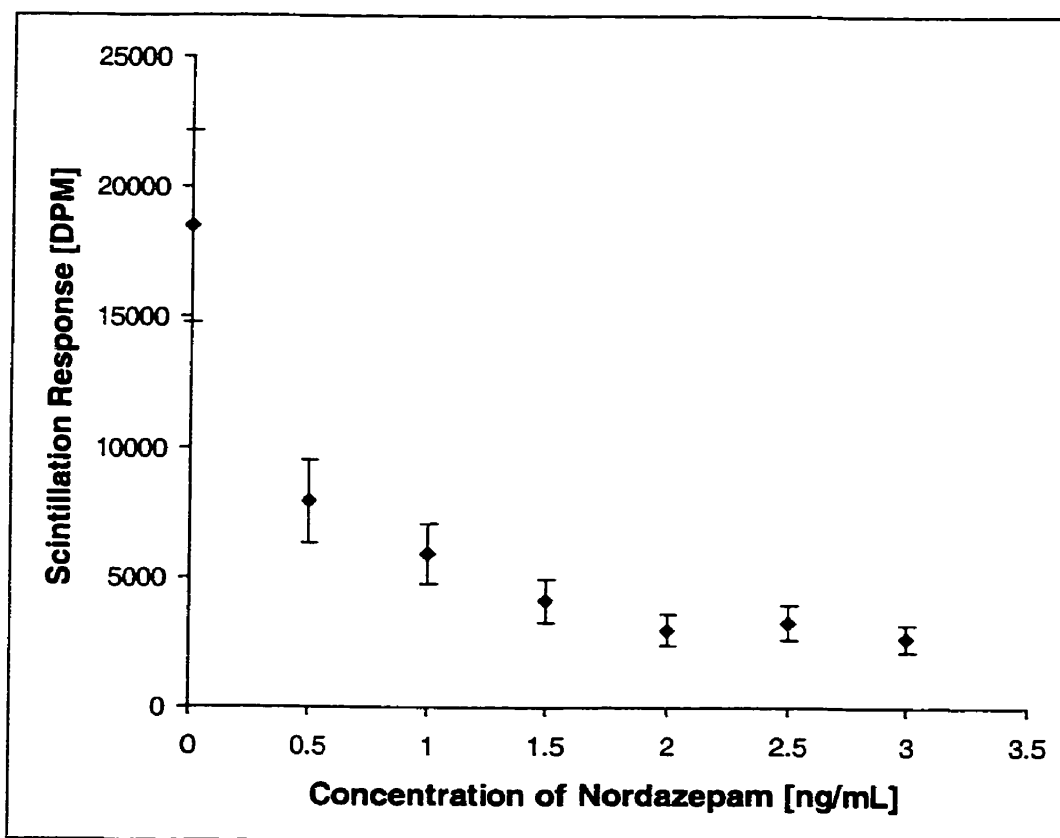


**Figure 4.6:** The competitive binding to nordazepam with  $^3\text{H}$ -diazepam in the binding to the anti-diazepam MIP fiber. The concentration of  $^3\text{H}$ -diazepam was 1 ng/mL.

According to (21), the cross-reactivity of nordazepam to anti-diazepam MIP is 27%. In our results, it is apparent that it takes a larger concentration of nordazepam than diazepam binding for the scintillation value to decrease to the base value.

#### 4.4 Conclusion

In this work, MIP has been applied to the SPME analysis. MIP particles were first glued on a SPME fiber and immunoassay were performed. Due to the tiny size of the SPME fiber, the capacity was too low to be detected either by GC or HPLC/MS. A radioimmunoassay with scintillation detection method was hence implemented. Although this work only represents some very preliminary results, the research results already show that the MIP is a promising molecular recognition material for the SPME analysis for biological samples. The only factor that restricts the work from broader application is that the technique of making the fiber manually was difficult and needs to be further improved. However, it is very likely that this disadvantage could be overcome. For example, MIPs have recently been electronically synthesized on fused silica surfaces with using polypyrrole conducting polymers (22).

#### 4.5 Reference

---

1. Pederson, C. J. *J. Am. Chem. Soc.*, **1967**, 89, 2495-2496.
2. Pederson, C. J. *J. Am. Chem. Soc.*, **1967**, 89, 7017-7036.
3. Ensing, K.; De Boer, T. *Trend. Anal. Chem.*, **1999**, 18, 140-145.
4. Wulff, G. *Angew. Chem. Int. Ed. Engl.* **1995**, 34, 1812-1832.



5. Mosbach, K. *Trend. Biochem. Sci.* **1994**, 19, 9-14.
6. Shea, K. J. *Trends Polym. Sci.* **1994**, 2, 166.
7. Ramström, O.; Ansell, R. J., *Chirality*, **1998**, 10, 195.
8. Stevenson, D. *Trends. Anal. Chem.*, **1999**, 18, 154-158.
9. Matsui, J.; Takeuchi, T. *Anal. Commun.*, **1997**, 34, 199-200.
10. Allender, C. J.; Heard, C. M.; Brain, K. R. *Chirality*, **1997**, 9, 238-242.
11. Remcho, V. T.; Tan, Z. J. *Anal. Chem.*, **1999**, 71, 248-255A.
12. Lin, J. M.; Nakagama, T.; Uchiyama, K.; Hobo, T. *Biomed. Chrom.*, **1997**, 11, 298-302.
13. Hedborg, E.; Winquit, F.; Lundstrom, I.; Andersson, L. I.; Mosbach, K. *Sens. Act. Phys.*, **1993**, 37, 796-799.
14. Hong, J. M.; Anderson, P. E.; Qian, J.; Martin, C. R. *Chem. Mat.* **1997**, 10, 1029-1033.
15. Andersson, L. I. *Anal. Chem.* **1996**, 68, 111-117.
16. Senholdt, M.; Sieman, M.; Mosbach, K.; Andersson, L. I.; *Anal. Lett.* **1997**, 30, 1809-1821.
17. Kriz, D.; Ramstrom, O.; Mosbach, K. *Anal. Chem.*, **1997**, 69, 345-349A.
18. Sellergren, B.; Lepistö, M.; Mosbach, K. *J. Am. Chem. Soc.*, **1988**, 110, 5853-5860.
19. Andersson, L. I.; Mosbach, K. *J. Chromatogr.*, **1990**, 516, 313-322.
20. Mullett, W. M. *Ph.D. Thesis*. Carleton University, 2000, p11.
21. Vlatakis, G.; Andersson, L. I.; Müller, R.; Mosbach, K. *Nature*, **1993**, 361: 645-647.
22. Deore, B.; Chen, Z.; Nagaoka, T. *Anal. Chem.*, **2000**, 72, 3089-3994.

## CHAPTER 5

### IN-TUBE SPME FOR BENZODIAZEPINE ANALYSIS

#### 5.1 Introduction

##### 5.1.1 Benzodiazepines

Benzodiazepines are an important class of drugs that are frequently used in clinical practice as tranquilizers, sleep inducers, antiepileptic hypnotics, anticonvulsants, and muscle relaxants (1, 2). Unfortunately, they are often subject to overdose in suicide attempts, abuse, tolerance and dependence. Therefore, they are frequently encountered in emergency toxicological screening, drug-of-abuse testing and forensic medicine examinations.

Since benzodiazepine is widely seen in clinical and forensic cases, its measurements in specimens are widely practiced (3, 4). Simple, accurate, and highly sensitive analytical techniques are often required for trace level quantification of benzodiazepines. The commonly used sample preparation techniques are liquid-liquid extraction (LLE) and solid-phase extraction (SPE). The SPME fiber extraction has also been studied in this application with limited results (5). Chromatographic techniques, particularly HPLC, GC and GC-MS, are most commonly used to identify specific benzodiazepines present in specimens (6, 7). GC-MS determination of benzodiazepines has been reviewed by Maurer (8). Further studies and comparisons have also been made between this technique and various immunoassays (9-13).

In recent years, the coupling of LC to MS has provided a useful and rugged technique for the analysis of drug compounds. It has become an alternative to GC-MS, in

which many thermally labile compounds decomposed to give a common metabolite (14, 15). The advent and development of soft-ionization techniques, such as electrospray ionization (16, 17), have further opened avenues for the specific detection and determination of various pharmaceuticals.

As stated in section 1.1.2, in-tube SPME has been applied to the analysis of many pharmaceutical compounds. In this study, as a class of common drug, benzodiazepines have been analyzed by in-tube SPME coupled with LC/ESI-MS.

### **5.1.2 Electrospray Ionization Mass Spectrometry**

Electrospray (ES) is a technique that allows ions to be transferred from solution to the gas phase and subjected to mass spectrometric analysis. Therefore, it is a perfect interface to allow HPLC coupling to mass spectrometry (MS) (16). The technique of electrospray ionization (ESI) was first introduced by Yamashita and Fenn in 1984 (18). However, it took a few more years before the importance of the method was recognized (19-21).

An LC/ESI-MS interface is shown in Figure 5.1 (HP 1100 LC/MS) (23). Unfortunately, a complete understanding of the ES mechanism is not yet available. However, the essence of the electrospray process can be described with simplicity (17) as follows. The ESI ion generation process is presented in Figure 5.2 (22). In ESI, the production of ions begins with charged polar analytes in the HPLC eluent. A solution of the analyte is passed through a capillary, which is held at a high potential. The effect of the high electric field as the solution emerges is to generate an aerosol of highly charged droplets, which pass down a potential and pressure gradient towards the analyzer portion

of the mass spectrometer. During the transition, the droplets reduce in size by evaporation of the solvent or by “Coulomb explosion” (droplet subdivision resulting from the high charge density). Ultimately, fully de-solvated ions result from complete evaporation of the solvent or by field desorption from the charged droplets. Nebulization of the solution emerging from the capillary may be facilitated by a sheath flow of nebulizer gas, a technique for which the term “ion-spray” was originally coined by its developers (20). Sampling of the fully or partially de-solvated ions is possible using a capillary or a skimmer device.

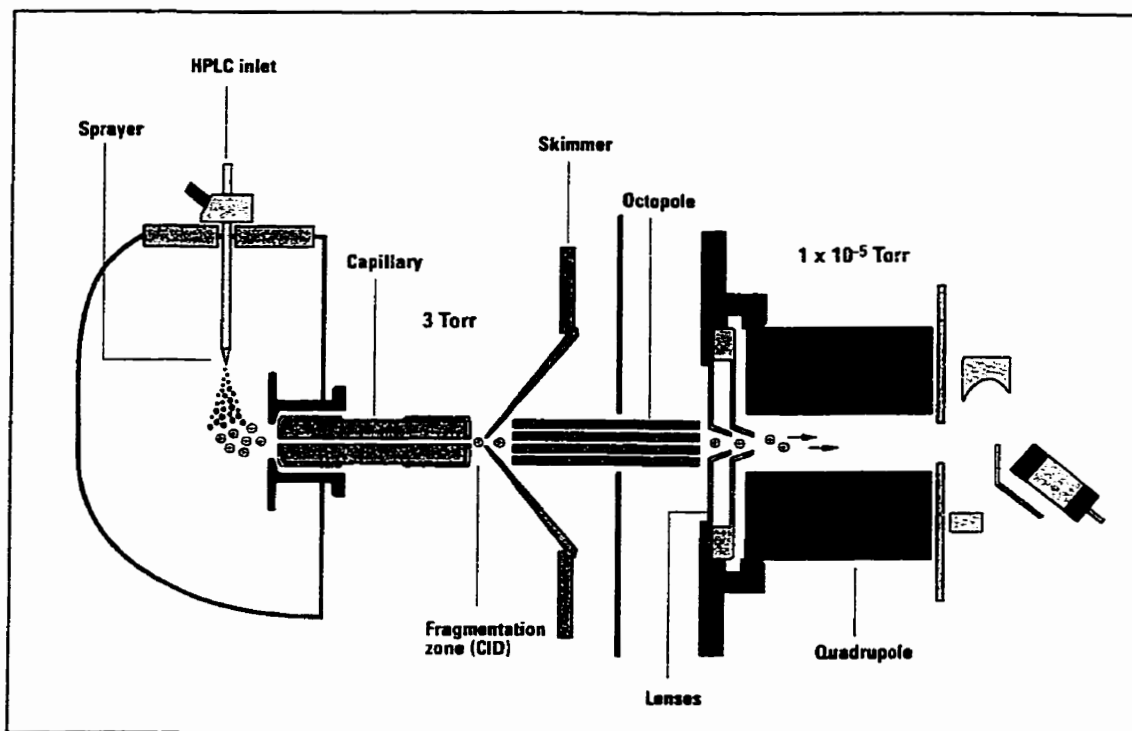


**Figure 5.1:** An LC/ESI/MS interface.

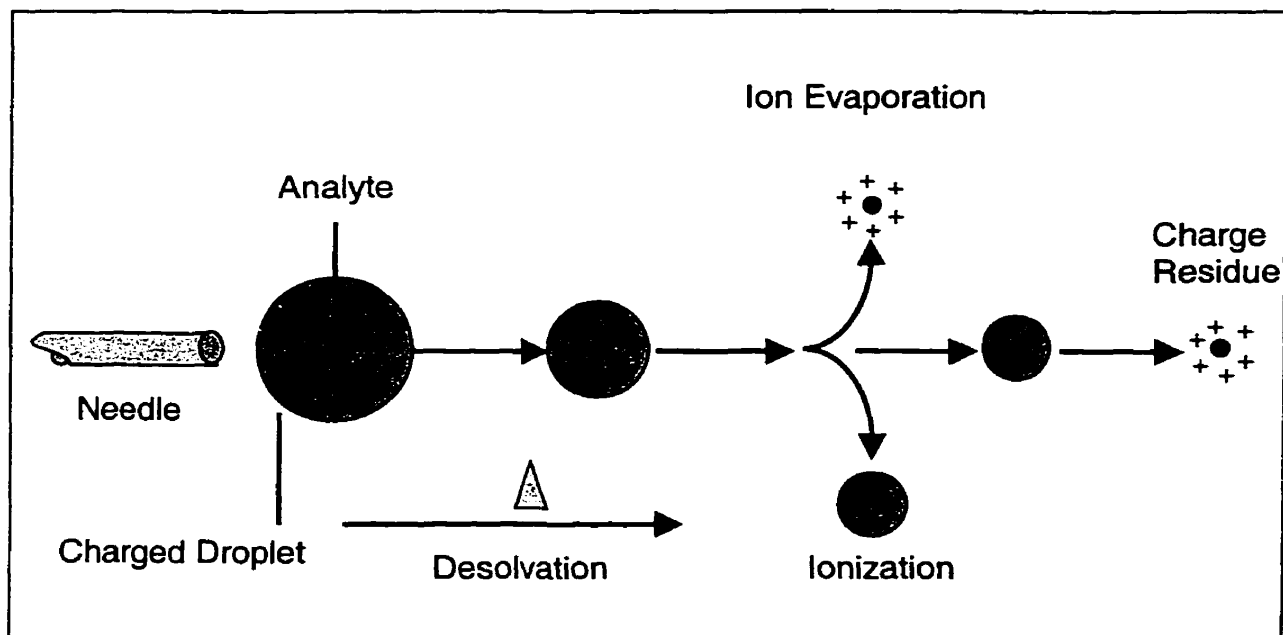


**Figure 5.2:** ESI ion generation process.

## 5.2 Theory

The configuration of the in-tube SPME using a Hewlett-Packard HP1100 LC/MS is shown in Figure 1.3. The technique is easily adapted into the Hewlett-Packard 1100 LC/MS system, as the configuration of the standard autosampler for this system (ALS 1100) is ideal for in-tube SPME.

In the experiment, a coated capillary GC column was mounted between the injection needle and the injection loop of the HPLC autosampler. The needle hosts the capillary when it is pierced through the septum of the vial containing the spiked aqueous sample.

The extraction process was achieved by aspirating (draw) and dispensing (eject) the aqueous sample a number of times between the sample and the capillary. The

extracted analyte was then released from the coating directly by the mobile phase or by a segment of desorption solvent previously aspirated into the capillary and injected into the system for separation.

For in-tube SPME, a higher extraction and separation efficiency could be achieved through manipulating several extraction conditions, including the types of the capillary column, pH value of the aqueous sample, the numbers draw/eject cycle, type of the desorption solvent, the speed of the draw/eject movement, etc.

In this research, seven commonly encountered benzodiazepines were analyzed by in-tube SPME coupled with HPLC/ESI/MS system. Their chemical structures are listed in Figure 5.3. The objective of this study was to develop a simple, rapid and reliable method to analyse selected benzodiazepines in aqueous solutions as well as in biological fluid by in-tube SPME.

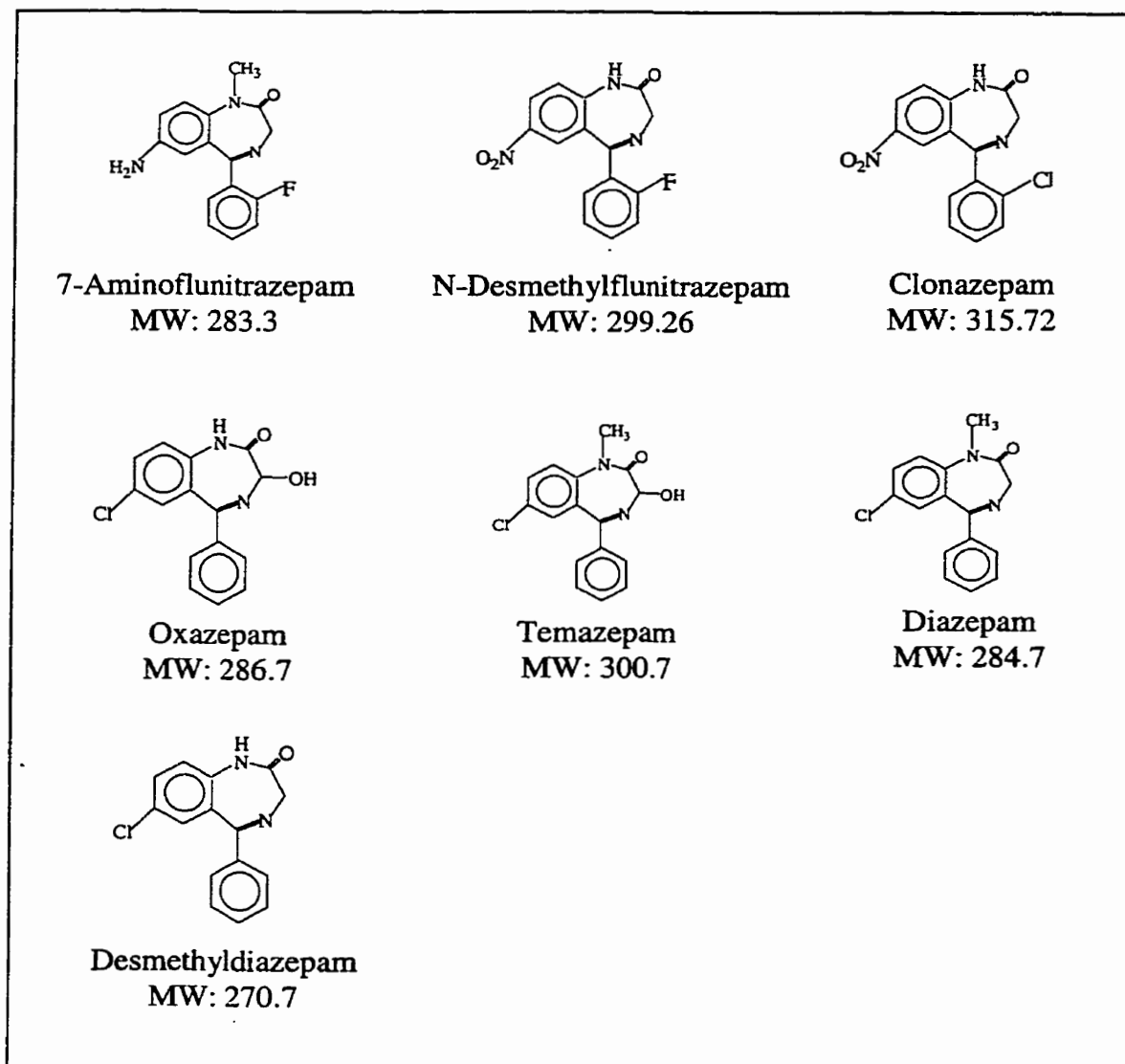


**Figure 5.3:** Structures of the target benzodiazepine compounds.

### 5.3 Experimental

*Chemicals and Materials.* All seven benzodiazepine compounds were purchased from Radian International (Texas, Austin, USA) as 1mg/ml methanol solutions. The solutions were diluted with methanol into 0.1mg/ml, 0.01mg/ml and 0.001mg/ml for experimental convenience and all solutions were stored at  $-10^{\circ}\text{C}$  when not in use. All the inorganic compounds used to prepare the buffer solution were purchased from Sigma (Mississauga, Ontario).

The solvents used in this study were all of HPLC grade and water filtered through a Milli-Q<sup>®</sup> ultrafiltration system (Millipore) was used during all experiments.

Capillaries (Supelco Q-PLOT, Supelcowax, Omegawax 250, SPB-5, SPB-1 and polar deactivated silica tubing) were purchased from Supelco (Bellefonte, PA).

*Preparation of Buffer Solutions.* The 100 mM pH 2.5, pH 4.0, pH 5.5, pH 7.0, pH 8.5 and pH 10.0 buffer were prepared separately. The pH 2.5 buffer was prepared by combining 0.1M phosphoric acid and 0.1M monobasic sodium monophosphate at certain ratios. The pH 4.0 and pH 5.5 buffer were prepared by 0.1 M acetic acid and 0.1 M sodium acetate at certain ratios. The pH 7.0 and pH 8.5 buffers were prepared from 0.1 M Tris (free base) and 0.1 M HCl. The pH 10.0 buffer was prepared by 0.1 M sodium carbonate and 0.1 M sodium hydrogen carbonate. The preparations for all of these buffers were performed under the monitoring of a pH meter.

*Instrumentation and Analytical Conditions.* The apparatus used was a HP 1100 LC/ESI/MS system (Hewlett-Packard, Palo. Alto, CA, USA) consisting of a degasser, a binary pump, an autosampler, a thermostatic column compartment, a variable wavelength detector and a mass selective detector (MSD). The ionization mode of the MSD was ESI.



The column used for the separation was a C<sub>18</sub> column (5.0 cm×2.1mm i.d., 3 μm particle size, Supelco, Bellefonte, PA). The mobile phase was composed of methanol (60%) and 50 mM ammonium acetate in water (40%). The flow rate was kept at 0.3 mL/min. The whole analytical time for each run took 12 minutes. All the separations were performed at 25°C.

ESI positive mode was used. Operation conditions were optimized as follows: drying gas (N<sub>2</sub>) was 10 mL/min; drying gas temperature was 350°C; nebulizer pressure was 25psi; capillary voltage was 3500 V; ions were observed at mass range m/z 100–400; fragmentor voltage was set at 70V. For the selected ion monitoring (SIM) mode, following ions were used: m/z 217 for nordazepam, 284 for 7-aminoflunitrazepam, 285 for diazepam, 287 for oxazepam, 300 for N-desmethylflunitrazepam, 301 for temazepam and 316 for clonazepam.

### 5.3.1 Methods

*In-tube SPME.* A GC capillary of 60 cm in length and 0.25 mm i.d. was used and the connections were facilitated by a 2.5cm sleeve of 1/16" polyetheretherketone (PEEK) tubing at each end. Normal 1/16" stainless steel nuts, ferrules and connectors were used to complete the connection. The inner volume for this capillary was 29.4μL. Vials (2 mL) filled with 1 mL of sample were set into the autosampler for analysis. In addition, two vials of 1.5 ml methanol were set on the autosampler to clean the capillary and needle. The extraction, desorption and injection procedure was controlled to give the best extraction and separation efficiency.

The capillary was washed and conditioned by a draw/eject cycle of 40  $\mu\text{L}$  methanol prior to extraction. During the extraction process, it was optimised to ten repeated draw/eject cycles. The draw/eject speed was set to 400  $\mu\text{L}/\text{min}$  in order to save analytical time without loss of extraction efficiency. After washing the injection needle by draw/eject cycle of 1.5  $\mu\text{L}$  methanol, the six-port valve was switched from LOAD to INJECT position and the extracted benzodiazepines were desorbed from the capillary coating with mobile phase flow and transported to the LC column for the separation. The sample would be further transferred to the MSD detector through the UV detector for detection.

*Preparation of Urine and Serum Sample.* Drug-free urine and serum samples were collected from a healthy volunteer. Urine samples were used after filtration by a syringe microfilter (0.45  $\mu\text{m}$ , Gelman Science). Serum samples were first diluted five times with 1% acetic acid and then ultrafiltered with NANOSEP centrifugal microconcentrator model 3K (Pall Filtron, Northborough, MA, USA) at 10,000 $\times g$  for 20 min. An aliquot of 0.5 mL of each sample was pipetted into a 2 mL vial. An additional 0.5 mL of buffer (pH 8.5) was spiked for each vial before it was set on the autosampler.

## **5.3.2 Results and Discussion**

### **5.3.2.1 Optimization of Analytical Conditions**

*Selection of Capillaries.* In order to optimize the extraction, several types of the capillary column were examined. The following capillaries were tested: Supelco Q-PLOT, Supelcowax, Omegawax 250, SPB-5, SPB-1 and polar silica tubing. The results were shown in Figure 5.4. The Supelco Q-PLOT column gave superior extraction

efficiency compared to the others due to the properties of divinylbenzene (DVB) polymer coating.

*Selection of pH Value of Matrix.* Since benzodiazepines are basic compounds, the pH value of the matrix affects the existing form of the molecule and, therefore, its extraction efficiency. The effect of pH was examined using several buffer solutions from pH 2.5 to pH 10.0, at intervals of 1.5 pH units. Different sensitivities were observed at different pH values. As shown in Figure 5.5, considering the overall performance, tris-HCl pH 8.5 gave the best extraction efficiency.

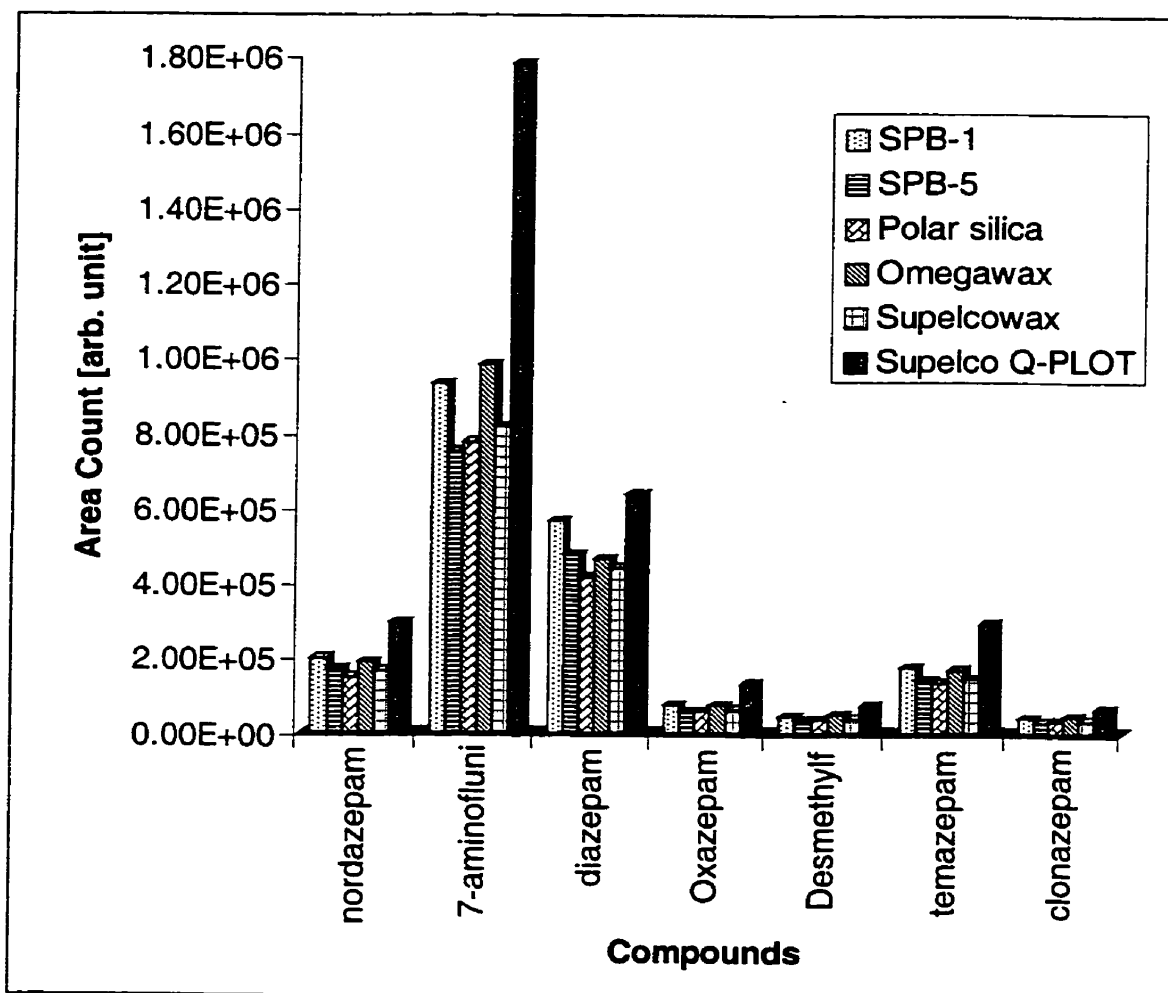


**Figure 5.4:** Comparison of various types of capillaries for in-tube SPME in the extraction of benzodiazepine compounds.

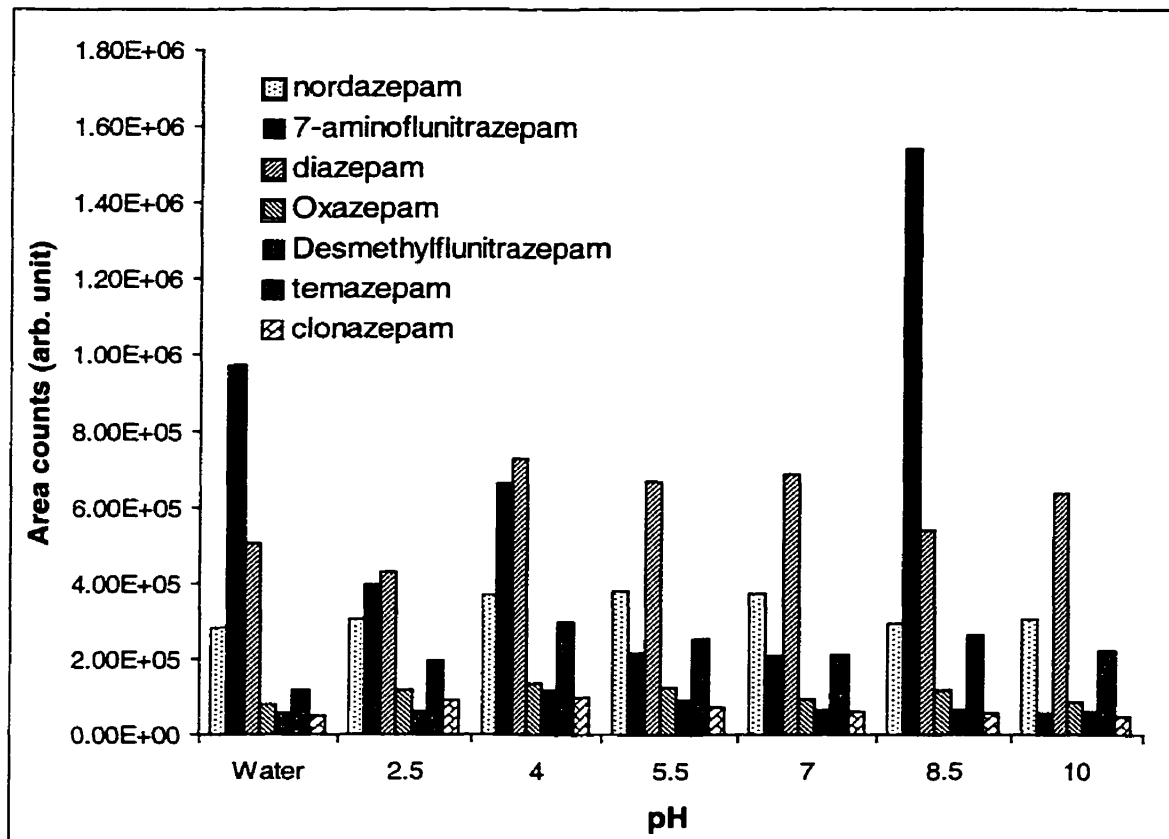


**Figure 5.5:** The effect of pH on in-tube SPME efficiency of benzodiazepine compounds using Supelco-Q PLOT capillary as the extraction medium.

*The Number of Draw/Eject Cycles.* The number of draw/eject cycles was varied over the range of 1 - 40 in order to investigate the equilibrium process of the extraction. A Supelco-Q plot capillary was used in this study. The extraction profile is shown in

Figure 5.6. From the figure, we can see that the equilibrium condition was still not reached for the compounds (especially for the four compounds with higher area counts) after 40 draw/eject cycles. Although the sensitivity was increased with more extraction cycles, a routine of ten draw/eject cycles was selected for the analysis in order to save analytical time while maintaining a sufficiently high extraction efficiency.

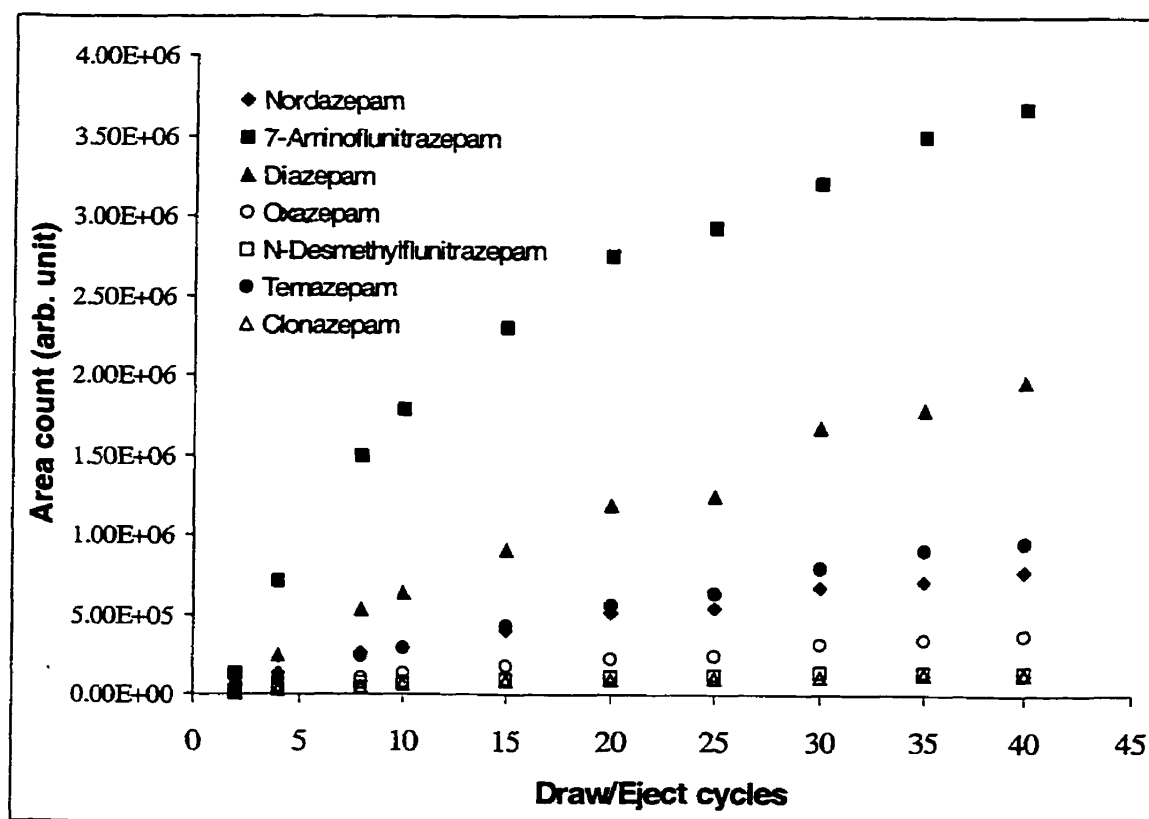


**Figure 5.6:** Extraction profile of benzodiazepine compounds illustrating the effect of draw/eject cycles on the in-tube SPME efficiency.

The absolute amount of benzodiazepines extracted by the capillary under optimal conditions (Supelco Q-PLOT capillary, pH of the sample solution = 8.5, the number of draw/eject cycles = 10) was calculated by direct injection of the sample solution to the LC column. Knowing the total amount of the analyte in the sample vial, the extraction efficiency can be subsequently calculated. As shown in Table 5.1, 26-83 ng (0.29-7.11%) was extracted by the in-tube SPME of benzodiazepines. These results were obtained by using 0.5 µg/mL sample solutions.

**Table 5.1:** Comparison of direct injection and in-tube SPME for the extraction of benzodiazepines.

| Compounds             | Area Counts ( $\times 10^6$ ) |                           | Extraction Yield <sup>c</sup> (%) |
|-----------------------|-------------------------------|---------------------------|-----------------------------------|
|                       | Direct injection <sup>a</sup> | In-tube SPME <sup>b</sup> |                                   |
| Nordazepam            | 0.12                          | 1.31 (26 ng)              | 9.2                               |
| 7-Aminoflunitrazepam  | 0.58                          | 7.11 (31 ng)              | 8.2                               |
| Diazepam              | 0.20                          | 3.41 (43 ng)              | 5.9                               |
| Oxazepam              | 0.028                         | 0.62 (56 ng)              | 4.5                               |
| Desmethyflunitrazepam | 0.020                         | 0.36 (46 ng)              | 5.6                               |
| Temazepam             | 0.081                         | 1.58 (49 ng)              | 5.1                               |
| Clonazepam            | 0.0087                        | 0.29 (83 ng)              | 3.0                               |

<sup>a</sup> 5 µL 500 ng/mL (2.5 ng) of benzodiazepines in 100 mM Tris HCl (pH 8.5) was directly injected.

<sup>b</sup> 1 mL of 0.5 µg/mL benzodiazepines in 100 mM Tris HCl (pH 8.5) was extracted by in-tube SPME, desorbed with mobile phase, and injected. Extracted amounts were calculated in comparison with area counts of benzodiazepines in direct injection and in-tube SPME.

<sup>c</sup> Percentages of extracted amount of benzodiazepines per initial amounts (500 ng) in sample solution using in-tube SPME.

*Sample Desorption.* The mobile phase was found to be the most suitable for desorption of benzodiazepines absorbed into the stationary phase of the capillary. Most conveniently, the desorbed benzodiazepines can be transported to the LC column with mobile phase flow. The entire in-tube SPME extraction and desorption process was accomplished automatically in 15 minutes. Carryover of benzodiazepines was not observed.

### 5.3.2.2 Quantitative Analysis

*Precision Analysis.* The precision analysis was based on the continuous analysis of 100 ppb benzodiazepines samples (n=9). The relative standard deviations for all the compounds were less than 10.0%.

*Calibration Curve and Limits of Detection.* The reliability of the present method was tested by quantitative measurements without an internal standard in SIM mode. Each peak area of the analytes was measured, and calibration curves were constructed. The calibration curves were linear in the range from 0.5 to 500 ng/mL for 7-aminoflunitrazepam, from 1 to 500 ng/mL for nordazepam, diazepam and oxazepam, from 2 to 500 ng/mL for N-desmethylflunitrazepam and temazepam, and from 5 to 500 ng/mL for clonazepam. No interference peaks from buffer solution was observed. The calibration curves are presented in Figure 5.7.



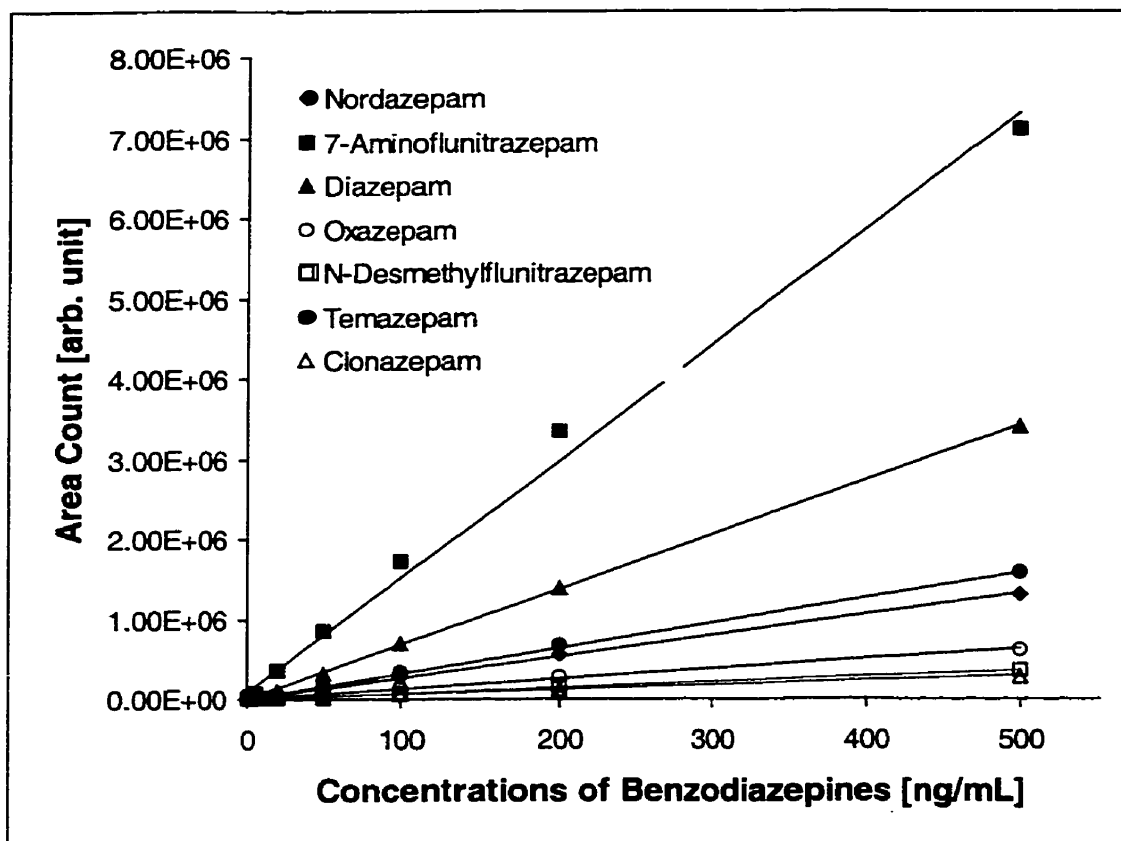


**Figure 5.7:** Calibration curves for benzodiazepine analysis by in-tube SPME.

**Table 5.2:** The regression coefficients of the calibration curves for benzodiazepines analysis by in-tube SPME.

| Compounds              | Regression Equation  | R <sup>2</sup> |
|------------------------|----------------------|----------------|
| 7-Aminoflunitrazepam   | $y = 14470x + 67590$ | 0.9943         |
| Diazepam               | $y = 6870x - 12130$  | 0.9997         |
| Temazepam              | $y = 3177x + 1829$   | 0.9992         |
| Nordazepam             | $y = 2633x + 4609$   | 0.9994         |
| Oxazepam               | $y = 1242x + 6391$   | 0.9979         |
| Desmethylflunitrazepam | $y = 707.2x + 3289$  | 0.9964         |
| Clonazepam             | $y = 563.1x + 5746$  | 0.9940         |

The blank and the 10 ng/mL standard from the linearity study were used to estimate the limit of detection of the procedure (25). The maximum baseline height of the blank was measured at the approximate retention time of each drug/metabolite peak and this peak height was multiplied by a factor of 3. The concentrations correspond to these values are used as the limits of detection (LOD). The limits of detection of the seven benzodiazepine compounds under the LC/MS conditions were 0.02 ng/mL for 7-aminoflunitrazepam, 1.0 ng/mL for diazepam, nordazepam and temazepam, 1.5 ng/mL for oxazepam, and 2.0 ng/mL for N-desmethylflunitrazepam and clonazepam. (Table 5.2). The detection limits could be further increased with more draw/eject cycles (Figure 5.6) with a sacrifice in analytical time. The in-tube SPME method gave 11-33 times higher sensitivity than the direct injection method (Table 5.1). The relative standard deviation for these compounds obtained at the same concentration of 500 ng/mL were 0.23-3.06% (n=3).

**Table 5.3:** The limits of detection of Benzodiazepine compounds by in-tube SPME.

| Compounds              | Limit of Detection (ng/mL) |
|------------------------|----------------------------|
| 7-Aminoflunitrazepam   | 0.024                      |
| Diazepam               | 1.0                        |
| Temazepam              | 1.5                        |
| Nordazepam             | 1.0                        |
| Oxazepam               | 1.5                        |
| Desmethylflunitrazepam | 2.0                        |
| Clonazepam             | 2.0                        |

### 5.3.2.3 Mass Spectra of Benzodiazepines

To select the monitoring ion for each of the benzodiazepines, ESI mass spectra were initially analyzed by direct liquid injection. Each drug gave a very simple spectrum in the mass scan range of  $m/z$  100-400 with  $[M+H]^+$  ion as the base ion. Each base ion accounted for more than 70% of the total ions, which was suitable for quantification in SIM mode for each benzodiazepine compound.

As shown in Figure 5.11 and Figure 5.12, 7-aminoflunitrazepam, N-desmethylflunitrazepam, clonazepam, oxazepam, temazepam, nordazepam and diazepam were eluted in well-separated peaks at 2.4, 3.8, 4.2, 5.8, 6.5, 8.2 and 9.5 min, respectively. However, perfect separations are not necessary due to the sensitivity and resolution power of SIM mode of ESI-quadrupole mass spectrometry.

The electrospray used in this study was a pneumatically assisted electrospray system. The theoretical advantage of this system is the low influence of the eluent composition for the nebulization efficiency. This permits the use of a wide range of

eluent without changing the performance of the nebulization and also permits the use of normal HPLC flow rates (0.3-1 mL/min).

The capillary voltage was applied between the spray chamber and nebulizer, with the potential of the nebulizer set at ground potential. (The polarity of the capillary voltage is always opposite to the polarity of the analyzed ion.) The charged capillary produces an electric field, which is the drawing force of the ion extraction from the fine droplets. The optimal voltage depends on the compounds and the geometric parameters of the spray chamber.

The fragmentor voltage was applied to the exit end of the capillary, which connects the spray chamber with the first vacuum zone of the MS. The applied voltage influences the fragmentation of the compounds and the transmission of ions. Theoretically, the higher that the fragmentation voltages are, the higher is the ion transmission. However, some unstable compounds can be easily fragmented in the collision induced dissociation (CID) zone.

Capillary voltages ranging from 1000 V to 6000 V were investigated. The samples for this study were 100 ng/mL and the fragmentor voltage was kept at 70 V for in-tube SPME analysis. The abundance of molecular ion  $[M+H]^+$  for each compound at different capillary voltages was shown in Figure 5.8. Each compound gave spectrum where the fragmentation patterns were dominated similar molecular ion ( $[M+H]^+$ ) for all the different capillary voltages. However, Figure 5.8 shows that all the compounds have the highest abundance of ions in the range of 2500 V-3500 V.

The fragmentor voltage from 20 V to 400 V was also investigated while keeping the capillary voltage at 3500V. With an increase in the fragmentor voltage, the

fragmentation pattern of the compounds became more complex. The abundance of molecular ion for each compound was decreased with an increase of the fragmentor voltage, while the characteristic ions started to appear. Depending on the structure of the compound, the characteristic ions appeared at a different fragmentor voltage. It was found that the compounds with hydroxyl group fragmented at relatively lower fragmentor voltage. This phenomenon can be clearly seen in Figure 5.9. It is obvious that the molecular ions of compounds with hydroxyl group, such as oxazepam and temazepam, give the highest abundance at lower voltage (~70V) as compared to the other compounds which do not possess hydroxyl groups (~100V).

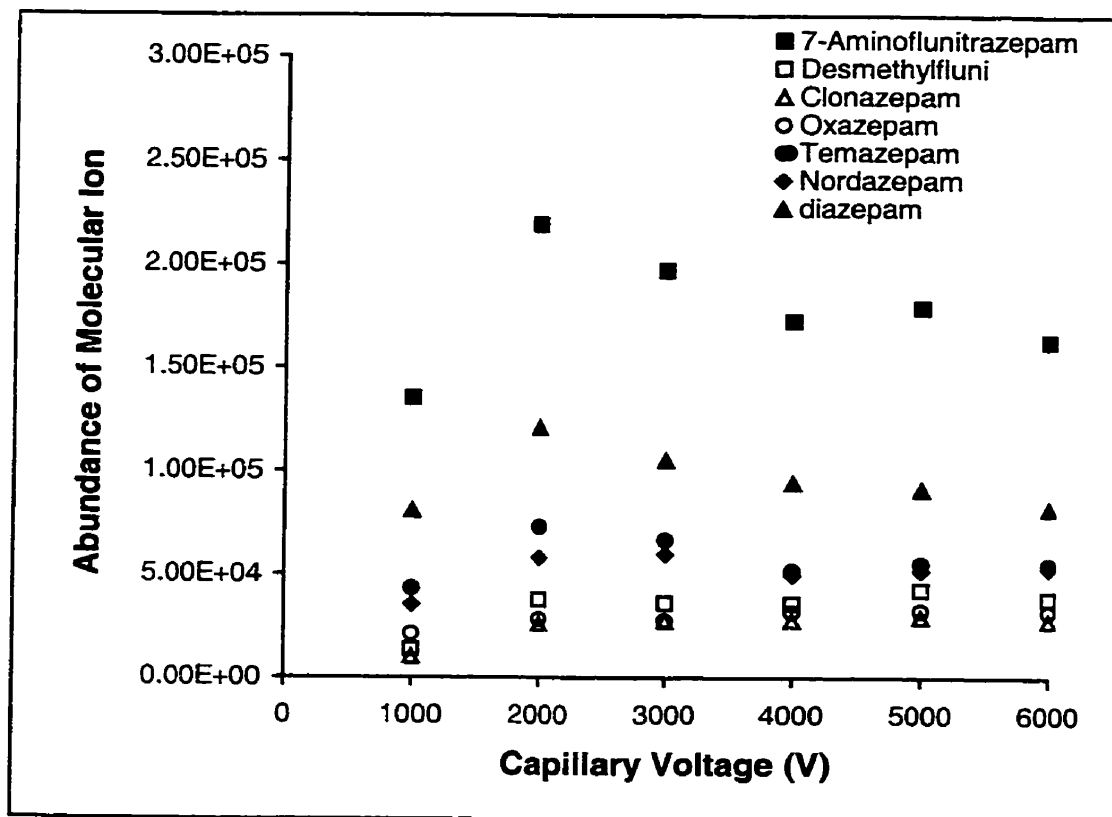


**Figure 5.8:** Influence of the capillary voltage on the fragmentation of the benzodiazepine compounds.

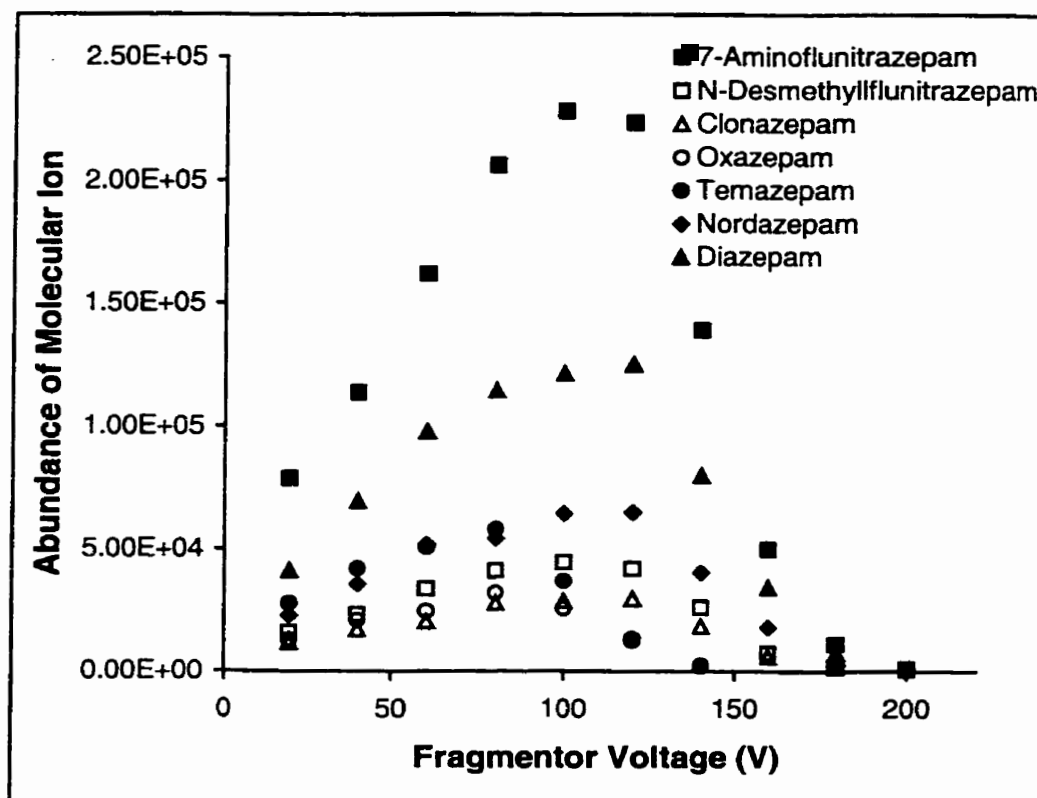
The spectra in Figure 5.10 were obtained by setting capillary voltage at 3500V.

Some characteristic ions were identified as listed in Table 5.4.

**Table 5.4:** The identified characteristic ions of the selected benzodiazepines.

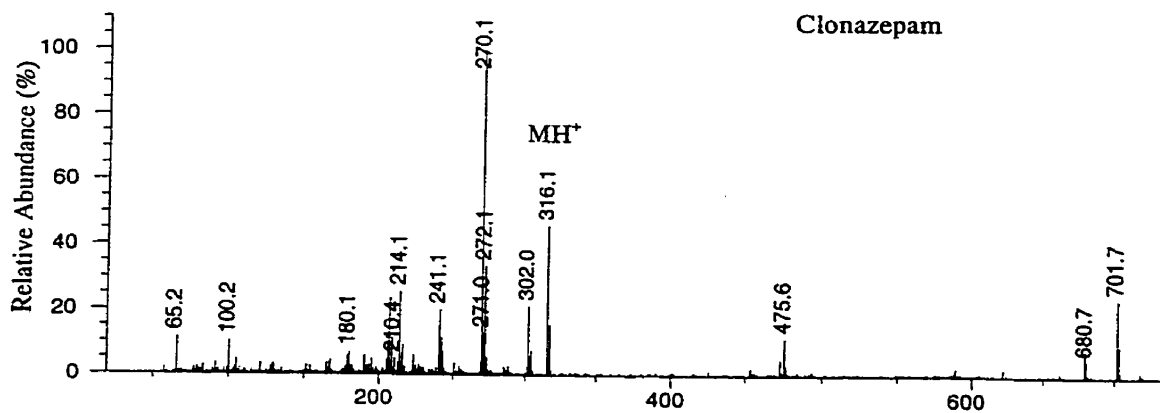
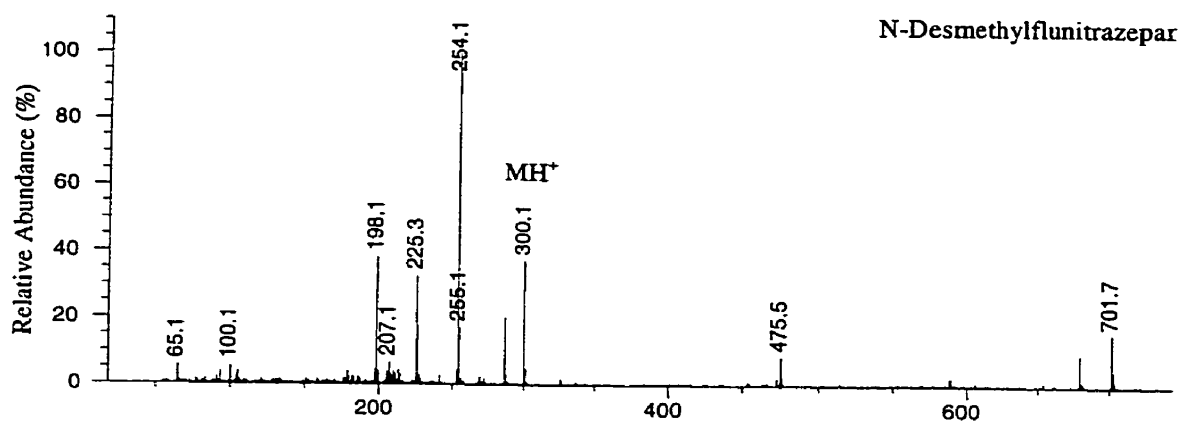
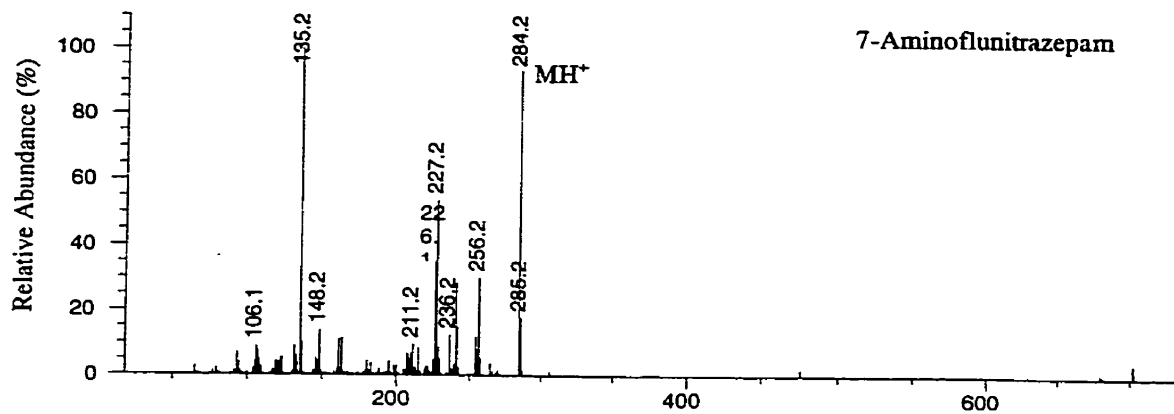
| Compounds                | Characteristic Ion   |
|--------------------------|--|
| 7-Aminoflunitrazepine    | (160V)* 284 [M+H] <sup>+</sup> , 256 [M+H-CO] <sup>+</sup> , 227 [M+H-CO-NCH <sub>3</sub> ] <sup>+</sup>   |
| N-desmethyflunitrazepine | (160V)* 300 [M+H] <sup>+</sup> , 254 [M+H-NO <sub>2</sub> ] <sup>+</sup> , 225 [M+H-C <sub>2</sub> N <sub>2</sub> OH <sub>7</sub> ] <sup>+</sup> |
| Clonazepam               | (140V)* 316 [M+H] <sup>+</sup> , 270 [M+H-NO <sub>2</sub> ] <sup>+</sup> , 241 [M+H-C <sub>2</sub> N <sub>2</sub> OH <sub>7</sub> ] <sup>+</sup> |
| Oxazepam                 | (100V)* 287 [M+H] <sup>+</sup> , 271 [M+H-NH] <sup>+</sup> , 241 [M+H-NOH] <sup>+</sup>  |
| Temazepam                | (100V)* 301 [M+H] <sup>+</sup> , 255 [M+H-CNOH] <sup>+</sup>   |
| Nordazepam               | (140V)* 271 [M+H] <sup>+</sup> , 243 [M+H-NO] <sup>+</sup> , 208 [M+H-NOCl] <sup>+</sup>   |
| Diazepam                 | (140V)* 285 [M+H] <sup>+</sup> , 257 [M+H-CO] <sup>+</sup>   |

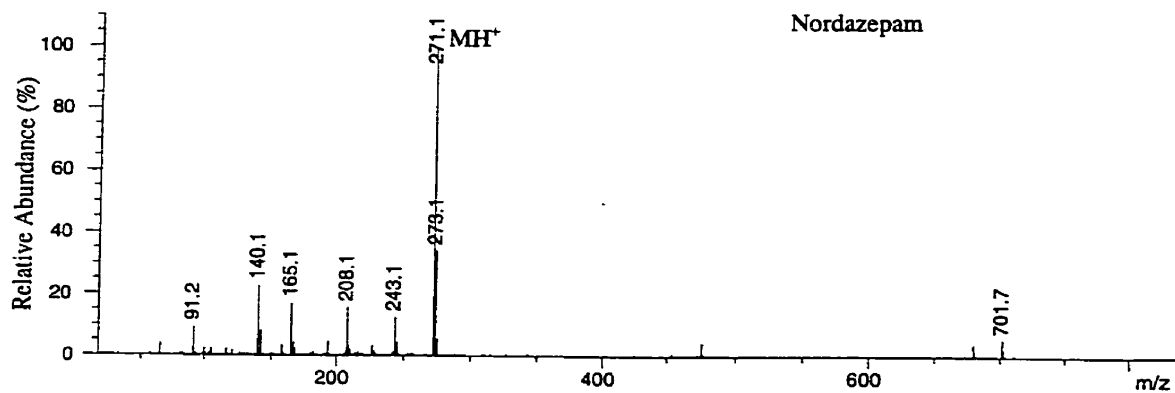
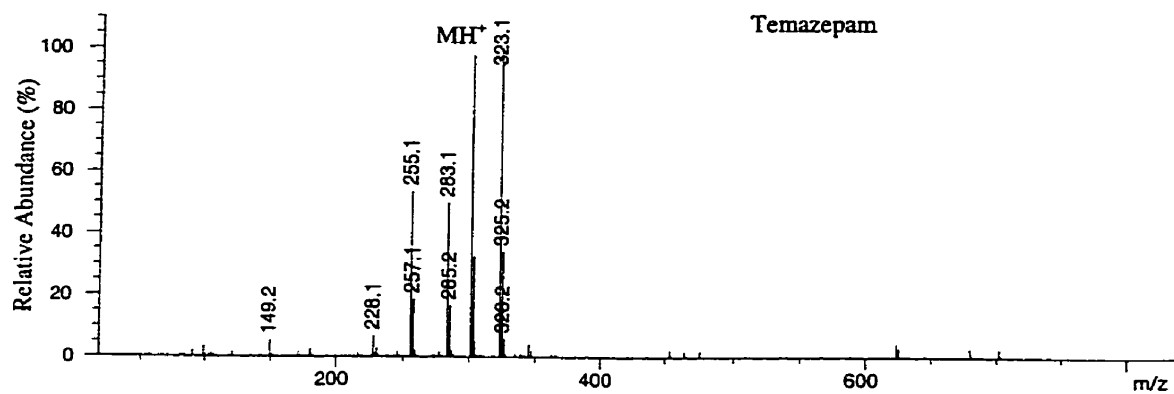
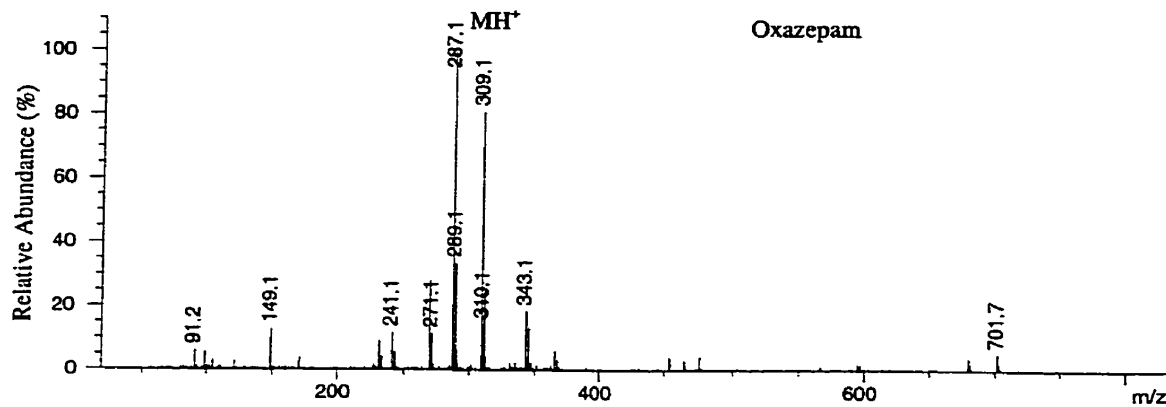
\* The fragmentor voltage.



**Figure 5.9:** Influence of the fragmentor voltage on the fragmentation of benzodiazepine compounds.







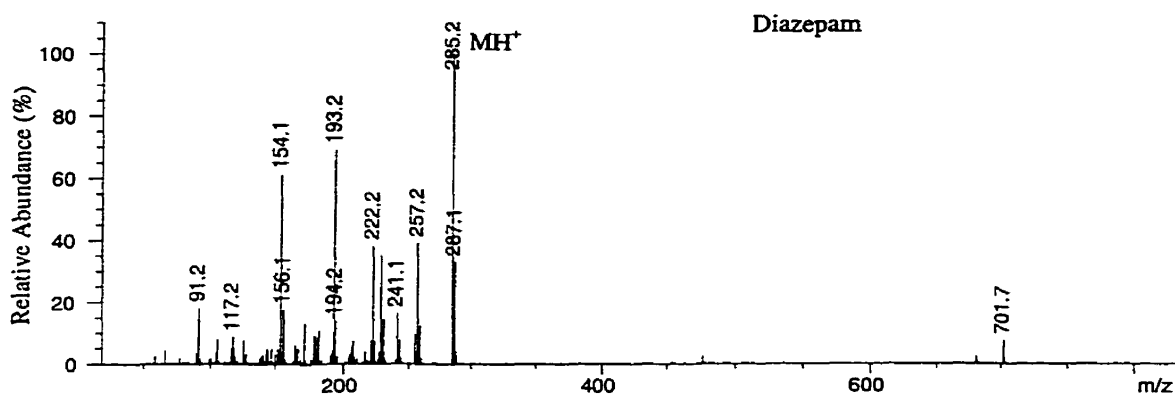


**Figure 5.10:** Mass spectra of benzodiazepine compounds obtained from HP 1100 LC/ESI/MS.

### 5.3.2.4 Analysis of Urine and Serum Samples

The method has also been applied to urine and serum sample analysis. As shown in Figures 5.11 and 5.12, no interference peaks were observed in non-spiked urine and serum samples. Benzodiazepines (each 50 or 500 ng) were spiked in the urine and serum samples and analyzed. As shown in Figure 5.11B and 5.12B, each of benzodiazepines in the urine and serum samples could be selectively detected in SIM mode. However, the peaks were broadened compared with direct liquid injection. As shown in Table 5.5, the recoveries from urine and serum samples were in the range of 75.8 to 106.8% and 35.4 to 53.7%, respectively. Recoveries from serum sample were lower than that of urine sample because of the protein binding. Clearly, the recoveries need to be further improved. The coefficients of variation of three replicate analyses were below 10%.

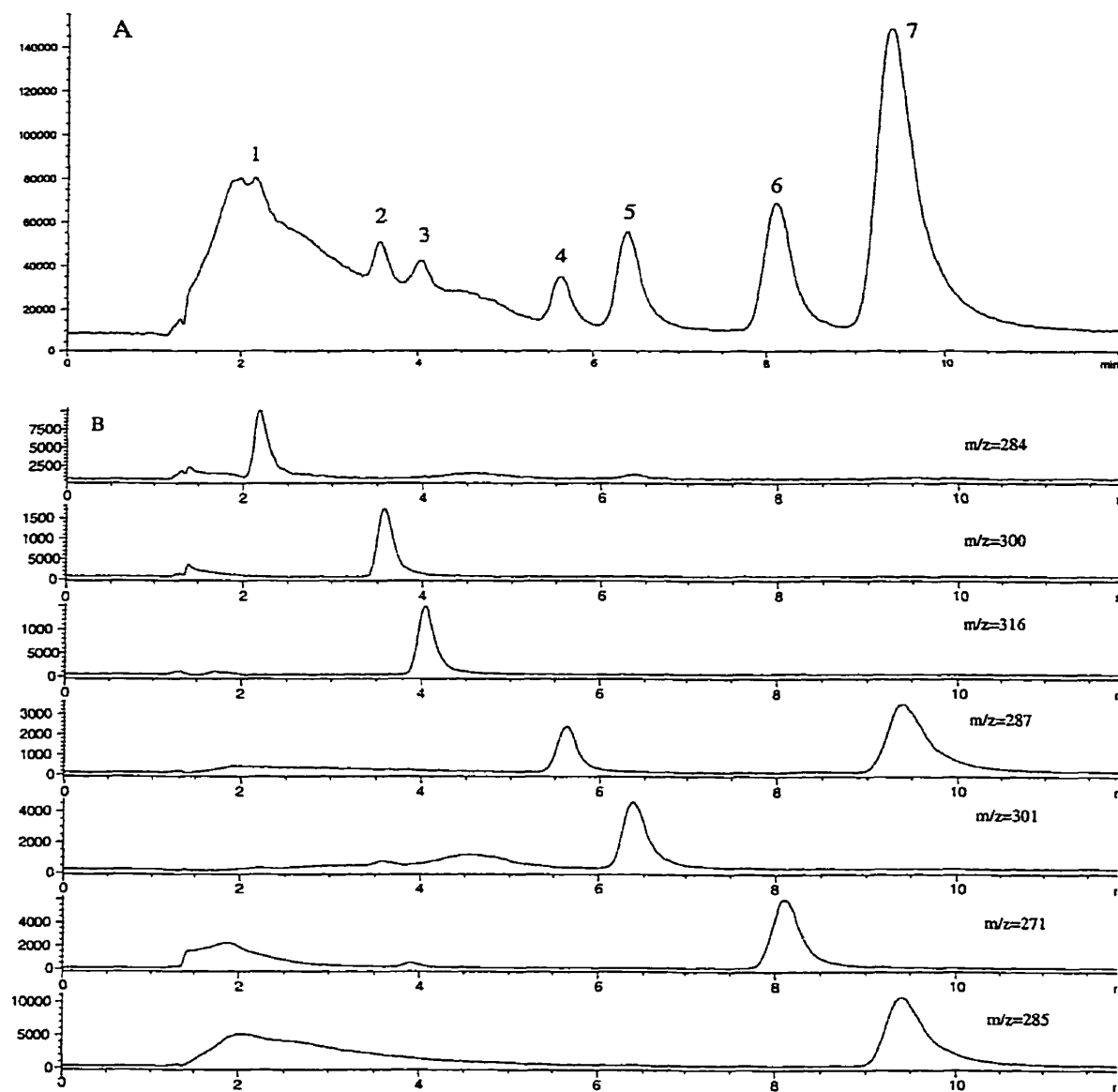


**Figure 5.11:** Total ion and SIM chromatograms obtained from urine samples

(0.5 $\mu$ g/mL) by in-tube SPME/LC/MS. A: Total ion chromatograms obtained from spiked urine sample. 1. 7-aminoflunitrazepam, 2. N-desmethyflunitrazepam, 3. clonazepam, 4. oxazepam, 5. temazepam, 6. nordazepam, 7. diazepam. B: SIM chromatograms obtained from spiked urine samples.

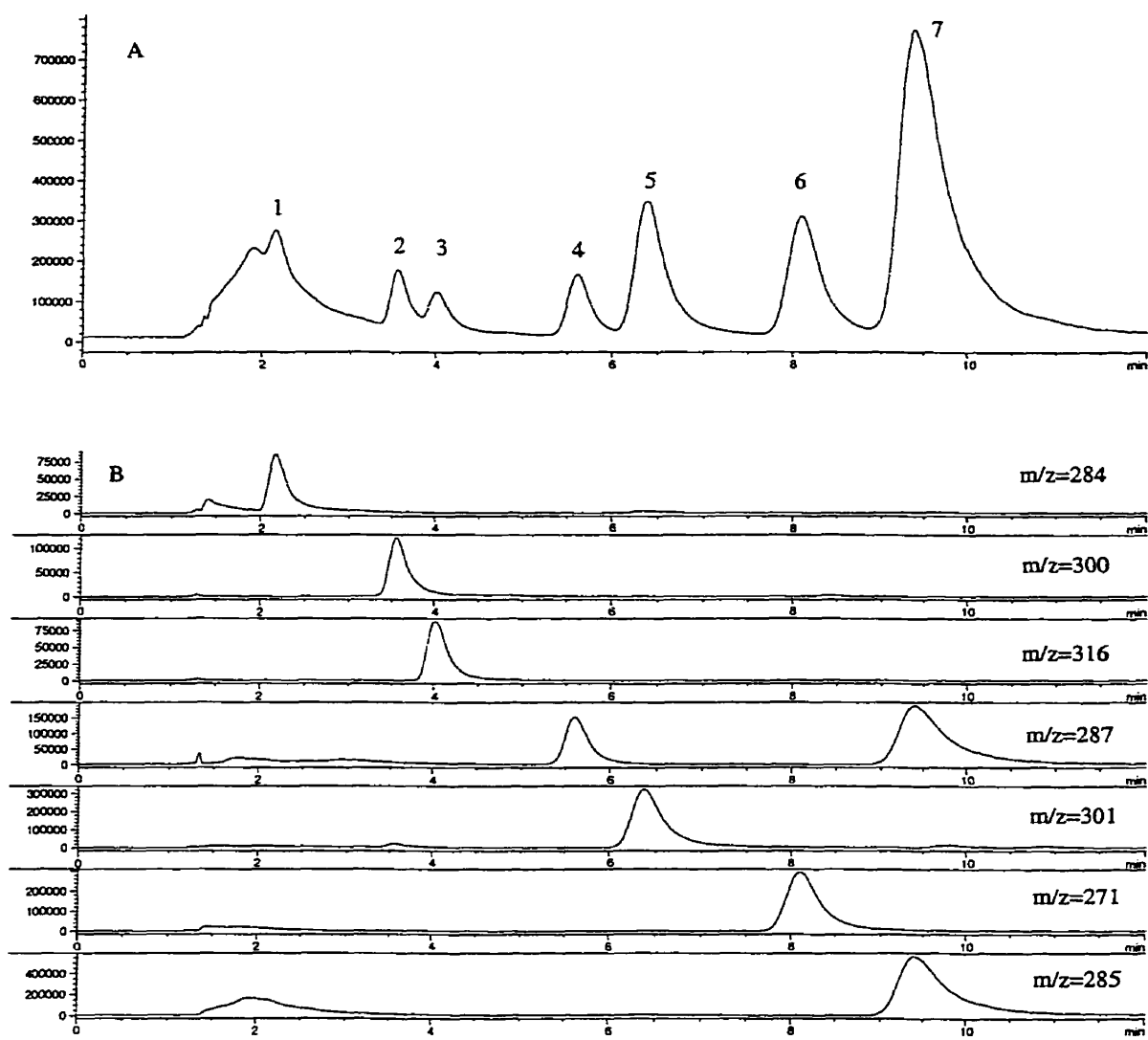


**Figure 5.12:** Total ion and SIM chromatograms obtained from serum samples (0.2 $\mu$ g/mL) by in-tube SPME/LC/MS. A: Total ion chromatograms obtained from spiked urine sample. 1. 7-aminoflunitrazepam, 2. N-desmethyflunitrazepam, 3. clonazepam, 4. oxazepam, 5. temazepam, 6. nordazepam, 7. diazepam. B: SIM chromatograms obtained from spiked urine samples.

**Table 5. 5:** Recoveries of seven benzodiazepines spiked into urine and serum samples.

| Compounds               | Recovery (%), Mean $\pm$ SD (n=3) |                 |                    |                |
|-------------------------|-----------------------------------|-----------------|--------------------|----------------|
|                         | Urine <sup>a</sup>                |                 | Serum <sup>b</sup> |                |
|                         | 50 ng/mL                          | 500 ng/mL       | 50 ng/mL           | 500 ng/mL      |
| Nordazepam              | 100.4 $\pm$ 1.2                   | 106.8 $\pm$ 6.8 | 41.5 $\pm$ 4.5     | 43.0 $\pm$ 3.2 |
| 7-Aminoflunitrazepam    | 94.2 $\pm$ 6.8                    | 96.9 $\pm$ 6.5  | 39.7 $\pm$ 2.3     | 44.4 $\pm$ 6.9 |
| Diazepam                | 97.2 $\pm$ 6.1                    | 101.4 $\pm$ 6.1 | 47.1 $\pm$ 3.1     | 51.8 $\pm$ 1.1 |
| Oxazepam                | 93.5 $\pm$ 7.9                    | 98.4 $\pm$ 8.9  | 40.0 $\pm$ 5.2     | 43.9 $\pm$ 1.7 |
| N-desmethyflunitrazepam | 82.8 $\pm$ 5.7                    | 98.5 $\pm$ 0.9  | 35.4 $\pm$ 4.1     | 39.7 $\pm$ 2.8 |
| Temazepam               | 75.8 $\pm$ 4.4                    | 82.1 $\pm$ 2.6  | 45.4 $\pm$ 2.3     | 53.7 $\pm$ 3.6 |
| Clonazepam              | 87.7 $\pm$ 7.9                    | 90.4 $\pm$ 6.3  | 44.2 $\pm$ 1.4     | 48.8 $\pm$ 2.1 |

<sup>a</sup> Benzodiazepines were spiked into 1 ml urine, the mixture was filtered using a syringe microfilter. 0.5 mL of the pH8.5 buffer was added to 0.5 mL mixture to make a 1 mL solution before analysis.

<sup>b</sup> Benzodiazepines were spiked into 100  $\mu$ L of serum, and the mixture was diluted 5 times with 1% acetic acid before analysis.

## 5.4 Conclusion

In-tube SPME is an excellent sample preparation technique because of its fast operation, simple automation, low solvent requirement and low expense. Its application to benzodiazepines analysis is very important due to their clinical significance. The diversity of the chemical structures of this class of compounds makes it difficult to find a universal traditional method to analyse and screen them all. However, after selecting the appropriate capillary, the automated in-tube SPME/LC/MS method demonstrated in this

study could continuously perform extraction of benzodiazepines from aqueous samples, followed by the identification through LC/MS analysis. However, due to the structural complexity of biomatrix, the recovery of some of the compounds from serum was fairly low. Further improvement in this respect is expected. Regardless, this method provided a useful tool for the screening and determination of benzodiazepines in clinical control and forensic analysis.

## 5.5 References

---

1. Linoila, M. in *The Benzodiazepines: From Molecular Biology to Clinical Practice*, E. Costa (Ed.), Raven, New York, **1983**, p. 267.
2. Cohen, S. *Psychiatr. Ann.* **1983**, 13, 65-70.
3. Drummer, O. H. *J. Chromatogr. B.* **1997**, 713, 201-225.
4. Huang, W.; D.E. Moody, D. E. *J. Anal. Toxicol.* **1995**, 19, 333-342.
5. Luo, Y.; Pan, L.; Pawliszyn, J. *J. Microcolumn Separation*, **1998**, 10, 193-201.
6. Ferrara, S. D.; Tedeschi, L.; Frison, G.; Castagna, F. *J. Anal. Toxicol.* **1993**, 17, 217-222.
7. Louter, A. J. H.; Bosma, E.; Schipperen, J. A. C.; Vreuls, J. J.; U. A. Th. Brinkman, U. A. Th. *J. Chromatogr. B.* **1997**, 689, 35-43.
8. Maurer, H. H. *J. Chromatogr.* **1992**, 580, 3-41.
9. Black, A. A.; Clark, G. D.; Haver, V. M.; Garbin, J. A.; A. J. Saxon, A. J. *J. Anal. Toxicol.*, **1994**, 18, 185-188.
10. Moore, C.; Long, G.; Marr, M. *J. Chromatogr. B.* **1994**, 655, 132-137.

11. Hold, K. M.; Crouch, D. J.; Rolloin, D. E.; Wilkins, D. G.; Canfield, D. V.; Maes, R. *A. J. Mass Spectrum*. **1996**, 31, 1033-1038.
12. Fitzgerald, R. I.; Rexin, D. A.; D. A. Herold, D. A. *Clin. Chem.*, **1994**, 40, 373-380.
13. Nishikawa, T.; Ohtani, H.; Herold, D. A.; Fitzgerald, R. L. *Am. J. Clin. Pathol.*, **1997**, 107, 345-352.
14. Essien, H.; Lai, S. J.; Binder, S. R.; King, D. L. *J. Chromatogr. B*. **1996**, 683, 199-208.
15. Lurie, I. S.; Cooper, D. A.; F. X. Klein, F. X. *J. Chromatogr.*, **1992**, 598, 59-66.
16. Kebarle, P.; Tang, L. *Anal. Chem.* **1993**, 65, 972A-968A.
17. Gaskell, J. *J. Mass Spectrum*. **1997**, 32, 677-688.
18. (a). Yamashita, M.; Fenn, J. B. *Phys. Chem.*, **1984**, 88, 4451. (b). Yamashita, M.; Fenn, J. B. *Phys. Chem.*, **1984**, 88, 4671.
19. Fenn, J. B.; Mann, M.; Meng, C. K.; Wong, S. F.; Whitehouse, C. M. *Science*, **1989**, 246, 64-71.
20. Covey, T. R.; Bonner, R. F.; Shushan, B. I.; Henion, J. *Rapid Commun. Mass Spectrum*. **1988**, 2, 249.
21. Smith, R. D.; Olivares, J. A.; Nguyen, N. T.; Udseth, H. R.; *Anal. Chem.*, **1988**, 60, 436-441.
22. Agilent Technology Inc. web site.  
<http://www.chem.agilent.com/temp/rad21313/00019847.pdf>
23. Crummtt, W. B. *Anal. Chem.*, **1980**, 52, 2242-49.



## CHAPTER 6

### CONCLUSIONS

#### 6.1 Scope of SPME in Biological Applications

As a relatively new analytical technique, SPME has experienced rapid development in the past decade, especially for volatile organic compounds in environmental sample analysis. In principle, SPME is distinguished from other sample preparation techniques, such as LLE and SPE, by providing three important features. First, the extraction phase of SPME is very small compared with the sample matrix. Second, instead of exhaustive extraction methods such as LLE and SPE, SPME is an extraction technique based on equilibrium processes. Furthermore, SPME is a solvent-free, rapid and simple analytical technique, which combines sampling, sample preparation and sample introduction into a single step.

The purpose of the work presented in this thesis was to investigate the viability of SPME for biological sample analysis. The entire work consists of three parts (Figure 6.1). First, the application of SPME to the study of drug-protein binding was investigated based on the equilibrium extraction process. Secondly, novel SPME coating materials with molecular recognition ability, i.e. antibody and MIP, have been developed and investigated for biological sample analysis. Finally, application to benzodiazepine compounds analysis by in-tube SPME has been performed with a LC/ESI/MS system.

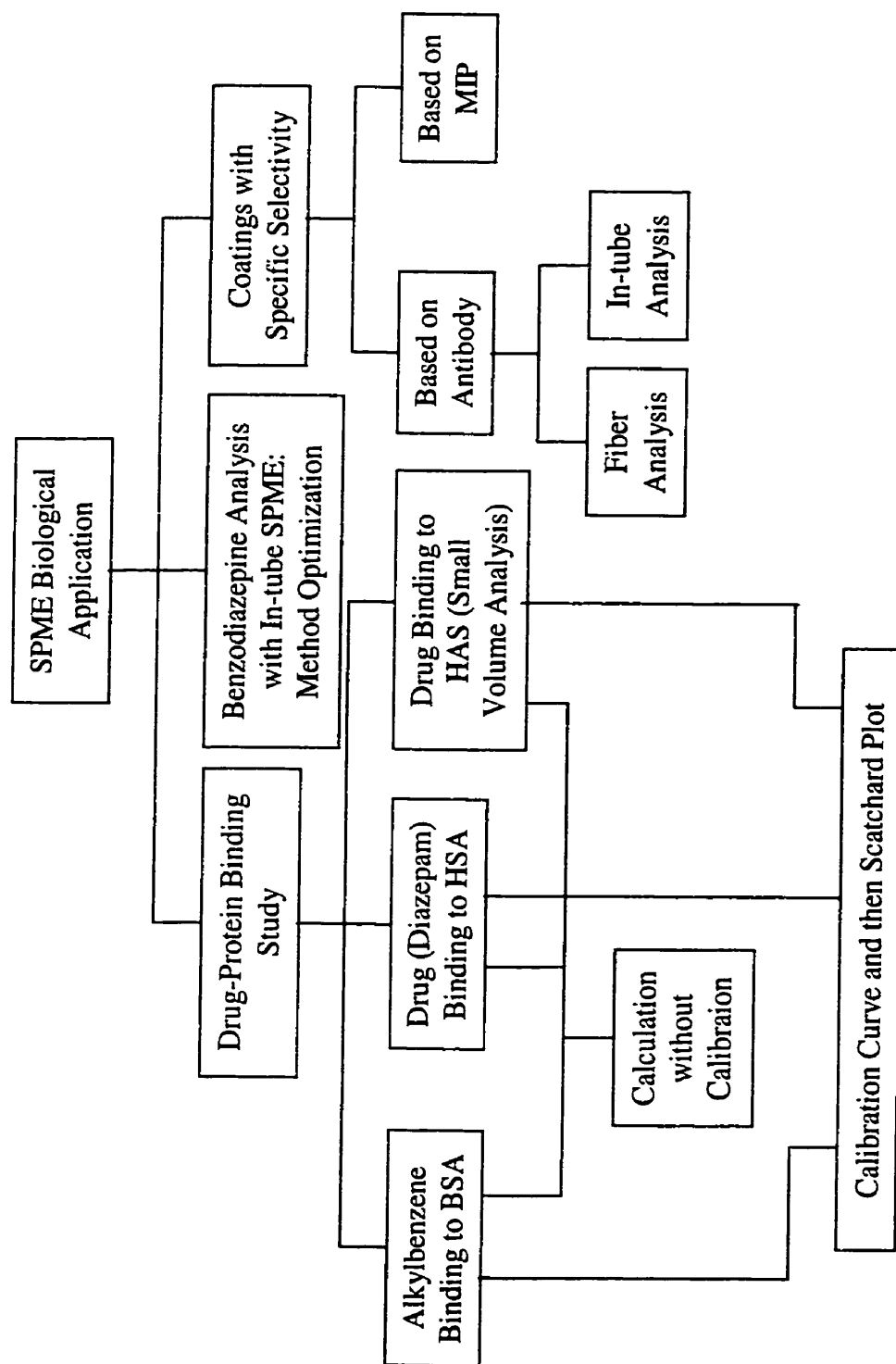


**Figure 6.1:** SPME for the biological applications – scope of the research performed in this thesis.

## 6.2 Protein Binding Study with SPME

The theory of SPME analysis of protein binding was thoroughly illustrated with five alkylbenzene compounds (benzene, toluene, ethylbenzene, propylbenzene and butylbenzene) and their binding to BSA in a model system. Since these alkylbenzene compounds are volatile, the extraction was performed in the headspace of the sample. Therefore, the system had four phases (sample solution-dissolved protein-headspace-fiber coating).

The theoretical as well as the experimental analysis demonstrated that SPME is a very simple and accurate method for such studies. In the experiment, a calibration curve was first constructed by employing the amount of the analytes partitioned on the fiber vs. the true free analyte concentration in the solution in the absence of protein. Special care should be exercised to make sure the correct concentrations in the calibration curve were utilized. Neglecting the amount of the analyte on the fiber and especially in the headspace must be verified before such an assumption is applied. The Scatchard plot was finally employed to obtain the number of binding sites and the equilibrium binding constants. The results from the SPME analysis demonstrated that the binding between alkylbenzene and BSA is first order. The equilibrium binding constants agree with the result from other methods, e.g. headspace GC analysis.

The main error of this experiment comes from the repeatability of the fiber and of the syringe injection (to obtain the GC response factor). However, for first order binding, the direct measurement initiated in this thesis does not need a GC response factor and calibration curves, which decreases the experimental error by eliminating the error introduced from such measurements. The only measurement needed is the area count

change (ratio) of the fiber injections before and after the protein was introduced into the system. This method is valid as long as both the GC and fiber extraction is linear. The direct measurement method greatly enhanced the accuracy of the binding study and reduced the workload by SPME. However, the limitation is that the number of binding sites has to be a pre-determined value.

Diazepam binding to HSA was also studied by SPME. Drug compounds, which are different from the alkylbenzene compounds, are normally non-volatile organic compounds. Therefore, direct extraction was employed instead of headspace SPME. This extraction system had three phases: sample solution-dissolved protein-fiber coating. It has been proven in this thesis that SPME is an appropriate method for the drug-protein studies. In small volume SPME application, by combining the loading and extraction into a single SPME fiber, it is extremely useful in the determination of drug binding to precious proteins since only very small amount (150  $\mu\text{L}$  for each extraction) of the protein solution and analyte is required.

### **6.3 Immunoaffinity SPME**

The major difficulty of biological sample analysis with the existing SPME coating material is the lack of selectivity, which normally results in poor chromatographic separations or/and the poor sensitivity. This adversely limits the scope of the applications of SPME in biological sample analysis. The solution proposed in this thesis is to find the coatings that have the selectivity towards the specific analyte. Therefore, immunoaffinity SPME has been developed based on two types of molecular recognition elements: antibody and MIPs.

Anti-theophylline was covalently immobilized on the surface of a fused silica fiber and on the inner surface of a fused silica capillary. The selectivity of the coating was demonstrated in the caffeine binding study, which showed lower caffeine-immobilized antibody cross reactivity compared with antibody of aqueous solutions. The results of human serum analysis showed that the methods are simple and effective.

Due to the small surface area of the fiber and low surface density of the immobilized antibody, the capacity of fiber/capillary is relatively low. Therefore, more sensitive scintillation detection instead of the chromatographic method was employed. However, the capacity could be improved by increasing the surface density which can be achieved either by investigation of other immobilization methods under different reaction conditions or by immobilization of only the Fab part of the antibody on the surface to decrease the size of the antibody. Once the capacity is increased, the antibody-immobilized capillary can be coupled with an HPLC system for in-tube SPME analysis.

Research on the application of MIP to SPME is still in a preliminary stage due to the limitation of the MIP coating technique. The research performed in this thesis demonstrated that such materials could have great potential for selective extraction once they can be coated on the fused silica surfaces more reliably and effectively.

#### **6.4 The Potential of SPME in Biological Applications**

In this thesis, the study of protein binding with SPME has been thoroughly discussed. Further improvement for SPME in the drug confirmation and concentration analysis will focus on the development of the coating techniques for materials with specific molecular recognition abilities.

One aspect of the improvements is to optimize the type and conditions of immobilization reactions. The aim is to increase the density of active immobilized antibody on the solid support surface, which will increase the capacity of the extraction media. This will allow for the smaller size of the extraction media, which is the trend of current analytical research, or more diversified detection methods coupling to either the antibody-immobilized fiber or the capillary.

Several methods can be explored to achieve this goal. One way is to improve the orientation of the antibody on the surface so that the binding sites (Fab) face towards the sample solution. This can be accomplished by taking advantage of various functional groups available for the linkage either on the protein molecule or the cross-linking reagent (1-3). The other way is to immobilize only the Fab portion of the antibody. Since the binding sites of the antibody is located in the Fab part of the molecule, the orientated immobilization of Fab of antibody could enhance the active density by saving the space each antibody occupied (4, 5). The Fab portion of the antibody can be obtained by digestion with pepsin followed by reduction with dithiothrietol (DTT) (5). Alternatively, efforts can be made to use different types of materials, which possess more active functional groups, such as the acrylate polymer and porous polydimethylsiloxane membranes (6, 7).

The major improvement for the application of MIP in SPME extraction is finding the proper method to attach the MIP on the solid support. Early studies by the author indicated that it is possible to polymerize the MIP directly on the fiber. However, it is very difficult to eliminate the imprint molecule. Recently, the MIP has been successfully synthesized on a solid support electrochemically with a conducting polymer technique

(8). If such methods can be successfully applied to SPME fibers and in-tube SPME capillaries, this could be a definite breakthrough for SPME techniques.

## 6.5 References

---

1. Qian, W.; Xu, B.; Wu, L.; Wang, C.; Song, Z.; Yao, D.; Lu, Z.; Wei, Y. *Journal of Inclusion Phenomena and Macrocyclic Chemistry*, **1999**, 35, 419-429.
2. Turková, J. *J. Chromatogr. B.*, **1999**, 722, 11-31.
3. Bílková, Z.; Mazuravá, J.; Churáček, J.; Horák, D.; Turková, J. *J. Chromatogr. A.*, **1999**, 852, 141-149.
4. Lu, B.; Xie, J.; Lu, C.; Wu, C.; Wei, Y. *Anal. Chem.*, **1995**, 67, 83-87.
5. Qian, W.; Yu, F.; Song, Z.; Liang, B.; Wei, Y. *Supramolecular Science*, **1998**, 5, 701-703.
6. Wang, H.; Kobayashi, T.; Saitoh, H.; Fujii, N. *Journal of Applied Polymer Science*, **1996**, 60, 2339-2346.
7. Hall, E. A. H.; Gooding, J. J.; Hall, C. E.; Martens, N. *Fresenius J. Anal. Chem.*, **1999**, 364, 58-65.
8. Deore, B.; Chen, Z.; Nagaoka, T. *Anal. Chem.*, **2000**, 72, 3089-3994.

## GLOSSARY

|           |   |
|-----------|---|
| Ab        | Antibody  |
| Ag        | Antigen   |
| AIBN      | (2,2'-azobis (2-methylpropionitrile)                            |
| APCI      | Atmospheric pressure chemical ionization                        |
| APTES     | (3-aminopropyl)triethoxysilane                                  |
| B.P.      | Boiling point   |
| BSA       | Bovine serum albumin  |
| CW        | Carbowax  |
| DVB       | Divinylbenzene  |
| EDMA      | Ethylene glycol dimethacrylate                                  |
| EMF       | Electro-magnetic field  |
| FID       | Flame Ionization Detector                                       |
| GC        | Gas Chromatography or Gas Chromatography                        |
| HPLC      | High performance liquid chromatography                          |
| HSA       | Human serum albumin   |
| i.d.      | Inside diameter   |
| IA        | Immunoassay   |
| LC/ESI/MS | Liquid Chromatography/Electrospray Ionization Mass Spectrometry |
| LLE       | Liquid-liquid extraction  |
| LOD       | Limit of detection  |
| MIP       | Molecularly imprinted polymer                                   |
| MAA       | Methacrylic acid  |
| PA        | Poly(acrylate)  |
| PBS       | Phosphate buffered saline                                       |
| PDMS      | Poly(dimethylsiloxane)  |
| PMT       | Photomultiplier tube  |
| ppb       | Part per billion  |
| ppt       | Part per trillion   |



|       |  |
|-------|--|
| PPY   | Polypyrrole  |
| RSD   | Relative standard deviation  |
| SEM   | Scanning Electronic Micrography                                      |
| SIM   | Selective Ionization Mode  |
| SPE   | Solid phase extraction   |
| SPI   | Septum-equipped temperature programmable injector, used in Varian GC |
| SPME  | Solid Phase Microextraction  |
| TFA   | Trifluoroacetic acid   |
| TR    | Template Resin   |
| V. P. | Vapor pressure   |